Modeling Chemical Vapor Deposition of Thin Solid Films

Thesis by

Michel E. Jabbour

In Partial Fulfillment of the Requirements

for the Degree of

Doctor of Philosophy

California Institute of Technology

Pasadena, California

2000

(Submitted August 30, 1999)

Acknowledgements

This work would not have been possible had it not been for the contributions of the following people:

My advisor, Kaushik Bhattacharya, has never failed to show great interest in all aspects of my research, and he has always been willing to discuss every detail of my work to whatever extent needed. He has provided crucial guidance and has taught me how to conduct a scientific investigation. He has above all taught me a strong work ethic and the virtue of perseverance. For these reasons and many others I am grateful to him.

Jim Knowles has shown much interest in my work. He was always willing to listen patiently to me, even when I was confused. He would always come down to my level and pedagogically explain things to me, repeatedly if needed. He has taught me that academic excellence and human kindness are not incompatible. This I will not forget.

I am grateful to S.I. Hariharan for his constant interest in my work and the many useful discussions we have had during his sabbatical stay at Caltech.

Robert Kukta has been an excellent friend and officemate. With him, I've had many useful discussions during which his insights have helped me clarify my own ideas. His companionship has created a lively work environment for me over the last two years.

Mark Brady's friendship as well as his pedagogical patience with me when it comes to computer-related issues have sustained me through the last difficult moments.

I want to thank Cem Gomel for the years of brotherhood, and Don Porcelli and Aude Tricca for their friendship and the many subtle ways in which they took care of me during the last stages of the process of writing my thesis.

To Alex Vittes I am grateful for so many things. She has never spared any effort to make my life more bearable during all the difficult moments over the past few years. She and Howard are my family here in Los Angeles and this is priceless to me.

Finally, thank you, Yaman and Elie Jabbour, for believing in me and the treasures of love you have never failed to give me. I am lucky to have you as parents.

Abstract

Chemical vapor deposition (CVD) is a process by which thin solid films are deposited on solid substrates for various technological applications. Roughly speaking, a multispecies chemically reacting gas flows past a heated substrate on top of which the deposition and subsequent formation of the alloy or compound of interest take place via a series of heterogeneous chemical reactions. The growth rate of the thin film is determined by the competition between the diffusive and convective transports of species in the gas phase, the homogeneous and heterogeneous chemical kinetics, and the morphology of the gas-film interface.

In chapter 2, a thermomechanical macroscopic model is proposed that couples the multicomponent chemically reactive gaseous flow to the bulk of the growing thin solid film via the equations that govern the morphological evolution of the film-gas interface. The surface is modeled as a separate anisotropic elastic phase, and such phenomena as surface species diffusion, heat conduction and chemistry are accounted for. In particular, the driving force at the surface is identified, and a thermodynamically consistent kinetic relation linking it to the growth velocity is proposed. A specialization of this general framework to the case of a multicomponent ideal gas and a linearly elastic solid film separated by an isotropic surface is considered.

In chapter 3, we examine a multicomponent gas flow in a vertical axisymmetric MOCVD reactor whose geometry is characterized by a small aspect ratio (defined as the ratio of the height of the reactor channel to the radius of the substrate) and operating under conditions insuring a small Mach number. A two-parameter asymptotic analysis yields, in the limit of vanishingly small aspect ratio and Mach number, a set of approximate equations governing the gas phase, combined with approximate boundary conditions at the showerhead and the gas-film interface. A specialization to the steady-state approximation is then proposed, and an analytical solution to the approximate problem is derived. It is found that this solution is of the similarity

type, thus insuring a uniform temperature and chemical composition profiles along the film surface.

Finally, in chapter 4, the growth of a generic thin film via a ledge-and-terrace mechanism is examined. Of particular interest is the interaction between the microstructure of the surface and the chemical kinetics by which the adsorption/desorption of species along the terraces and the formation of the compound at the steps occur. A simple step-flow model is proposed and its specialization to the case of a binary compound is used to illustrate the complex dependence of the averaged growth rate on the chemical composition of the gas phase as well as on the morphology of the evolving surface.

Contents

Chapter 1 Introduction

1.1 Background

Chemical vapor deposition (CVD) is a widely used technique for the deposition of thin solid films on solid substrates. Its main industrial applications are the fabrication of integrated circuits, in particular Silicon-based semiconductor devices such as computer chips, the production of compound semiconductors (such as Gallium-Arsenide films) for opto-electronic applications, the synthesis of diamond films for such applications as cutting tools, the filling of grooves for interconnect lines, as well as the manufacture of various anticorrosion and antiwear industrial coatings (cf., e.g., Kleijn [K] and Goodwin and Butler [GB]). A more recent technological development has been the use of CVD to grow high-temperature superconducting $YBa_2Cu_3O_{7-\delta}$ films which are incorporated in high-performance microwave filters for commercial wireless and aerospace communications (e.g., cf. Bourdillon and Bourdillon [BB]).

As a deposition process, metallorganic CVD is more attractive than other production methods (such as molecular beam epitaxy (MBE) or pulsed laser deposition (PLD)) because of a variety of factors. It typically has higher growth rates and it is a low-unit-cost manufacturing technique. Most importantly, it has the capability of depositing highly uniform films, both in terms of thickness (even on irregular surfaces) and chemical composition (e.g., cf. Houtman et al. [HGJ]).

The huge technological progress accomplished over the recent years in the production of semiconductor devices, leading to the current generation of ultra-large-scale-integration (ULSI) circuits, characterized by the presence of millions of components on a single chip whose typical dimensions are of the order of a micron or less, has led to increasing demands on the performance of CVD processes. Thus the need to understand quantitatively the fundamental physics and chemistry of such processes, in the hope that physically-based theoretical models and numerical simulations can

help in the design, optimization, and control of CVD reactors. Moreover, the recent interest in the deposition of compounds such as $YBa_2Cu_3O_{7-\delta}$ superconductors and $PbTiO_3$ ferroelectrics poses the additional challenge of providing a very accurate controllability of the chemical composition of the grown thin films in order to prevent the formation of secondary phases with disastrous consequences on the performance of the manufactured devices. As an example, consider $YBa_2Cu_3O_{7-\delta}$ films. Even a slight excess in Ba can lead to the degradation of the superconductivity of the film (e.g., Waffenschmidt et al. [W]), while the formation of Cu-rich precipitates interferes with line patterning thus making it difficult to produce multilayers.

Roughly speaking, chemical vapor deposition of compounds consists of flowing a multispecies chemically reacting gas past a heated substrate on top of which the deposition of the desired species occurs via a series of adsorption reactions. The adatoms diffuse along the surface and react chemically to form the compound of interest. From the brief description above, it can be seen that chemical vapor deposition is a highly complex process. This complexity results mainly from two reasons: (a) the multitude of physical and chemical mechanisms present in the reactor, and (b) the presence of multiple length scales.

In order to discuss (a), consider the growth of a thin film by MOCVD. The atoms to be deposited on top of the substrate are carried by metallorganic precursor compounds, more or less diluted with an inert carrier gas (usually Hydrogen or Nitrogen). These precursors are chosen so that they have the adequate volatility at the source temperature (i.e., in the separate temperature-controlled ovens containing each of the precursors of interest), but they must also decompose to release the atoms from the organic ligands at the substrate temperature. The precursors and the carrier gas mix and flow into the reactor channel in which the heated substrate is positioned. The transport of species in the gas phase occurs both by convection and diffusion. In parallel, a series of heat-activated homogeneous chemical reactions take place in the gas flow, leading to the formation of reactive intermediate products. These intermediates reach the surface of the substrate where they adsorb, releasing the organic ligands into the gas. The adatoms (i.e., the adsorbed particles) then diffuse along the

surface, and react chemically, ultimately leading to the formation of the compound of interest, while the exhaust gases leave the reactor through the vacuum ports. From the description given above, it can easily be seen that the rate of growth of the film depends on the competition between homogeneous and heterogeneous chemical kinetics, as well as the convective and diffusive transport phenomena. It should be noted here that the chemical kinetics and transport properties are functions of the process conditions, i.e., they depend on the temperature, pressure, chemical composition of the gas mixture, and inlet conditions (flowrates, inlet temperature, etc.), as well as on the reactor geometry. Various mathematical models have been successfully developed to describe the behavior of the gas flow, complemented by chemistry and heat transfer models (on general CVD models, cf., e.g., Winters, Evans and Moen [WEM], Coltrin, Kee and Rupley [CKR], and the excellent review article by Kleijn [K] and the references therein; on stagnation-point flow CVD, see, e.g., Houtman, Graves and Jensen [HGJ] and Evans and Greif [EG]; on Silicon CVD, cf., e.g., Coltrin, Kee and Miller [CKM1] and [CKM2], Pollard and Newman [PN], and Houf, Grcar and Breiland [HGB]; on $GaAs$ CVD, see, e.g., Mountziaris and Jensen [JM] and Omstead et al. [OSLJ], as well as Coltrin and Kee [CK]). We note here that a common feature of these models is the assumption that the film surface is flat.

The presence of multiple length scales is obvious from the observation that the typical dimension of the reactor chamber is of the order of inches, while the height of the grown thin film is typically less than a micron. It is this observation that justifies the assumption of flatness of the surface of the film in the various gas-phase models mentioned above. In reality, the surface is not flat, and a crucial question concerns the dependence of the deposition kinetics on the morphological details of the evolving gas-film interface.

The morphological evolution of the surface has been the focus of numerous studies ranging from particle-based Monte Carlo simulations at the atomistic or molecular scale to continuum models at the macrosopic scale and passing by semi-continuum models at the mesoscopic scale. Monte Carlo simulations of the deposition kinetics during epitaxial growth are based on solid-on-solid (SOS) models. These atomistic

models describe the random deposition of particles onto lattice sites and their surface migration via nearest-neighbor hopping mechanisms (for a brief description of the Monte Carlo procedure, cf. Saito [S] and the references therein). Vvedensky et al. have focused mainly on simple deposition kinetics such as those characterizing MBE processes (one reason for this being that the kinetics underlying the SOS models contain free parameters that can either be determined based on molecular-dynamics calculations or obtained by indirect comparison with in-situ experimental observations, thus the choice of MBE because of its simple deposition kinetics and the relative ease with which in-situ measurements can be performed in its ultra-vaccum environment– cf., e.g., Vvedensky [V], Vvedensky, Haider, Shitara et al. [VHS] and Ratsch, Smilauer, Vvedensky et al. [RSV]). Recently, Srolovitz et al. have studied the CVD of diamond using Monte Carlo simulations based on kinetics parameterized by conventional surface chemical reaction-rate coefficients (see, e.g., Battaile, Srolovitz and Butler [BSB1, BSB2, BSB3]). However, due to computational limitations, these simulations remain essentially too microscopic (the surfaces simulated have typical dimensions of the order of nanometers). Semi-continuum mesoscopic models find their justification in the experimental observation that, under certain growth conditions, epitaxially deposited films grow by the "terrace and ledge" mechanism. That is, atoms are adsorbed to large terraces separated by unit-cell ledges; they then diffuse along these terraces and are finally incorporated into the film at the ledges. This terrace-and-ledge model has been studied extensively since the seminal work of Burton, Cabrera and Frank [BCF] (also see, e.g., Zangwill [Z], Bales and Zangwill [BZ], Villain [V], Villain and Pimpinelli [VP] and Elkanini and Villain [VE], as well as the references therein for more recent studies). These studies, however, concentrate on the growth of films of a single chemical species or element. In addition, they are often confined to the case of deposition by a ballistic flux of atoms, thus reducing the complexity of the coupling with the gas-phase. Finally, macroscopic continuum models have been developed that describe the morphological evolution of the surface at length scales sufficiently large so that the microstructure can be neglected, i.e., the evolving surface is modeled as a smooth two-dimensional manifold. These models

were pioneered by the works of Mullins [M] and Mullins and Sekerka [MS] (for more recent works, cf. Spencer, Voorhees and Davis [SVD] and Davi and Gurtin [DG], as well as the references therein). These studies have mostly focused on the growth of single-component films, and more recently, there has been a growing interest in alloy films (cf., e.g., Guyer and Voorhees [GV]).

1.2 Scope of the Present Work

The objective of the present work is to address several issues concerning the modeling of thin film growth by chemical vapor deposition. The context within which most of this investigation was conducted is the growth of $YBa_2Cu_3O_{7-\delta}$ high-temperature superconducting films by MOCVD. This is a highly complex process still suffering from an incomplete theoretical knowledge and experimental characterization of many of its underlying fundamental physical mechanisms, the most significant handicap being perhaps the very partial knowledge we possess of the gas-phase and surface chemical kinetics. As a result, the approach espoused here was to treat the general case of a multicomponent system with N constituents, where $N \geq 2$. In doing so, our ambition was to acquire some qualitative understanding of the physics underlying CVD processes rather than the quantitative characterization of a specific physical system.

The goal was to build upon the impressive body of work already available. As mentioned above, models exist that deal with the very complex chemistry that characterizes many CVD systems which have been extensively investigated (such as Silicon or Gallium-Arsenide CVD), and the interplay between the various transport phenomena that occur in the gas phase (i.e., species and momentum transport as well as heat transfer) and the deposition chemistry. But these models have mostly payed little attention to the morphology of the surface separating the gas phase from the bulk of the film. On the other hand, microscopic Monte Carlo, mesoscopic terrace-and-ledge and macroscopic continuum models that have investigated the influence of surface morphology and elastic stress on the growth of thin films have been mostly confined

to single-species or binary alloy systems growing by MBE (or other ballistic deposition techniques), thus reducing the complexity of the gas-phase transport phenomena and the heterogeneous chemical deposition kinetics. In chapter 2, we attempt to provide a unified macroscopic framework within which to model the morphological evolution of multispecies films grown by CVD.

In chapter 3, the focus is on the modeling of the multispecies reactive gas flow. The specialization to a vertical axisymmetric reactor with small aspect ratio (defined as the ratio of the height of the reactor's channel to the radius of the substrate on top of which the deposition occurs) and operating under conditions insuring a small Mach number is the consequence of our involvement in the VIP (Virtual Integrated Prototyping) project whose experimental MOCVD reactor can be idealized to correspond to the one we study. A two-parameter asymptotic expansion yields a set of approximate equations governing the behavior of the flow and boundary conditions at the showerhead and the substrate. This approximate problem can be solved analytically, leading to a similarity-type solution which guarantees the uniformity of the temperature and chemical composition on most of the substrate.

Finally, in chapter 4, the interaction between the microstructure of a generic thin film grown by MOCVD and the surface chemistry by which the adsorption and incorporation of adatoms take place is examined in the light of experimental observations suggesting that, within a certain operating regime, the growth of $YBa_2Cu_3O_{7-\delta}$ films occurs via a terrace-and-ledge mechanism. A simple one-dimensional step-flow model is proposed, and its application to a binary compound illustrates the interesting nonlinear effects of the morphology of the terraced surface and the gas-phase chemical composition on the overall growth rate of the thin film.

Chapter 2 A Macroscopic Thermomechanical Model of Multispecies Film Growth by CVD

2.1 Introduction

The present chapter is an attempt to provide a unified continuum treatment of the growth process of multicomponent thin solid films (either substitutional alloys or compounds) by chemical vapor deposition (CVD). The basic setup is shown in Figure 2.1 which represents the schematic of a vertical stagnation-point flow reactor such as are used to deposit high-temperature superconducting thin films of $YBa_2Cu_3O_{7-\delta}$ on MgO substrates via MOCVD (metallorganic CVD). A chemically reactive gas mixture with N constituents ($N \geq 2$) flows through a showerhead into the reactor chamber and past an independently heated substrate on top of which it deposits various chemical species whose conglomeration forms the compound or alloy of interest (for a general and extensive overview of the modeling of chemical vapor deposition processes, we refer the reader to the excellent article by Kleijn [K]). Our goal is to formulate a set of equations governing both the fluid flow in the channel and the growth of the thin solid film on the substrate (via the morphological evolution of the vapor-solid interface). In both the gas flow and the bulk of the solid film, we allow for the transport of species by convection and diffusion, and the diffusive species fluxes can suffer discontinuities across the gas-film evolving interface. Homogeneous and heterogeneous chemical reactions are also accounted for, where the former are confined to the gas phase (and thus involve only gaseous species), while the latter occur along the gas-film interface and typically involve gaseous, bulk and superficial species. Heat transport by conduction and radiation is considered under the con-

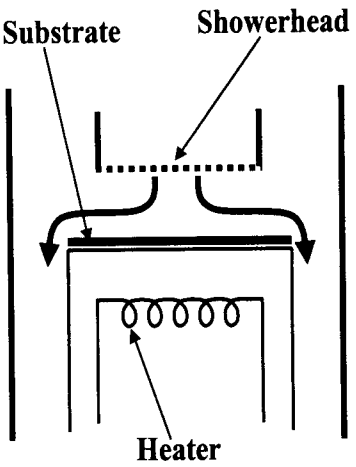

Figure 2.1: Schematic of a vertical axisymmetric stagnation-flow reactor used to grow $YBa_2Cu_3O_{7-\delta}$ high-T_c superconducting thin films on MgO heated substrates by MOCVD. The flow of carrier gas (Nitrogen), Oxygen, and the three precursor species ($Ba(tmhd)_2$, $Cu(tmhd)_2$ and $Y(tmhd)_3$) enters the reactor channel through the showerhead. The gas exhausts axisymmetrically through the annular gap surrounding the substrate (cf. [G1]).

straint of continuity of the temperature, but the bulk heat flux can jump across the interface. Along the interface, we permit for surface species diffusion and heat conduction (both defined in the limit of an infinitely thin surface as tangential vectorial fields). Finally, we consider only coherent surfaces, i.e., surfaces across which the deformation is continuous but its derivatives with respect to time (material velocity) and position (deformation gradient) can suffer discontinuities.

In section 2.2, we introduce a number of key concepts at the core of the continuum model we propose. Essential to our description of the problem is the treatment of the flowing gas mixture as a single phase (an approach which is consistent with the fact that it is a *miscible* mixture). In each phase, we view the diffusion of a given chemical species as the motion of those particles belonging to the species in question *relative* to the motion of the mixture as a *whole*. We begin by introducing, in the current configuration, the species mass density and velocity spatial fields. We then define a mass-averaged (convective) velocity field and use it to introduce a reference configuration in the material space (subsection 2.2.1). Next, we use the Eulerian framework once more to introduce the Cauchy stress tensor (section 2.2.2). We can then define its Lagrangian counterpart, the Piola-Kirchhoff stress, in the reference configuration introduced above. Finally, we adopt a Gibbsian view of the interface (or surface) separating the growing thin solid phase from the 'mother' gas phase. That

is, we view the surface as a separate phase endowed with mass and volume. Hence the requirement that the fundamental principles (i.e., the conservation of mass and other balance laws) along the surface be satisfied. However, we assert that the thickness of the surface is much smaller than any of the other characteristic dimensions of the physical system at hand (e.g., the height of the reactor channel or the typical thickness of the thin film). Consequently, when formulating the balance laws at a macroscopic scale, we treat the surface as a smoothly evolving two-dimensional manifold (subsection 2.2.3).

In section 2.3, we introduce a number of preliminary results and mathematical identities that are indispensable for the formulation of the equations governing the growth process.

In section 2.4, we formulate the various equations resulting from the requirement that the fundamental principles of mechanics and thermodynamics be satisfied. More specifically, in each of the three phases (gas, surface and bulk), the balances of mass for the various chemical species present, the conservation of the linear and angular momenta, the balance of configurational forces, the balance of energy and the entropy inequality are expected to be satisfied. We note here that, given a material surface, there exist two physical mechanisms by which the area of the surface can be changed: one is by deformation (think of the stretching of an elastic membrane), and the other is by accretion, that is, by addition (or deletion) of material particles to the surface of interest. The former mechanism maintains the mass of the surface intact, but its properties (such as the density of particles per unit area or the state of strain of the surface) can be greatly affected. The latter mechanism modifies the total mass of the surface, but its local characteristics remain unaffected. Following Gurtin (e.g., cf. [G3]), we view the standard forces as accounting for the first (deformational) mechanism, while the configurational forces are associated with the second (accretive) mechanism. The existence of two separate force balances (the standard balance of forces or conservation of linear momentum and the additional balance of configurational forces) is then an adequate way of accounting for those two distinct mechanisms separately.

In section 2.5, we make constitutive assumptions on the behavior of the various phases. The gas mixture behaves like a multicomponent fluid which is assumed, in addition, to be viscous and Newtonian. The solid phase behaves like a multicomponent elastic material, while the driving force at the surface is identified and a kinetic relation linking it to the growth velocity is proposed. Of particular relevance to CVD processes is the Soret effect, i.e., the dependence of the species diffusion on the temperature gradient, and this is accounted for in our constitutive formulation. That the Soret effect should not be neglected in our setting can easily be seen from the fact that the variation in temperature between the inlet and the substrate is of the order of a few hundred degrees Celsius. Also, if the temperature along the interface is not uniform, it is conceivable that the surface Soret effect would lead to phase segregation and the formation of unwanted secondary phases such as BaO- or CuO-islands with disastrous consequences on the superconducting properties of the thin film (cf. [W]).

In section 2.6, we list all the evolution equations, thus providing the reader with a condensed formulation of the general free-boundary problem. Here, we make the additional assumptions that the gas mixture behaves like a multicomponent *ideal* gas and that the thin film is *linearly* elastic. This is followed, in section 2.7, by a specialization to the case of 'local equilibrium' with a particular emphasis on single-species systems for which we obtain the Mullins-Sekerka type of evolution equations (cf. [MS]). Finally, we conclude, in section 2.8, with a comparaison of our thermomechanical model to the more classical treatment of similar physical systems within the conceptual framework of the theory of mixtures (cf., e.g., [BD] and the references therein).

2.2 Key Concepts

2.2.1 Kinematics

Consider a continuum composed of N species[1], where $N \geq 2$, and let the mass density $\bar{\rho}_k$ and the velocity $\bar{v}_k$ of the k^{th} species be given as functions of position (in the current configuration) and time:

$$\bar{\rho}_k = \bar{\rho}_k(y,t) \quad \text{and} \quad \bar{v}_k = \bar{v}_k(y,t), \qquad \forall\ k = 1, \ldots, N. \tag{2.1}$$

We define the total mass density as the sum (over all species present) of the species densities and a mass-averaged (convective) velocity as follows:

$$\bar{\rho}(y,t) \stackrel{def}{=} \sum_{k=1}^{N} \bar{\rho}_k(y,t), \tag{2.2}$$

$$\bar{\rho}(y,t)v(y,t) \stackrel{def}{=} \sum_{k=1}^{N} \bar{\rho}_k(y,t)\bar{v}_k(y,t). \tag{2.3}$$

We also define the (spatial) diffusive mass fluxes associated with the various chemical species present: $\forall\ k = 1, \ldots, N$,

$$\bar{h}_k \stackrel{def}{=} \bar{\rho}_k(\bar{v}_k - \bar{v}); \tag{2.4}$$

that is, the diffusive motion of the k^{th} species is a motion relative to the (convective) motion of the mixture as a whole. From the definitions (2.4), (2.2) and (2.3), it follows that the total diffusive mass flux is identically null:

$$\bar{h} \stackrel{def}{=} \sum_{k=1}^{N} \bar{h}_k \ = \ 0. \tag{2.5}$$

We are interested in chemically reacting mixtures such as can be found in chemical vapor deposition processes. Hence, we introduce the notion of mass production due

[1] We use the terms constituent and chemical species interchangeably.

to chemical reactions: let $\bar{R}_k = \bar{R}_k(y,t)$ be the mass production rate of the k^{th} species due to the creation or destruction of k-particles by all the chemical reactions involving it. In addition, we postulate that there is no net production of mass due to chemical reactions, i.e.,

$$\bar{R} \stackrel{def}{=} \sum_{k=1}^{N} \bar{R}_k = 0. \tag{2.6}$$

We now use the mass-average spatial velocity field $\bar{v}$ introduced above to define a reference configuration. Our goal is to find a time-dependent mapping $y(x,t)$ from the material space into the current configuration Ω_t (a time-dependent region in the physical space) such that:

$$\frac{\partial y}{\partial t}(x,t) = \bar{v}(y(x,t),t), \qquad \text{and} \tag{2.7}$$

$$y(x,0) = y_0(x). \tag{2.8}$$

In what follows, fix an arbitrary x in the material space and suppress it from the notation. Consequently, for this fixed x, the equations (2.7)-(2.8) may be written as:

$$y'(t) = \bar{v}(y(t),t), \qquad \text{and}$$

$$y(0) = y_0.$$

The following theorem guarantees the local existence of a solution y to these equations:

Theorem. If $\bar{v}(y,t)$ satisfies the Lipschitz condition for y in some domain $\mathcal{D}$ in $\mathbb{R} \times \mathbb{R}^+$, then there exist $h \in \mathbb{R}^+$ and an exact solution $y = y(t)$ of the equation $y' = \bar{v}(y,t)$ for $|t| \leq h$, such that $y(0) = y_0$ (see, for example, Hurewicz [H2]).

It can also be shown that such a solution is unique. We repeat this for each material point x, thus defining the mapping $y(x,t)$. Now, we can also show that if the function $y_0(x)$ is smooth in x and with $\det \nabla y_0$ positive, then the function $y(x,t)$ is also smooth in x with $\det \nabla y$ positive locally in time. In addition, let us assume that the mapping $x \mapsto y$ is invertible for small times. We can then use the mapping

y^{-1} to define the reference configuration.

We have thus implicitly defined a *single* reference configuration in the material space whose image by y, at an arbitrary instant in time t, is the observable current configuration in the physical space at that time.

In this reference configuration, we can now define the species densities, partial velocities, diffusive fluxes and production rates as the Lagrangian (i.e., material) counterparts of the Eulerian (i.e., spatial) fields introduced above: $\forall\ k = 1, \ldots, N$,

$$\begin{aligned} \rho_k(x,t) &= J(x,t)\bar{\rho}_k(y(x,t),t), \\ v_k(x,t) &= \bar{v}_k(y(x,t),t), \\ h_k(x,t) &= J(x,t)F^{-T}(x,t)\bar{h}_k(y(x,t),t), \qquad \text{and} \\ R_k(x,t) &= J(x,t)\bar{R}_k(y(x,t),t), \end{aligned}$$

where $F(x,t) \stackrel{def}{=} \nabla_x y(x,t)$ and $J(x,t) \stackrel{def}{=} \det F(x,t)$. Making use of (2.5) and (2.6), it can be seen that:

$$\begin{aligned} h &\stackrel{def}{=} \sum_{k=1}^{N} h_k = 0, \qquad \text{and} \\ R &\stackrel{def}{=} \sum_{k=1}^{N} R_k = 0. \end{aligned}$$

We note here that the introduction of the mass averaged velocity and the reference configuration has many advantages in our treatment as it will enable us to make four key assumptions about the species velocity fields, namely equations (2.40), (2.56), (2.57) and (2.83), all of which will be instrumental in the formulation of the governing equations.

2.2.2 Deformational stresses

We begin by postulating that the contact forces exerted by one part of the body on another across the surface S_t separating them in the current configuration (at time

t) can be written as

$$\int_{S_t} \mathbf{t}(y,t;n_y)da_y, \tag{2.9}$$

where $\mathbf{t}(y,t;n_y)$ is the traction per unit current area and n_y is the unit normal to S_t at y. It is important to note that this definition of the total traction is independent of the chemical nature of the continuum at hand. That is, the total traction (2.9) is caused by the interactions between the particles of *all* species lying on both sides of the surface. Then, following the usual arguments (see for example Gurtin [G2]), we deduce the existence of the Cauchy stress tensor T such that

$$\mathbf{t}(y,t;n_y) = T(y,t)n_y.$$

We now recall the deformation mapping $y(x,t)$ defined earlier, and use it to introduce the material description of the Cauchy stress

$$\hat{T}(x,t) \stackrel{def}{=} T(y(x,t),t),$$

and, consequently, the Piola-Kirchoff (or nominal) stress tensor defined as

$$S \stackrel{def}{=} J\hat{T}F^{-T}.$$

As usual then, if S is the pre-image of S_t in the reference configuration, it is easy to verify that

$$\int_{S_t} Tn_y \; da_y \;=\; \int_S Sn_x \; da_x.$$

2.2.3 The surface phase

We consider a physical system constituted of three phases (each containing multiple chemical species): the gas or fluid phase, the solid or bulk phase and the surface phase. Following Gibbs [G], we treat the surface as a separate phase, which can be

viewed as a 'layer' of material of finite thickness. Because it is a separate phase, the surface is endowed with a set of thermodynamic variables that account for its structure. Of particular relevance are the mass densities of chemical species present in the interfacial phase. Being three-dimensional, the surface phase has two interfaces, one with the vapor and the other with the bulk. This way of conceiving the surface will be central when we study the balance of mass of the various chemical species present at the surface. More specifically, we will postulate three separate mass balances: one holding between the vapor and the surface phases (2.27), one within the surface phase (2.25) and third between the bulk and the surface phases (2.28).

We will assume that the thickness of this three-dimensional phase is much smaller than any other characteristic length of the system in question such as the height of the thin film (typically, the surface phase is a few monolayers high, i.e., of the order of Angströms, while the growing film's height is of the order of microns). Consequently, even though it is a three-dimensional phase, the surface can be reasonably modeled, in the setting of macroscopic continuum mechanics, as a two-dimensional smoothly evolving surface. Put differently, we treat the surface as a phase endowed with mass and structure but of negligible volume. We do so by introducing a parameter τ (of dimension length) such that, as the surface becomes infinitesimally thin, $\tau \longrightarrow 0$.

More specifically, consider a closed region in the material space (the reference configuration) and divide it into three time-dependent regions: $\Omega_g(t)$, $\Omega_s(t)$, and $\Omega_f(t)$, the gas, surface and film phases (respectively). This dependence on time is merely a way of accounting for the fact that the solid phase is growing at the expense of the gaseous one, via the motion of the interfacial phase in the reference configuration. The following limits hold:

$$\begin{aligned} \forall\ \hat{f} : \Omega_s(t) \times [0,\infty) \to \mathbb{R}^3, \quad \exists\ \tilde{f} : S(t) \times [0,\infty) \to \mathbb{R}^3 \text{ s.t.} \\ \frac{1}{\tau}\int_{\Omega_s(t)} \hat{f}\ dv \xrightarrow{\tau\to 0} \int_{S(t)} \tilde{f}\ da, \\ \forall\ \hat{g} : \Omega_s(t) \times [0,\infty) \to \mathbb{R}, \quad \exists\ \tilde{g}\ : S(t) \times [0,\infty) \to \mathbb{R} \text{ s.t.} \\ \frac{1}{\tau}\int_{\Omega_s(t)} \hat{g}\ \dot{y}\ dv \xrightarrow{\tau\to 0} \int_{S(t)} \tilde{g}\ \langle \dot{y} \rangle\ da, \end{aligned}$$

where $S(t)$ is the two-dimensional manifold representing the limit of $\Omega_s(t) \subset \mathbb{R}^3$ as $\tau \to 0$, and

$$\begin{aligned} \langle \dot{y} \rangle &\stackrel{def}{=} \frac{1}{2}(\dot{y}^+ + \dot{y}^-), \text{ with} \\ \dot{y}^+ &\stackrel{def}{=} \lim_{x \in \Omega_g(t) \to x \in S(t)} \dot{y}(x,t), \quad \text{and} \\ \dot{y}^- &\stackrel{def}{=} \lim_{x \in \Omega_f(t) \to x \in S(t)} \dot{y}(x,t). \end{aligned}$$

Now define $f = \tau \tilde{f}$ and $g = \tau \tilde{g}$. It follows that the previous limits can be rewritten as:

$$\begin{aligned} \int_{\Omega_s(t)} \hat{f} \, dv &\stackrel{\tau \to 0}{\longrightarrow} \int_{S(t)} f \, da, \qquad \text{and} \\ \int_{\Omega_s(t)} \hat{g} \, \dot{y} \, dv &\stackrel{\tau \to 0}{\longrightarrow} \int_{S(t)} g \, \langle \dot{y} \rangle \, da. \end{aligned}$$

2.3 Preliminaries

2.3.1 Control volume

As mentioned above, we consider a physical system characterized by the presence of N chemical species, where $N \geq 2$. It should be noticed that we do not make the distinction between species present in some phases but absent from others. In such a case, the variables relative to the species of interest are set to zero in the phases from which these species are absent.

Let $P(t)$ denote an arbitrary *evolving* control volume in the reference configuration (cf. Figure 2.2). When $P(t)$ contains material in all three phases, the portions $P_g(t)$, $P_f(t)$, and $S(t)$ that lie, respectively, in the gas phase, the solid phase and the surface phase will be functions of time. The interface is oriented such that its unit normal field n_s points into the vapor. We denote v_s the velocity of the interface and v_n its normal component in the direction of its normal (i.e., $v_n = v_s \cdot n_s$). Also, u denotes the velocity of the boundary of the control volume $\partial P(t) = \partial P_f(t) \cup \partial P_g(t)$ and U represents its normal component in the direction of its normal field n. In what follows,

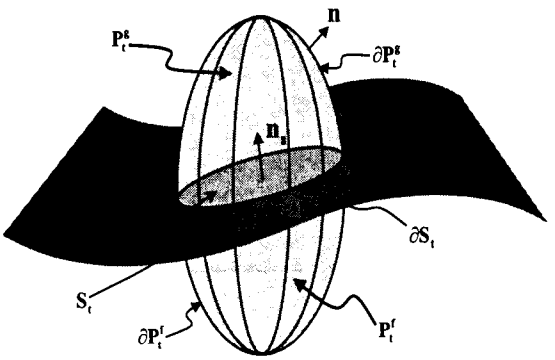

Figure 2.2: The evolving control volume in the reference configuration whose intersections with the flow phase, the bulk, and the moving surface are P_t^g, P_t^f and S_t (respectively). The unit normal to $\partial P_t = \partial P_t^g \cup \partial P_t^f$ is denoted n. The normal to S_t is n_s, while the unit normal and tangent to ∂S_t are ν and t respectively.

we shall rely heavily on the property that *only* the normal components v_n and U of the two velocity fields defined above are intrinsic, i.e., do not depend on the local parametrization of $S(t)$ and $\partial P(t)$ (respectively).

2.3.2 Surface kinematics

In the reference configuration, the evolving surfaces $S(t)$ and $\partial P(t)$ can be parametrized as follows:

$$\begin{aligned} S(t) &\stackrel{def}{=} \{x = \tilde{x}(\alpha_1, \alpha_2, t) \parallel (\alpha_1, \alpha_2) \in \mathcal{D} \subset \mathbb{R}^2, t \in \mathbb{R}^+\}, \qquad \text{and} \\ \partial P(t) &\stackrel{def}{=} \{x = \hat{x}(\beta_1, \beta_2, t) \parallel (\beta_1, \beta_2) \in \mathcal{D}' \subset \mathbb{R}^2, t \in \mathbb{R}^+\}. \end{aligned}$$

We define the velocities of $S(t)$ and $\partial P(t)$ (respectively) as follows:

$$v_s \stackrel{def}{=} \frac{\partial \tilde{x}}{\partial t} \quad \text{and} \quad u \stackrel{def}{=} \frac{\partial \hat{x}}{\partial t},$$

where $\frac{\partial f}{\partial t}$ denotes the derivative of $f(\gamma, t)$ with respect to t holding γ fixed. If either evolving surface is reparametrized, only the normal component of the surface velocity remains unchanged. This dependence of the tangential velocities on the parametrization will yield important identities when combined with the requirement that the working of the various forces acting on the moving surfaces be independent of the particular parametrization chosen.

Let $\bar{S}(t)$ and $\partial\bar{P}(t)$ denote the images of $S(t)$ and $\partial P(t)$ respectively in the deformed configuration:

$$\bar{S}(t) \;=\; y(S(t),t) \;\text{ and }\; \partial\bar{P}(t) \;=\; y(\partial P(t),t).$$

Consequently, these two surfaces can be parametrized in the current configuration as:

$$\bar{S}(t) = \{y = y(\tilde{x}(\alpha_1,\alpha_2,t),t) \stackrel{def}{=} \tilde{y}(\alpha_1,\alpha_2,t) \parallel \; (\alpha_1,\alpha_2) \in \mathcal{D} \subset \mathbb{R}^2, t \in \mathbb{R}^+\}, \text{ and}$$
$$\partial\bar{P}(t) = \{y = y(\hat{x}(\beta_1,\beta_2,t),t) \stackrel{def}{=} \hat{y}(\beta_1,\beta_2,t) \parallel \; (\beta_1,\beta_2) \in \mathcal{D}' \subset \mathbb{R}^2, t \in \mathbb{R}^+\}.$$

Let $\bar{v}_s$ and $\bar{u}$ be the velocities of $\bar{S}(t)$ and $\partial\bar{P}(t)$ respectively:

$$\bar{v}_s \stackrel{def}{=} \frac{\partial\tilde{y}}{\partial t} \;\text{ and }\; \bar{u} \stackrel{def}{=} \frac{\partial\hat{y}}{\partial t}. \tag{2.10}$$

It can then easily be shown that:

$$\bar{v}_s \;=\; \dot{y}^{\pm} + F^{\pm}v_s \;=\; \langle\dot{y}\rangle + \langle F\rangle v_s, \qquad \text{and} \tag{2.11}$$
$$\bar{u} \;=\; \dot{y} + Fu. \tag{2.12}$$

Also, for a coherent interface, we have the classical Hadamard jump condition at the interface, stated as follows:

$$[[F]] = a \otimes n_s \quad \text{with} \quad a \stackrel{def}{=} [[F]]n_s,$$

which we rewrite as:

$$[[F]](\mathbf{1} - n_s \otimes n_s) = 0,$$

or equivalently:

$$[[F]]\mathbf{P} = 0, \tag{2.13}$$

where $\mathbf{P} \in Lin(\mathbb{R}^3, \mathbb{R}^3)$ is the *projection* tensor, i.e.,

$$\forall\, a \in \mathbb{R}^3,\ Pa \stackrel{def}{=} a - (a \cdot n_s)n_s \in \mathbb{R}^3. \tag{2.14}$$

Finally, the combination of (2.13) and (2.11) yields an additional compatibility condition:

$$[[\dot{y}]] \ = \ -v_n\ [[F]]\ n_s. \tag{2.15}$$

2.3.3 Surface deformational stress

In this subsection we define the superficial Piola-Kirchhoff (or nominal) stress. Consider the time-dependent closed region of the physical space P_t introduced previously, and let P be its codomain in the material space, i.e., the closed region in the reference configuration whose image in the deformed configuration is P_t. Assume now that P is traversed by an evolving surface whose intersection with P we label S_t. We denote by $\bar{S}_t$ the corresponding evolving surface in the current configuration, i.e., $\bar{S}_t \ = \ y(S_t, t)$. We begin by postulating that the contact forces exerted by one part of the deformed surface on an adjacent part can be represented by a traction $\mathbf{t}(y \in \mathcal{C}_t, t; \nu_y)$ along the oriented curve $\mathcal{C}_t$ separating them, where ν_y is the unit normal to the curve. Following Gurtin & Murdoch (cf. [GM]), we deduce the existence of the superficial Cauchy stress tensor, $T^s \in Lin(\bar{n}_s^{\perp}, \mathbb{R}^3)$, such that:

$$\mathbf{t}(y \in \mathcal{C}_t \subset \bar{S}_t, t; \nu_y) \ = \ T^s(y \in \mathcal{C}_t \subset \bar{S}_t, t)\nu_y.$$

Next, by making a change of variables from the current configuration into the reference one, we have the following relation:

$$\int_{\partial \bar{S}_t} T^s \nu_y \ dl_y \ = \ \int_{\partial S_t} j\hat{T}^s \hat{F}^{-T} \nu_x \ dl_x,$$

where $\hat{T}^s$ is the material representation of the Cauchy surface stress:

$$T^s(y \in \bar{S}_t,\ t) = T^s(y(x \in S_t,\ t), t) \stackrel{def}{=} \hat{T}^s(x \in S_t,\ t),$$

and $\hat{F}$ is the restriction of F to the surface, i.e.,

$$\hat{F} \stackrel{def}{=} \bar{P}\langle F\rangle I,$$

and $j \stackrel{def}{=} \det \hat{F}$. Here, the inclusion tensor *in the reference configuration* is defined as:

$$I \in Lin(n_s^{\perp},\ \mathbb{R}^3) \text{ such that } Ia \stackrel{def}{=} a,\ \forall\ a \in n_s^{\perp},$$

and the projection tensor *in the current configuration* is given by:

$$\bar{P} \in Lin(\mathbb{R}^3,\ \bar{n}_s^{\perp}) \text{ such that } \bar{P}a \stackrel{def}{=} a - (a \cdot \bar{n}_s)\bar{n}_s,\ \forall\ a \in \mathbb{R}^3.$$

Consequently, $\hat{F} \in Lin(n_s^{\perp},\ \bar{n}_s^{\perp})$, and j and $\hat{F}^{-1}$ are defined accordingly.

It follows that:

$$\int_{\partial \bar{S}_t} T^s \nu_y\ dl_y = \int_{\partial S_t} S^s \nu_x\ dl_x,$$

where:

$$S^s \stackrel{def}{=} j\hat{T}^s \hat{F}^{-T}$$

is the superficial Piola-Kirchhoff stress tensor.

2.3.4 Transport theorems

Let φ be any (scalar or vectorial) bulk field and φ^s be any (scalar or vectorial) surface field. We introduce the following terminology:

$$\begin{aligned}
\int_{P(t)} \varphi \, dv &\stackrel{def}{=} \int_{P(t)} \varphi(x,t) \, dv(x), \\
\int_{\partial P(t)} \varphi \, da &\stackrel{def}{=} \int_{\partial P(t)} \varphi(x,t) \, da(x), \\
\int_{S(t)} \varphi^s \, da &\stackrel{def}{=} \int_{S(t)} \varphi^s(\alpha_1,\alpha_2,t) \, da(\alpha_1,\alpha_2), \qquad \text{and} \\
\int_{\partial S(t)} \varphi^s \, ds &\stackrel{def}{=} \int_{\partial S(t)} \varphi^s(\alpha_1,\alpha_2,t) \, ds(\alpha_1,\alpha_2),
\end{aligned}$$

where $\varphi^s(\alpha_1,\alpha_2,t)$ is an arc-length description of φ^s.

A normal arc-length trajectory through a point (α_1,α_2,t_0) of the domain of $\tilde{x}$ is a path $(\bar{\alpha}_1(t),\bar{\alpha}_2(t))$ such that:

$$\mathbf{t}(\bar{\alpha}_1(t),\bar{\alpha}_2(t),t) \cdot \frac{d\tilde{x}}{dt}(\bar{\alpha}_1(t),\bar{\alpha}_2(t),t) \;=\; 0,$$

where $\mathbf{t}$ is any vector tangential to $S(t)$ and

$$\bar{\alpha}_1(t_0) = \alpha_1, \quad \bar{\alpha}_2(t_0) = \alpha_2.$$

We can then define the *normal time derivative* $\overset{\circ}{\varphi}{}^s(s,t)$ as

$$\overset{\circ}{\varphi}{}^s(\alpha_1,\alpha_2,t) \stackrel{def}{=} \frac{d\varphi^s}{dt}(\bar{\alpha}_1(t),\bar{\alpha}_2(t),t).$$

We can now state the bulk and surface transport theorems (respectively):

$$\frac{d}{dt}\int_{P(t)} \varphi \, dv \;=\; \int_{P(t)} \dot{\varphi} \, dv - \int_{S(t)} [[\varphi]] v_n \, da + \int_{\partial P(t)} \varphi U \, da, \tag{2.16}$$

$$\frac{d}{dt}\int_{S(t)} \varphi^s \, dv \;=\; \int_{S(t)} (\overset{\circ}{\varphi}{}^s - \varphi\kappa v_n) \, da + \int_{\partial S(t)} \varphi^s v_s \cdot \nu \, ds, \tag{2.17}$$

where for any scalar, vector or tensor field f that suffers a discontinuity across the

surface $S(t)$, $[[f]] = f^+ - f^-$, with f^+ the limit as f approaches the surface from the vapor phase (the phase towards which n_s points) and f^- the limit as f approaches $S(t)$ from the film phase. κ denotes the mean curvature of the surface, and ν is the in-plane unit normal field (or *binormal*) to $\partial S(t)$.

2.3.5 Bulk and surface divergence theorems

Let a be a vector field and A be a tensor field in the bulk, both of which are discontinuous across the evolving interface, then the following identities hold:

$$\int_{P(t)} \nabla \cdot a \, dv = \int_{\partial P(t)} a \cdot n \, da - \int_{S(t)} [[a]] \cdot n_s \, da, \quad \text{and} \tag{2.18}$$

$$\int_{P(t)} \nabla \cdot A \, dv = \int_{\partial P(t)} A \, n \, da - \int_{S(t)} [[A]] \, n_s \, da. \tag{2.19}$$

Identically, if a^s and A^s are superficial vector and tensor fields, then the following identities are valid:

$$\int_{S(t)} \nabla_s \cdot a \, da = \int_{\partial S(t)} a \cdot \nu \, ds, \quad \text{and} \tag{2.20}$$

$$\int_{S(t)} \nabla_s \cdot A \, da = \int_{\partial S(t)} A\nu \, ds. \tag{2.21}$$

2.4 Balance Laws

2.4.1 The mass balances or species equations

We begin by writing the integral version of the mass balance for the k^{th} species ($1 \leq k \leq N$) as it applies to the evolving control volume defined previously. We postulate that the temporal rate of change of mass of the k-species in the control volume is balanced by the diffusive flux of this species into (or out of) the volume, the chemical reactions that generate or consume particles of the species of interest in the volume and the accretion by the motion of the boundary (see Figure 2.2 for sign

conventions):

$$\begin{aligned}
&\frac{d}{dt}\int_{P_g(t)} \rho_k^g \, dv + \frac{d}{dt}\int_{S(t)} \rho_k^s \, da + \frac{d}{dt}\int_{P_f(t)} \rho_k^f \, dv = \\
&\quad - \int_{\partial P_g(t)} h_k^g \cdot n_g \, da - \int_{\partial S(t)} h_k^s \cdot \nu \, ds - \int_{\partial P_f(t)} h_k^f \cdot n_f \, da \\
&\qquad + \int_{P_g(t)} R_k^g \, dv + \int_{S(t)} R_k^s \, da \\
&\quad + \int_{\partial P_g(t)} \rho_k^g u \cdot n_g \, da + \int_{\partial S(t)} \rho_k^s v_s \cdot \nu \, ds + \int_{\partial P_f(t)} \rho_k^f u \cdot n_f \, da, \qquad (2.22)
\end{aligned}$$

where we have adopted the following terminology: ρ_k^α is the mass density of the k^{th} species present in the phase α, h_k^α is the diffusive mass flux of the k^{th} species across the part of the boundary of the control volume that lies within the phase α, and R_k^α is the net mass production of species k by all the chemical reactions involving the k^{th} species that take place inside of the phase α.

Consider the left-hand side of (2.22). The first term represents the temporal change in the mass of species k present in the gas phase. The second and third terms account for the temporal changes in mass of the same species present in the interfacial and solid phases respectively. Now consider the right-hand side of the equation. The first three integrals account for the mass exchanged between the control volume and its exterior via diffusion across its boundaries. Notice that h_k^s, the interfacial diffusive mass flux associated with the k-particles along the surface, is tangential to the surface by definition. The next two terms represent the net mass production of species k by all the chemical reactions involving the species in question that take place in the vapor and at the surface respectively. Note that we have assumed that there are no chemical reactions taking place in the bulk of the thin film. Such would not be the case if we allow for the chemical formation of secondary phases (precipitates) in the bulk, but such mechanisms are confined, in our model, to the surface phase where chemical phase segregation is often observed experimentally (cf. [W]). The remaining three integrals account for the exchange of species k between the control volume and its environment due solely to the motion of its boundaries.

Making use of the transport and divergence theorems stated above, and then localizing, we obtain the following local versions of the species equations:

$$\dot{\rho}_k^g + \nabla \cdot h_k^g - R_k^g = 0 \quad \text{in the gas phase,} \tag{2.23}$$

$$\dot{\rho}_k^f + \nabla \cdot h_k^f = 0 \quad \text{in the film,} \tag{2.24}$$

$$\overset{\circ}{\rho}_k^s - ([[\rho_k]] + \rho_k^s \kappa) v_s + [[h_k]] \cdot n_s + \nabla_s \cdot h_k^s - R_k^s = 0 \quad \text{at the surface,} \tag{2.25}$$

where $\nabla \cdot (\ )$ and $\nabla_s \cdot (\ )$ are the bulk and surface divergences respectively in the reference configuration.

In order for our formulation to be complete, we now write additional mass balance laws for the k^{th} species at the two interfaces of the surface phase as discussed earlier (subsection 2.2.3). Consider first the interface separating the gas from the surface phase. We write the integral version of the mass balance for species k as it holds in the evolving control volume $P_g(t)$ whose boundary is $\partial P_g(t) \cup S(t)$:

$$\frac{d}{dt}\int_{P_g(t)} \rho_k^g \, dv - \int_{\partial P_g(t)} \rho_k^g \, u \cdot n_g \, da = - \int_{\partial P_g(t)} h_k^g \cdot n_g \, da + \int_{S(t)} (j_k^g + \frac{1}{\tau}\rho_k^s v_n) \, da + \int_{P_g(t)} R_k^g \, dv, \tag{2.26}$$

where j_k^g is an interfacial (scalar) field accounting for the mass flow of species k out of the surface and into the vapor (and vice-versa). Shrinking $P_g(t)$ to its interface with the surface phase, which is mathematically identical to the surface itself, we obtain:

$$-\rho_k^g v_n = -h_k^g \cdot n_s + j_k^g + \frac{1}{\tau}\rho_k^s v_n. \tag{2.27}$$

An identical procedure applied to $P_f(t)$ yields the following localized version of the mass balance for species k at the interface separating the bulk of the film from the surface phase:

$$\rho_k^f v_n = h_k^f \cdot n_s + j_k^f - \frac{1}{\tau}\rho_k^s v_n. \tag{2.28}$$

Finally, from (2.27) and (2.28), we deduce the following relations which will be useful at later stages:

$$[[h_k]] \cdot n_s = [[\rho_k]] v_n + 2\langle j_k \rangle, \qquad \text{and} \tag{2.29}$$

$$\langle h_k \rangle \cdot n_s = \frac{1}{2}[[j_k]] + (\langle \rho_k \rangle + \frac{1}{\tau}\rho_k^s) v_n. \tag{2.30}$$

In each phase, the total mass density is defined as the sum of the partial densities over all the species present in the phase of interest: $\rho^{g,f,s} \stackrel{def}{=} \sum_{k=1}^{N} \rho_k^{g,f,s}$. It follows that we can choose as our set of independent fundamental variables (i.e., those variables describing the chemical composition of a given phase) either $\{\rho_k^{g,f,s}\}_{k=1}^{N}$ or $\{\rho^{g,f,s}, \{\rho_k^{g,f,s}\}_{k=1}^{N-1}\}$. It is common in the literature on the modeling of the gas phase behavior during CVD to adopt the latter representation (e.g., cf. Kleijn [K] and Coltrin and Kee [CK]). We thus provide localized versions of the global mass balance by summing the (already derived) localized versions of the species equations, but it is important in doing so to keep in mind that the following relations hold:

$$h^{g,f} \stackrel{def}{=} \sum_{k=1}^{N} h_k^{g,f} = 0, \quad h^s \stackrel{def}{=} \sum_{k=1}^{N} h_k^s = 0, \quad R^{g,s} \stackrel{def}{=} \sum_{k=1}^{N} R_k^{g,s} = 0.$$

It can then easily be shown that:

$$\dot{\rho}^g = 0 \qquad \text{in the gas phase,} \tag{2.31}$$

$$\dot{\rho}^f = 0 \qquad \text{in the bulk of the thin film,} \tag{2.32}$$

$$\overset{\circ}{\rho}{}^s - ([[\rho]] + \rho^s \kappa) v_s \cdot n_s = 0 \qquad \text{at the surface,} \tag{2.33}$$

$$(\rho^g + \frac{1}{\tau}\rho^s) v_s \cdot n_s + j^g = 0 \qquad \text{at the vapor-surface interface,} \tag{2.34}$$

$$(\rho^f + \frac{1}{\tau}\rho^s) v_s \cdot n_s - j^f = 0 \qquad \text{at the film-surface interface.} \tag{2.35}$$

2.4.2 The balance of deformational forces

We postulate that the deformational contact forces acting on the evolving control volume introduced above are balanced by the body forces:

$$\int_{\partial P_g(t)} S^g n_g \, da + \int_{\partial P_f(t)} S^f n_f \, da + \int_{\partial S(t)} S^s \nu \, dl + \int_{P_{g,f}(t)} (b^{g,f} + b_e^{g,f}) \, dv + \int_{S(t)} b^s \, da = 0, \tag{2.36}$$

where we have decomposed the density of body forces in the gas and bulk phases into a purely inertial component $b^{g,f}$ and an external noninertial component $b_e^{g,f}$. An example of an external noninertial boby force that plays an important role in the setting of *vertical* CVD reactors is gravity. Its omission would lead to an incomplete modeling of the behavior of the fluid flow.

We note that this statement of the balance of deformational forces for a multi-component physical system is approximate and valid only under the assumption

$$\sum_{k=1}^{N} \rho^k v^k \otimes v^k \cong \rho v \otimes v. \tag{2.37}$$

More specifically, let us consider a single-phase mutli-species physical system in the Eulerian setting. The *exact* statement of the balance of forces as it applies to a fixed control volume D in the current configuration is:

$$\frac{\partial}{\partial t}\left(\sum_{k=1}^{N} \int_D \bar{\rho}^k \bar{v}^k \, dv\right) = \int_{\partial D} Tn \, da - \sum_{k=1}^{N} \int_{\partial D} (\bar{\rho}^k \bar{v}^k) \bar{v}^k \cdot n \, da + \sum_{k=1}^{N} \int_D \bar{b}^k \, dv, \tag{2.38}$$

where the linear momentum of the system is defined as the sum of all the the linear momenta associated with the individual species, T is the Cauchy stress tensor and $\bar{b}^k$ is the density (per unit current volume) of body force acting on particles of the k^{th} species. Now, making use of the divergence and localization theorems, we can state

the exact localized version of the momentum equation in the current configuration:

$$\frac{\partial}{\partial t}(\sum_{k=1}^{N} \bar{\rho}^k \bar{v}^k) + \nabla \cdot (\sum_{k=1}^{N} \bar{\rho}^k \bar{v}^k \otimes \bar{v}^k) = \nabla \cdot T + \bar{b}, \tag{2.39}$$

where

$$\bar{b} \stackrel{def}{=} \sum_{k=1}^{N} \bar{b}^k$$

and $\nabla \cdot (\ )$ is the spatial divergence. If we assume that the Eulerian counterpart of (2.37) holds, i.e., if

$$\sum_{k=1}^{N} \bar{\rho}^k \bar{v}^k \otimes \bar{v}^k \cong \bar{\rho}\bar{v} \otimes \bar{v}, \tag{2.40}$$

then we can *approximate* the localized momentum equation as:

$$\frac{\partial}{\partial t}(\bar{\rho}\bar{v}) + \nabla \cdot (\bar{\rho}\bar{v} \otimes \bar{v}) = \nabla \cdot T + \bar{b}. \tag{2.41}$$

The integral formulation of the force balance (2.36) is therefore to be viewed as a Lagrangian *approximation* of the exact formulation of the linear momentum equation as it applies to a multiphase multicomponent physical system when approximation (2.37) holds.

Now back to (2.36). Applying the divergence theorems and then localizing yields the following pointwise equations:

$$\nabla \cdot S^g + b^g + b_e^g = 0 \qquad \text{in the gas phase,} \tag{2.42}$$

$$\nabla \cdot S^f + b^f + b_e^f = 0 \qquad \text{in the bulk of the film,} \tag{2.43}$$

$$[[S]]n_s + \nabla_s \cdot S^s + b^s = 0 \qquad \text{at the surface.} \tag{2.44}$$

In addition, following Gurtin and Podio-Guidugli [GP], we postulate that for an

evolving control volume:

$$\begin{aligned}
&\int_{P_g(t)} b^g \, dv + \int_{P_f(t)} b^f \, dv + \int_{S(t)} b^s \, da \\
&\quad - \int_{\partial P_g(t)} (\rho^g \dot{y}) u \cdot n \, da - \int_{\partial P_f(t)} (\rho^f \dot{y}) u \cdot n \, da - \int_{\partial S_t} (\rho^s \langle \dot{y} \rangle) v_s \cdot \nu \, dl \\
&\quad = -\frac{d}{dt} \int_{P_g(t)} \rho^g \dot{y} \, dv - \frac{d}{dt} \int_{P_f(t)} \rho^f \dot{y} \, dv - \frac{d}{dt} \int_{S_t} \rho^s \langle \dot{y} \rangle \, da. \qquad (2.45)
\end{aligned}$$

Away from the interface, the use of the bulk transport and localization theorems, as well as the recourse to the total mass balances in the bulk phases (2.31) and (2.32) yield the following identities:

$$b^g = -\rho^g \ddot{y} \qquad \text{in the gas phase,} \qquad (2.46)$$

$$b^f = -\rho^f \ddot{y} \qquad \text{in the bulk of the film.} \qquad (2.47)$$

Along the surface, the surface transport and localization theorems yield:

$$b^s = ([[\rho \dot{y}]] + \kappa \rho^s \langle \dot{y} \rangle) v_s \cdot n_s - (\rho^s \langle \dot{y} \rangle)^{\circ}. \qquad (2.48)$$

Now, making use of the identity

$$[[fg]] = [[f]]\langle g \rangle + \langle f \rangle [[g]] \qquad (2.49)$$

and the compatibility condition (2.15) as well as the surface total mass balance (2.33), we obtain the following relation:

$$b^s = -\rho^s \langle \dot{y} \rangle^{\circ} - v_n^2 \langle \rho \rangle [[F]] n_s. \qquad (2.50)$$

2.4.3 The balance of configurational forces

As mentioned above, the surface separating the vapor from the bulk of the film can be viewed as a phase boundary. In situations of growth of thin films by vapor deposition (whether physical or chemical), the atoms deposited on the top mono-

layer are ultimately incorporated into the bulk phase, thus causing the motion of the surface (during the chemical vapor deposition of compound films, the adatoms react chemically to form the compound in question). That is, as soon as the compound is formed, it is identified as being part of the bulk, thus forcing the 'redefinition' of the bulk-vapor interface so as to incorporate the newly formed compound into the bulk. Consequently, the motion of the surface is relative to the particles of the system and it results in changes in the reference configuration (i.e., changes that would occur even in the absence of any deformation of the physical system in question).

A convenient framework for studying changes in the reference configuration is through the introduction of *configurational forces* following Gurtin [G3]. These forces may be viewed as the work-conjugate 'generalized' forces associated with the kinematic variables that describe the changes which take place in the reference configuration. The classical body forces and stresses are deformational and are work-conjugate to the kinematic variables accounting for changes in the current (i.e., deformed) configuration. The postulate that there are two distinct balance laws, one balancing configurational forces and the other balancing deformational forces, can then be viewed as reflecting the fact that these two sets of forces act in two distinct configurations (the reference and deformed ones respectively).

Following Gurtin we postulate the existence of two types of configuration forces. The first is a contact force and hence may be expressed in terms of a stress tensor (C^g, C^s, C^f in the gas, surface and film respectively), while the second is a body force (g^g, g^s, g^f in the gas, surface and film respectively). We postulate that the configurational contact forces acting on any part of the body are balanced by the configurational body force:

$$\int_{\partial P_g(t)} C^g n_g \, da + \int_{\partial P_f(t)} C^f n_f \, da + \int_{\partial S(t)} C^s \nu \, ds + \int_{P_g(t)} g^g \, dv + \int_{P_f(t)} g^f \, dv + \int_{S(t)} g^s \, da = 0. \tag{2.51}$$

Using the bulk and surface divergence theorems and then localizing, we obtain the

following pointwise equations:

$$\nabla \cdot C^g + g^g = 0 \qquad \text{in the gas phase,} \tag{2.52}$$

$$\nabla \cdot C^f + g^f = 0 \qquad \text{in the bulk of the film,} \tag{2.53}$$

$$[[\mathbf{C}]]n_s + \nabla_s \cdot C^s + g^s = 0 \qquad \text{at the surface.} \tag{2.54}$$

Moreover, we decompose g^g, g^f, and g^s into an internal and an external component each:

$$g^{g,f,s} \stackrel{def}{=} g^{g,f,s}_{ext} + g^{g,f,s}_{int}.$$

2.4.4 The energy balance

We begin by postulating that the rate of change of the internal energy of the evolving control volume introduced above $P(t) \cup S(t)$, where $P(t) = P_g(t) \cup P_f(t)$ is balanced by the rate at which energy is supplied to the control volume:

$$\frac{d}{dt}\int_{P(t)} \epsilon \, dv + \frac{d}{dt}\int_{S(t)} \epsilon^s \, da = W(P(t)) + W(S(t)), \tag{2.55}$$

where $W(P(t)) + W(S(t))$ is the rate at which energy is supplied to the body (the splitting of the energy supply rate into the rate of energy supplied to the bulk of the control volume $P(t)$ and that supplied to the surface $S(t)$ will turn out to be useful at later stages in simplifying the formulation of the problem which is already quite complex).

In addition to (2.40), we make the following approximations

$$\sum_{k=1}^{N} \bar{b}_k \cdot \bar{v}_k \cong \bar{b} \cdot \bar{v}, \qquad \text{and} \tag{2.56}$$

$$\sum_{k=1}^{N} (\bar{\rho}_k \bar{v}_k \otimes \bar{v}_k)\bar{v}_k \cong (\bar{\rho}\bar{v} \otimes \bar{v})\bar{v} \tag{2.57}$$

in order to explicitly write the expressions corresponding to the rates of energy sup-

plies $W(P(t))$ and $W(S(t))$.

More specifically, consider for now a single-phase multi-species mixture occupying a fixed region in space D. The balance of energy in this region is given by

$$\frac{\partial}{\partial t}\int_D (\bar{\rho}\bar{\epsilon} + \frac{1}{2}\sum_{k=1}^{N} \bar{\rho}_k \bar{v}_k \cdot \bar{v}_k)\, dv = \int_{\partial D} Tn \cdot \bar{v}\, da + \sum_{k=1}^{N} \int_D \bar{b}_k \cdot \bar{v}_k\, dv - \int_{\partial D} \bar{q} \cdot n\, da + \int_D \bar{Q}\, dv - \sum_{k=1}^{N} \int_{\partial D} (\bar{\rho}_k \bar{\mu}_k + \frac{1}{2}\bar{\rho}_k \bar{v}_k \cdot \bar{v}_k)\bar{v}_k \cdot n\, da. \tag{2.58}$$

The first term in the integrand on the LHS of the above equality represents the internal energy of the physical system which occupies the fixed region D at the time t, with the mass-averaged internal energy density defined as

$$\bar{\rho}\bar{\epsilon} \overset{def}{=} \sum_{i=1}^{N} \bar{\rho}_i \bar{\mu}_i + \bar{\epsilon}_{\text{mix}}, \tag{2.59}$$

wherein $\bar{\epsilon}_{\text{mix}}$ is the energy density of mixing (per unit current volume), i.e., the excess energy resulting from the mixing process and the ensuing interactions between the various species. The second term of the integrand on the LHS is the exact kinetic energy of the multi-species system. On the RHS of (2.58), the first integral is the working of the deformational stress, the second term is the sum of the workings of the various non-inertial body forces associated with the species present, the third integral represents heat conduction, the fourth accounts for heat radiation, and the last integral accounts for the supply of energy (into or out of D) due to the motion of the various species across its boundary ∂D.

Using the trace of (2.40), (2.56) and (2.57), we can rewrite the above equation as:

$$\frac{\partial}{\partial t}\int_D (\bar{\rho}\bar{\epsilon} + \frac{1}{2}\bar{\rho}\bar{v} \cdot \bar{v})\, dv = \int_{\partial D} Tn \cdot \bar{v}\, da + \int_D \bar{b} \cdot \bar{v}\, dv - \int_{\partial D} \bar{q} \cdot n\, da + \int_D \bar{Q}\, dv - \sum_{k=1}^{N} \int_{\partial D} (\bar{\rho}_k \bar{\mu}_k \bar{v}_k \cdot n + \frac{1}{2}\bar{\rho}(\bar{v} \cdot \bar{v})\bar{v} \cdot n)\, da. \tag{2.60}$$

For later use, we state the localized Eulerian version of the energy balance as it applies to a single-phase multi-species physical system. Making use of the (Eulerian versions of the) divergence and localization theorems, the definition of the species diffusive mass fluxes (2.4), the species mass balances (2.23) and (2.24), as well as the momentum equation (2.41), we obtain the following equation:

$$\bar{\rho}\frac{d\bar{\epsilon}}{dt} - \sum_{k=1}^{N} \bar{\mu}_k \frac{d\bar{\rho}_k}{dt} + \sum_{k=1}^{N} \bar{h}_k \cdot \nabla \bar{\mu}_k + \sum_{k=1}^{N} \bar{\mu}_k \bar{R}_k$$
$$+\nabla \cdot \bar{q} + \bar{Q} - T \cdot D - \left(\sum_{k=1}^{N} \bar{\rho}_k \bar{\mu}_k \right) \nabla \cdot \bar{v} = 0, \tag{2.61}$$

where

$$\frac{d}{dt}(\,) \stackrel{def}{=} \frac{\partial}{\partial t}(\,) + v \cdot \nabla(\,).$$

It should be noted here that in deriving (2.61) we have neglected the mixing energy. This is a reasonable approximation when the mixture of interest is dilute (a situation often encountered in CVD processes). In the limit of a multicomponent ideal gas, a case of interest as it approximates properly many CVD gas mixtures, the mixing energy is identically zero.

Let us now consider an evolving control volume in the reference configuration $P(t)$ whose image coincides with the region D in the current configuration at time t. We can use (2.60) to postulate the following energy balance for $P(t)$:

$$\frac{d}{dt}\int_{P(t)} \epsilon \, dv = \int_{\partial P(t)} (Sn \cdot \bar{u} + Cn \cdot u) \;\; da + \int_{P(t)} (b + b_e) \cdot \dot{y} \, dv$$
$$- \int_{\partial P(t)} q \cdot n \, da + \int_{\partial P(t)} Qu \cdot n \, da + \int_{P(t)} \mathcal{Q} \, dv$$
$$+ \sum_{k=1}^{N} \{ \int_{\partial P(t)} \mu_k \rho_k u \cdot n \, da - \int_{\partial P(t)} \mu_k h_k \cdot n \, da \}, \tag{2.62}$$

where we have added the working of the configurational stress tensor as it accounts for the incorporation or removal of material into the evolving control volume via the

motion of its boundary $\partial P(t)$ in the reference configuration. The additional terms

$$\int_{\partial P(t)} Qu \cdot n \; da \quad \text{and} \quad \sum_{k=1}^{N} \int_{\partial P(t)} \mu_k \rho_k u \cdot n \; da$$

come from the fact that the control volume considered is an evolving one in the reference configuration.

Now let us return to a multi-phase, multi-species body and the postulate (2.55). Generalizing the argument above, we write:

$$\begin{aligned} W(P(t)) \stackrel{def}{=} & \int_{\partial P(t)} (Sn \cdot \bar{u} + Cn \cdot u) \; da + \int_{P(t)} (b + b_e) \cdot \dot{y} \; dv \\ & - \int_{\partial P(t)} q \cdot n \; da + \int_{\partial P(t)} Qu \cdot n \; da + \int_{P(t)} \mathcal{Q} \; dv \\ & + \sum_{k=1}^{N} \{ \int_{\partial P(t)} \mu_k \rho_k u \cdot n \; da - \int_{\partial P(t)} \mu_k h_k \cdot n \; da \}, \qquad \text{and} \qquad (2.63) \\ W(S(t)) \stackrel{def}{=} & \int_{\partial S(t)} (S^s \nu \cdot \bar{v}_s + C^s \nu \cdot v_s) \; ds + \int_{S(t)} (g^s_{ext} \cdot v_s + b^s \cdot \overline{v}_s) \; da \\ & - \int_{\partial S(t)} q^s \cdot \nu \; ds + \int_{\partial S(t)} Q^s v_s \cdot \nu \; ds + \int_{S(t)} \mathcal{Q}^s \; da \\ & + \sum_{k=1}^{N} \{ \int_{\partial S(t)} \mu^s_k \rho^s_k v_s \cdot \nu \; ds - \int_{\partial S(t)} \mu^s_k h^s_k \cdot \nu \; ds \}. \qquad (2.64) \end{aligned}$$

Consider the equality (2.63). The first integral on the RHS of the equality represents the mechanical workings of the bulk deformational and configurational stresses on the evolving boundary of the control volume $\partial P(t) = \partial P_g(t) \cup \partial P_f(t)$. The velocity conjugate to the Piola-Kirchhoff stress is the velocity of the boundary in the deformed configuration, while the velocity conjuguate to the configurational stress is that of the moving boundary in the reference configuration[2]. The third integral is the standard working of the inertial and noninertial external body forces. Notice that $g^{g,f}_{int}$ perform

[2]The working of the Cauchy stress on the boundary of a moving control volume in space $D(t)$ is typically written as $\int_{\partial D(t)} T n_y \cdot \bar{u} \; da_y$ where $\bar{u}$ is the velocity of the boundary and n_y its unit outer normal. It is then just a matter of changing variables between the current and the reference configurations to obtain the working of the nominal stress. On the other hand, the configurational stress acting on a moving surface in the material space, it seems only natural to take the velocity of the surface in question as its work-conjuguate variable.

no work as they are internal to the control volume, while $g_{ext}^{g,f}$ perform no work because material points in the reference configuration are stationary. The fourth integral accounts for the exchange of heat between $P(t)$ and its environment by conduction, while the fifth term represents the amounts of heat exchanged between $P(t)$ and its exterior as its boundary $\partial P(t)$ evolves. The sixth integral represents the external radiative supply of heat to the control volume.

Finally, for each k $(1 \leq k \leq N)$, μ_k^α represents the amount of energy (per unit mass) associated with the k^{th} species present in the α phase ($\alpha = g,\ f$). Consequently, $\mu_k^\alpha h_k^\alpha \cdot n_\alpha$ is the amount of energy transported by diffusion of particles of the k^{th} species (per unit area and unit time) and $\mu_k^\alpha \rho_k^\alpha u \cdot n_\alpha$ is the amount of energy associated with the incorporation (or detachment) of particles of species k into $P_\alpha(t)$ solely due to the motion of its boundary (per unit area and unit time). Notice that the rate of production of energy associated with the gas-phase chemical reactions involving the k^{th} species (either as a reactant or a product) does not appear in $W(P(t))$ as it is *internal* to the control volume.

Now consider (2.64). The first integral accounts for the working of the superficial deformational and configurational stresses in an analogous fashion to their bulk counterparts: the first component represents the standard working done on the evolving surface, while the second accounts for the working associated with the supply of mass to the surface via addition or removal of particles. The second integral accounts for the working of the surperficial inertial and noninertial body forces. The third integral represents the conductive heat supply to the surface, where q^s is a tangential vector field by definition, while the fourth integral represents heat supply to the surface solely due to its tangential (or in-plane) motion. The sixth integral accounts for the external supply of heat to the surface by radiation. The last two integrals account for the energy supply to the surface due to the incorporation of particles via the tangential motion of the surface and the surface diffusion of adatoms (by definition a tangential vector field). Finally, it should be remarked that the production rate of energy associated with the heterogeneous chemical reactions[3] is absent from $W(S(t))$

[3]By heterogeneous chemical reactions,we mean those reactions taking place at the surface that

as it represents an *internal* production of energy.

2.4.5 The invariance of the working under reparametrization

First, define the mechanical working on $P(t)$ as follows:

$$W_m(P(t)) \stackrel{def}{=} \int_{\partial P(t)} (Sn \cdot (\dot{y} + Fu) + Cn \cdot u)\ da + \int_{P(t)} (b + b_e) \cdot \dot{y}\ dv,$$

where we have used (2.12). Next, rearrange $W_m(P(t))$ as follows:

$$W_m(P(t)) \stackrel{def}{=} \int_{\partial P(t)} \{(C + F^T S)n \cdot u + Sn \cdot \dot{y}\}\ da + \int_{P(t)} (b + b_e) \cdot \dot{y}\ dv.$$

We now require that the mechanical working be independent of the local parametrization of $\partial P(t)$. But, under reparametrization, the only invariant component of the velocity field u is the normal one. Consequently, if $W_m(P(t))$ is to remain unchanged, the following relation should be satisfied:

$$(C + F^T S)n \cdot m = 0, \quad \forall\ m \text{ such that } m \cdot n = 0.$$

It then follows that:

$$C = \pi I - F^T S, \tag{2.65}$$

where π is a scalar (yet to be determined).

Making use of the bulk divergence theorem (2.18) and the balances of deformational forces (2.42) and (2.43), we can rewrite the bulk mechanical working as

$$W_m(P(t)) \ = \int_{\partial P(t)} \pi u \cdot n\ da + \int_{P(t)} S \cdot \dot{F}\ dv + \int_{S(t)} [[Sn_s \cdot \dot{y}]]\ da. \tag{2.66}$$

involve *only* surface species. As for those chemical reactions involving *both* vapor and surface species, they are already accounted for in the terms j_k^g of the species equations at the gas-surface interface (2.27).

Identically, define the mechanical working on the $S(t)$ as:

$$W_m(S(t)) = W_m^{(1)}(S(t)) + W_m^{(2)}(S(t)),$$

where

$$W_m^{(1)}(S(t)) \stackrel{def}{=} \int_{\partial S(t)} C^s \nu \cdot v_s \, ds + \int_{\partial S(t)} S^s \nu \cdot (\langle \dot{y} \rangle + \langle F \rangle v_s) \, ds,$$

and

$$W_m^{(2)}(S(t)) \stackrel{def}{=} \int_{S(t)} [g_{ext}^s \cdot v_s + b^s \cdot (\langle \dot{y} \rangle + \langle F \rangle v_s)] \, da.$$

We begin by rewriting $W_m^{(1)}(S(t))$ as:

$$W_m^{(1)}(S(t)) = \int_{\partial S(t)} S^s \nu \cdot \langle \dot{y} \rangle \, ds + \int_{\partial S(t)} (C^s + \langle F \rangle^T S^s) \nu \cdot v_s \, ds. \tag{2.67}$$

We now require that the superficial mechanical working be invariant under reparametrization of $\partial S(t)$. This requirement holds if and only if:

$$(C^s + \langle F \rangle^T) \nu \cdot t = 0, \quad \text{where} \quad t \stackrel{def}{=} n_s \times \nu. \tag{2.68}$$

It can then be shown that:

$$C^s \; = \; \sigma \mathbf{P} + n_s \otimes \hat{c} - \langle F \rangle^T S^s, \tag{2.69}$$

where

$$\hat{c} \stackrel{def}{=} (C^s + \langle F \rangle^T S^s)^T n_s.$$

Note that we have defined the superficial configurational stress tensor as a linear

transformation from $\mathbb{R}^3$ to $\mathbb{R}^3$ that satisfies the following relation:

$$C^s n_s \;=\; 0. \tag{2.70}$$

We can rewrite (2.69) as follows:

$$C^s \;=\; \sigma \mathbf{P} + n_s \otimes c - \bar{F}^T S^s, \tag{2.71}$$

where the scalar σ is the surface tension and

$$c \stackrel{def}{=} C^{sT} n_s$$

is the (tangential) surface shear, and the surface deformation gradient

$$\bar{F} \stackrel{def}{=} F^{\pm}\mathbf{P} = \langle F \rangle \mathbf{P}$$

has been defined so as to be in $Lin(\mathbb{R}^3, \mathbb{R}^3)$ and to satisfy the relation $\bar{F} n_s = 0$.

Making use of the surface divergence theorem (2.20) and (2.21), as well as the following two identities (cf., e.g., Simha and Bhattacharya [SB])

$$\begin{aligned} \nabla_s(\langle \dot{y} \rangle + v_n \langle F \rangle n_s) \;&=\; (\langle F \rangle^{\circ} - \langle F \rangle n_s \otimes n_s^{\circ} - v_n \langle F \rangle L)\, \mathbf{P}, \qquad \text{and} \\ n_s^{\circ} \;&=\; -\nabla_s v_n, \end{aligned}$$

we obtain the following expression for $W_m^{(1)}(S(t))$:

$$\begin{aligned} W_m^{(1)}(S(t)) = &\int_{\partial S(t)} \sigma v_s \cdot \nu \; ds + \\ &\int_{S(t)} \left\{ (\nabla \cdot S^s) \cdot \langle \dot{y} \rangle + S^s \cdot \langle F \rangle^{\circ} - [S^{sT} \langle F \rangle n_s + c] \cdot n_s^{\circ} \right\} \; da + \\ &\int S(t) \left\{ (\nabla_s \cdot S^s) \cdot \langle F \rangle n_s + \nabla_s \cdot c - \langle F \rangle^T S^s \cdot L \right\} v_n \; da, \end{aligned} \tag{2.72}$$

where the curvature tensor L is defined as

$$L \stackrel{def}{=} -\nabla_s n_s.$$

Now back to (2.4.5). We rearrange $W_m^{(2)}(S(t))$ as follows:

$$W_m^{(2)}(S(t)) = \int_{S(t)} \left\{ [g_{ext}^s + \langle F \rangle^T b^s] \cdot v_s + b^s \cdot \langle \dot{y} \rangle \right\} \, da. \tag{2.73}$$

We also require that the mechanical working remain unchanged if $S(t)$ were to be reparametrized. This can be true only if there exists a scalar β^s such that:

$$g_{ext}^s = \beta^s n_s - \langle F \rangle^T b^s. \tag{2.74}$$

Consequently, (2.73) reduces to

$$W_m^{(2)}(S(t)) = \int_{S(t)} [\beta^s v_n + b^s \cdot \langle \dot{y} \rangle] \, da. \tag{2.75}$$

Grouping (2.72) and (2.75), and making use of the interfacial balance of standard forces (2.44), we obtain the following expression for the mechanical working on the surface:

$$\begin{aligned} W_m(S(t)) = & \int_{\partial S(t)} \sigma v_s \cdot \nu \, ds - \int_{S(t)} [[S]] n_s \cdot \langle \dot{y} \rangle \, da + \\ & \int_{S(t)} \left\{ S^s \cdot \langle F \rangle^{\circ} - (S^{sT} \langle F \rangle n_s + c) \cdot n_s^{\circ} \right\} \, da + \\ & \int_{S(t)} \left\{ (\nabla_s \cdot S^s) \cdot \langle F \rangle n_s + \nabla_s \cdot c - \langle F \rangle^T S^s \cdot L + \beta^s \right\} v_n \, da. \end{aligned} \tag{2.76}$$

It then follows from (2.66) and (2.76) that

$$
\begin{aligned}
W_m(P(t)\cup S(t)) = \; & W_m(P(t)) + W_m(S(t)) \; = \\
& \int_{\partial P(t)} \pi u\cdot n \; da + \int_{\partial S(t)} \sigma v_s\cdot \nu \; ds + \int_{P(t)} S\cdot \dot{F} \; dv \\
& + \int_{S(t)} \left\{ (\nabla_s \cdot S^s)\cdot \langle F\rangle n_s + \nabla_s \cdot c - \langle F\rangle^T S^s \cdot L + \beta^s - \langle S\rangle n_s \cdot [[F]] n_s \right\} v_n \; da \\
& + \int_{S(t)} \left\{ S^s \cdot \langle F\rangle^{\circ} - (S^{sT}\langle F\rangle n_s + c)\cdot n_s^{\circ} \right\} \; da, \qquad (2.77)
\end{aligned}
$$

where we have used the compatibility condition (2.15).

Finally, define the nonmechanical rates of energy supply to $P(t)$ and $S(t)$, i.e., those supplies due to bulk and surface heat exchange, species diffusion, external supply of heat as well as the motion of the boundary of the control volume in the reference configuration, as follows:

$$
W_d(P(t)) \stackrel{def}{=} W(P(t)) - W_m(P(t)), \; W_d(S(t)) \stackrel{def}{=} W(S(t)) - W_m(S(t)).
$$

Using the bulk and surface divergence theorems, we obtain the following integral expressions:

$$
\begin{aligned}
W_d(P(t)) \; = \; & -\int_{P(t)} \nabla\cdot q \; dv - \int_{S(t)} [[q]]\cdot n_s \; da + \int_{\partial P(t)} Qu\cdot n \; da + \int_{P(t)} \mathcal{Q} \; dv \\
& + \sum_{k=1}^{N} \{ \int_{\partial P(t)} \mu_k \rho_k u\cdot n \; da - \int_{P(t)} \nabla\cdot(\mu_k h_k) \; dv - \int_{S(t)} [[\mu_k h_k]]\cdot n_s \; da \}, \\
W_d(S(t)) \; = \; & -\int_{S(t)} \nabla_s \cdot q^s \; da + \int_{\partial S(t)} Q^s v_s \cdot \nu \; ds + \int_{S(t)} \mathcal{Q}^s \; da \\
& + \sum_{k=1}^{N} \{ \int_{\partial S(t)} \mu_k^s \rho_k^s v_s \cdot \nu \; ds - \int_{S(t)} \nabla_s \cdot (\mu_k^s h_k^s) \; da \}.
\end{aligned}
$$

We are now in a position to explicitly formulate the first law of Thermodynamics which, as stated above, requires that the temporal changes in the energy of the system (i.e., the sum of the bulk and surface energies) be exactly compensated for by the

power supplied to the system by its environment.

2.4.6 The energy balance (continued)

Now, return to (2.55). Making use of the bulk and surface transport theorems, we can rewrite (2.55) as follows:

$$\int_{P(t)} \dot{\epsilon}\, dv - \int_{S(t)} [[\epsilon]] v_s \cdot n_s\, da + \int_{\partial P(t)} \epsilon u \cdot n\, da + \int_{S(t)} (\overset{\circ}{\epsilon^s} - \epsilon^s \kappa v_s \cdot n_s)\, da + \int_{\partial S(t)} \epsilon^s v_s \cdot \nu\, ds = W_m(P(t)) + W_d(P(t)) + W_m(S(t)) + W_d(S(t))$$

Using the previously derived expressions for the bulk and interfacial power supplies, and then recombining various terms, we arrive at the following statement of the first law of thermodynamics as it applies to the evolving control volume:

$$\begin{aligned}
&\int_{P(t)} \{\dot{\epsilon} - S \cdot \dot{F} + \nabla \cdot q - \mathcal{Q} + \sum_{k=1}^{N} (\nabla \cdot (\mu_k h_k)\}\, dv \\
&\quad + \int_{\partial P(t)} \{\epsilon - \pi - Q - \sum_{k=1}^{N} \mu_k \rho_k\} u \cdot n\, da \\
&\quad + \int_{S(t)} \{\overset{\circ}{\epsilon^s} - S^s \cdot \langle F \rangle^{\circ} + (S^{sT} \langle F \rangle n_s + c) \cdot \overset{\circ}{n}_s \\
&-([[\epsilon]] + \epsilon^s \kappa + (\nabla_s \cdot S^s) \cdot \langle F \rangle n_s + \nabla_s \cdot c - \langle F \rangle^T S^s \cdot L + \beta^s - \langle S \rangle n_s \cdot [[F]] n_s) v_n \\
&\quad + [[q]] \cdot n_s - \mathcal{Q}^s + \nabla_s \cdot q^s + \sum_{k=1}^{N} (\nabla_s \cdot (\mu_k^s h_k^s) + [[\mu_k^s h_k]] \cdot n_s\}\, da \\
&\quad + \int_{\partial S(t)} \{\epsilon^s - \sigma - Q^s - \sum_{k=1}^{N} \mu_k^s \rho_k^s\} v_s\, ds = 0.
\end{aligned} \tag{2.78}$$

At any time t we can define another evolving control volume $P'(t)$ such that $P'(t) = P(t)$, but its boundary velocity field u' is such that $u' \cdot n' \neq u \cdot n$ where $n(x,t) = n'(x,t)$, i.e., the normal velocities of the two control volumes are not identical even though they coincide at the instant in time under consideration. The energy

balance in the bulk should hold for both control volumes $P(t)$ and $P'(t)$. This can be the case if and only if:

$$\epsilon - \pi - Q - \sum_{k=1}^{N} \mu_k \rho_k = 0. \tag{2.79}$$

Identically, at any instant t in time, we can define a moving surface $S'(t)$ that coincides with $S(t)$ at that instant but whose boundary velocity field is distinct from that of $S(t)$, i.e., $v_s \cdot \nu \neq v'_s \cdot \nu'$,where $\nu(x,t) = \nu'(x,t)$. Again, the interfacial energy balance is expected to hold for both surfaces, which implies that:

$$\epsilon^s - \sigma - Q^s - \sum_{k=1}^{N} \mu_k^s \rho_k^s = 0. \tag{2.80}$$

2.4.7 The dissipation inequality

The second law of Thermodynamics

We postulate the following statement of the second law of Thermodynamics (or law of entropy growth):

$$\frac{d}{dt}\int_{P(t)} \eta \, dv + \frac{d}{dt}\int_{S(t)} \eta^s \, da \geq -\int_{\partial P(t)} \frac{1}{\theta} q \cdot n \, da + \int_{P(t)} \frac{\mathcal{Q}}{\theta} \, dv + \int_{\partial P(t)} \frac{Q}{\theta} u \cdot n \, da - \int_{\partial S(t)} \frac{1}{\theta^s} q^s \cdot \nu \, ds + \int_{S(t)} \frac{\mathcal{Q}^s}{\theta^s} \, da - \int_{\partial S(t)} \frac{Q^s}{\theta^s} v_s \cdot \nu \, ds \tag{2.81}$$

where θ^s is the superficial temperature field, η and η^s are the mass-averaged bulk and superficial entropy densities, i.e.,

$$\rho\eta = \sum_{k=1}^{N} \rho_k \eta_k + \eta_{\text{mix}}, \quad \text{and} \quad \rho^s \eta^s = \sum_{k=1}^{N} \rho_k^s \eta_k^s + \eta_{\text{mix}}^s, \tag{2.82}$$

with η_{mix} and η_{mix}^s the bulk and surface entropy densities of mixing (resulting from the molecular interactions between the various chemical species present in the mixture).

We note that this statement is once again approximate and relies on the following

approximation:

$$\sum_{k=1}^{N} \rho_k^\alpha \eta_k^\alpha v_k = \rho^\alpha \eta^\alpha v, \tag{2.83}$$

where $\alpha = g, f, s$.

Now back to (2.81). Applying the divergence and transport theorems, and assuming that the temperature field is *continuous* accross the surface, i.e., $\theta^- = \theta^+ = \theta^s$, we arrive at the following integral version of the second law of thermodynamics:

$$\begin{aligned} &\int_{P(t)} \{\dot{\eta} + \nabla \cdot (\frac{1}{\theta} q) - \frac{\mathcal{Q}}{\theta}\}\, dv + \int_{\partial P(t)} (\eta - \frac{Q}{\theta}) u \cdot n \, da \\ &+ \int_{S(t)} \{\mathring{\eta} - ([[\eta]] + \eta^s \kappa) v_s + \frac{1}{\theta^s} [[q]] \cdot n_s + \nabla_s \cdot (\frac{1}{\theta^s} q^s) - \frac{\mathcal{Q}^s}{\theta^s}\}\, da \\ &+ \int_{\partial S(t)} (\eta^s - \frac{Q^s}{\theta^s}) v_s \cdot \nu \, ds \geq 0. \end{aligned} \tag{2.84}$$

Next, using an argument identical to that which yields (2.79) and (2.80), we obtain the following identities:

$$\eta - \frac{Q}{\theta} = 0, \qquad \text{and} \tag{2.85}$$

$$\eta^s - \frac{Q^s}{\theta^s} = 0. \tag{2.86}$$

Combining (2.79) and (2.85) provides us with a definition of the scalar π as the grand canonical energy density of the bulk phase in question:

$$\pi = G, \tag{2.87}$$

where

$$G \stackrel{def}{=} \epsilon - \theta\eta - \sum_{k=1}^{N} \mu_k \rho_k.$$

Identically, combining (2.80) and (2.86) enables us to define the (scalar) surface

tension as the grand canonical energy density of the surface phase:

$$\sigma = G^s \quad \text{with} \quad G^s \stackrel{def}{=} \epsilon^s - \theta^s \eta^s - \sum_{k=1}^{N} \mu_k^s \rho_k^s. \tag{2.88}$$

The gas and solid dissipation inequalities

Localization of the energy balance and the growth inequality in the gas phase, away from the surface, yields the following equations:

$$\begin{aligned} \dot{\epsilon}^g - S^g \cdot \dot{F} + \nabla \cdot q^g - \mathcal{Q} + \sum_{k=1}^{N} h_k^g \cdot \nabla \mu_k^g + \sum_{k=1}^{N} \mu_k^g \nabla \cdot h_k^g &= 0, \qquad \text{and} \\ \dot{\eta}^g + \frac{1}{\theta} \nabla \cdot q^g - \frac{1}{\theta^2} q^g \cdot \nabla \theta - \frac{\mathcal{Q}}{\theta} &\geq 0. \end{aligned}$$

Next, making use of the species equations in the vapor phase (2.23) and combining the above two equations, we obtain the localized version of the dissipation inequality in the gas phase:

$$\dot{\psi}^g + \eta^g \dot{\theta} - S^g \cdot \dot{F} - \sum_{k=1}^{N} \mu_k^g \dot{\rho}_k^g + \sum_{k=1}^{N} \mu_k^g R_k^g + \sum_{k=1}^{N} h_k^g \cdot \nabla \mu_k^g + q^g \cdot \nabla (\ln \theta) \leq 0. \tag{2.89}$$

An identical procedure yields an analogous localized dissipation inequality in the bulk of the thin solid film:

$$\dot{\psi}^f + \eta^f \dot{\theta} - S^f \cdot \dot{F} - \sum_{k=1}^{N} \mu_k^f \dot{\rho}_k^f + \sum_{k=1}^{N} h_k^f \cdot \nabla \mu_k^f + q^f \cdot \nabla (\ln \theta) \leq 0, \tag{2.90}$$

where $\psi^\alpha \stackrel{def}{=} \epsilon^\alpha - \theta \eta^\alpha$ is the Helmholtz free energy density (per unit volume) in the α phase.

The dissipation inequality at the surface

Localization of the energy balance and entropy inequality at the suface yields the following interfacial equations:

$$\begin{aligned}
&\overset{\circ}{\epsilon^s} - S^s \cdot \langle F \rangle^{\mathrm{o}} + (S^{sT}\langle F \rangle n_s + c) \cdot n_s^{\mathrm{o}} - \bar{f} v_n + [[q]] \cdot n_s - \mathcal{Q}^s + \nabla_s \cdot q^s \\
&\quad + \sum_{k=1}^{N} \mu_k^s \nabla_s \cdot h_k^s + \sum_{k=1}^{N} h_k^s \cdot \nabla \mu_k^s + \sum_{k=1}^{N} (\langle \mu_k \rangle [[h_k]] \cdot n_s + [[\mu_k]] \langle h_k \rangle \cdot n_s) \;=\; 0, \text{ and} \\
&\overset{\circ}{\eta^s} - ([[\eta]] + \eta^s \kappa) v_n + \frac{1}{\theta^s}[[q]] \cdot n_s + \frac{1}{\theta^s} \nabla_s \cdot q^s - \frac{1}{\theta^{s2}} q^s \cdot \nabla_s \theta^s - \frac{\mathcal{Q}^s}{\theta^s} \geq 0,
\end{aligned}$$

where

$$\bar{f} \overset{def}{=} [[\epsilon]] + \epsilon^s \kappa + (\nabla_s \cdot S^s) \cdot \langle F \rangle n_s + \nabla_s \cdot c - \langle F \rangle^T S^s \cdot L + \beta^s - \langle S \rangle n_s \cdot [[F]] n_s.$$

Multiplying the entropy inequality by θ and subtracting the resulting equation from the energy balance, and then using the species equations at the surface (2.25), we obtain the dissipation inequality at the surface:

$$\begin{aligned}
&\overset{\circ}{\psi^s} + \eta^s \overset{\circ}{\theta} - \sum_{k=1}^{N} \mu_k^s \overset{\circ}{\rho_k^s} - S^s \cdot \langle F \rangle^{\mathrm{o}} + (S^{sT}\langle F \rangle n_s + c) \cdot n_s^{\mathrm{o}} \\
&\qquad + \sum_{k=1}^{N} \mu^s R^s + \sum_{k=1}^{N} h_k^s \cdot \nabla \mu_k^s + q^s \cdot \nabla_s (\ln \theta) - \tilde{f} v_n \\
&\qquad + \sum_{k=1}^{N} \{ (\langle \mu_k \rangle - \mu_k^s)[[h_k]] \cdot n_s + [[\mu_k]] \langle h_k \rangle \cdot n_s \} \leq 0,
\end{aligned}$$

where

$$\begin{aligned}
\tilde{f} \overset{def}{=}\; & [[\psi]] + \psi^s \kappa - \sum_{i=1}^{N} \mu_i^s ([[\rho_i]] + \rho_i^s \kappa) \\
& + (\nabla_s \cdot S^s) \cdot \langle F \rangle n_s + \nabla_s \cdot c - \langle F \rangle^T S^s \cdot L + \beta^s - \langle S \rangle n_s \cdot [[F]] n_s,
\end{aligned}$$

and $\psi^s \overset{def}{=} \epsilon^s - \theta^s \eta^s$ is the Helmholtz free energy density (per unit area) of the surface. The temperature is assumed to be continuous across the surface.

Define, for the k^{th} species, the mass flux from the phase α into the *moving* surface

phase as:

$$J_k^\alpha \stackrel{def}{=} j_k^\alpha - \frac{1}{\tau}\rho_k^s v_s \cdot n_\alpha, \qquad \forall\ k = 1, \ldots, N, \tag{2.91}$$

with $n_g = -n_s$ and $n_f = n_s$.

Making use of the interfacial species balances (2.27), (2.28), the identity $\mathbf{P} \cdot L = \kappa$, as well as the interfacial balance of deformational forces (2.44), and after some tedious but straightforward algebra, we obtain the following version of the dissipation inequality at the surface:

$$\begin{aligned} &\overset{\circ}{\psi}{}^s + \eta^s \overset{\circ}{\theta} - S^s \cdot \langle F \rangle^{\circ} + (S^{sT}\langle F \rangle n_s + c) \cdot n_s^{\circ} \\ &\quad - \sum_{k=1}^{N} \mu_k^s \overset{\circ}{\rho}{}_k^s + \sum_{k=1}^{N} h_k^s \cdot \nabla \mu_k^s + q^s \cdot \nabla_s (\ln \theta) + \sum_{k=1}^{N} \mu_k^s R_k^s \\ &\quad - f v_n + \sum_{k=1}^{N} (\mu_k^g - \mu_k^s) J_k^g + \sum_{k=1}^{N} (\mu_k^f - \mu_k^s) J_k^f \leq 0, \end{aligned} \tag{2.92}$$

where

$$f \stackrel{def}{=} n_s \cdot [[G\mathbf{1} - F^T S]] n_s + (G^s \mathbf{P} - \langle F \rangle^T S^s) \cdot L + \nabla_s \cdot c - b^s \cdot \langle F \rangle n_s + \beta^s \tag{2.93}$$

is identified as the driving force at the surface whose conjugate variable is the normal velocity of the surface v_n. Here,

$$G^\alpha \stackrel{def}{=} \psi^\alpha - \sum_{i=1}^{N} \mu_i^\alpha \rho_i^\alpha$$

is the density of the grand canonical energy in the phase α ($\alpha = g, f, s$) and b^s is given by (2.48).

In order to explicitly identify β^s, we postulate the equivalence of the inertial working and the temporal changes in the kinetic energy (cf. [GP]). In the bulk

phases g, f, the densities (per unit volume) of kinetic energy are given by:

$$k^{g,f} \stackrel{def}{=} \frac{1}{2}\rho^{g,f}\dot{y}\cdot\dot{y},$$

where $\rho^{g,f}$ are the total mass densities in the vapor and film phases respectively. Along the surface, the density (per unit area) of kinetic energy is given by

$$k^{s} \stackrel{def}{=} \frac{1}{2}\rho^{s}\langle\dot{y}\rangle\cdot\langle\dot{y}\rangle,$$

where ρ^s is the total interfacial mass density and $\langle\dot{y}\rangle$ is the (mass-averaged) material velocity associated with the particles along the surface. We now require that the production of kinetic energy in the *evolving* control volume defined previously $P(t)$ be equal to the negative of the working of the *inertial* forces on $P(t)$:

$$\frac{d}{dt}\int_{P_{g,f}(t)} k^{g,f}\,dv - \int_{\partial P^{g,f}(t)} k^{g,f}u\cdot n\,da + \frac{d}{dt}\int_{S(t)} k^{s}\,da$$
$$- \int_{\partial S(t)} k^{s}v_s\cdot\nu\,ds = -\int_{P_{g,f}(t)} b^{g,f}\cdot\dot{y}\,dv - \int_{S(t)}(b^{s}\cdot\bar{v}_s + g^{s}_{ext}\cdot v_s)\,da. \quad (2.94)$$

Making use of the bulk and surface transport theorems, we rewrite (2.94) as:

$$\int_{P_{g,f}(t)} \dot{k}^{g,f}\,dv - \int_{S(t)}[[k]]v_s\cdot n_s\,da + \int_{S(t)}(\overset{\circ}{k^{s}} - \kappa k^{s}v_s\cdot n_s)\,da$$
$$= -\int_{P_{g,f}(t)} b^{g,f}\cdot\dot{y}\,dv - \int_{S(t)} b^{s}\cdot\langle\dot{y}\rangle\,da - \int_{S(t)}(g^{s}_{ext} + \langle F\rangle^{T}b^{s})\cdot v_s\,da, \quad (2.95)$$

where we have used (2.11).

Away from the surface, localization yields the following identity:

$$\dot{k}^{b,f} = -b^{g,f}\cdot\dot{y}. \quad (2.96)$$

The definitions of the bulk kinetic energies as well as the relations (2.46) and (2.47) show that (2.96) is identically satisfied.

At the surface, localization and (2.74) yield the following relation:

$$-\overset{\circ}{k^s} + ([[k]] + k^s\kappa)v_n = \beta^s v_n + b^s \cdot \langle \dot{y} \rangle. \tag{2.97}$$

Using the relation (2.50), the compatibility condition (2.15), the identity (2.49), the total mass balance at the surface (2.33), and assuming that $v_n \neq 0$, we obtain the following relation:

$$\beta^s = \frac{1}{2}(\langle \rho \rangle \langle \dot{y} \rangle - \langle \rho \dot{y} \rangle) \cdot [[F]] n_s v_n, \tag{2.98}$$

which can be rewritten, with the help of (2.15), as:

$$\beta^s = \frac{1}{4} v_n^2 [[\rho]] ([[F]] n_s \cdot [[F]] n_s). \tag{2.99}$$

It follows that the generalized thermodynamic driving force at the interface reduces to:

$$f = n_s \cdot [[G\mathbf{1} - F^T S]] n_s + (G^s \mathbf{P} - \langle F \rangle^T S^s) \cdot L + \nabla_s \cdot c - b^s \cdot \langle F \rangle n_s + \beta^s \tag{2.100}$$

with

$$\begin{aligned} b^s &= -\rho^s \langle \dot{y} \rangle^\circ - v_n^2 \langle \rho \rangle [[F]] n_s, \qquad \text{and} \\ \beta^s &= \frac{1}{4} v_n^2 [[\rho]] ([[F]] n_s \cdot [[F]] n_s). \end{aligned}$$

2.5 The Constitutive Equations

2.5.1 The gas phase

First, model the gas mixture as a viscoelastic multicomponent material, i.e., assume that the behavior of the multispecies gas depends on the temperature, the state of strain, the local chemical composition as well as the velocity gradient. More

specifically, we begin by making the following constitutive assumptions:

$$\begin{aligned}
\bar{\psi}^g &= \bar{\psi}^g(\theta, F, \{Y_k^g\}_{k=1}^N), \\
\bar{\eta}^g &= \bar{\eta}^g(\theta, F, \{Y_k^g\}_{k=1}^N), \\
\bar{\mu}_k^g &= \bar{\mu}_k^g(\theta, F, \{Y_i^g\}_{i=1}^N), \ \forall\ k = 1, \ldots, N, \\
T &= \hat{T}(\theta, F, \{Y_k^g\}_{k=1}^N) + \sigma(\theta, F, \{Y_k^g\}_{k=1}^N)[L], \\
\bar{q} &= \bar{q}(\theta, F, \{Y_k^g\}_{k=1}^N, \nabla_y(\ln\theta), \{\nabla_y \mu_k^g\}_{k=1}^N), \\
\bar{h}_k^g &= \bar{h}_k^g(\theta, F, \{Y_i^g\}_{i=1}^N, \nabla_y(\ln\theta), \{\nabla_y \mu_i^g\}_{i=1}^N), \ \forall\ k = 1, \ldots, N, \qquad \text{and} \\
\bar{R}_k^g &= \bar{R}_k^g(\theta, F, \{Y_i^g\}_{i=1}^N), \ \forall\ k = 1, \ldots, N, \qquad (2.101)
\end{aligned}$$

where

$$Y_k^g \stackrel{def}{=} \frac{\bar{\rho}_k^g}{\bar{\rho}^g}$$

is the mass fraction of the k^{th} chemical species present in the mixture, and

$$L \stackrel{def}{=} \nabla_y \bar{v}$$

is the velocity gradient. Here (as previously), the bar denotes a *spatial* scalar, vectorial or tensorial field and the subscript y denotes differentiation with respect to the position in the *current* configuration. Note that we have decomposed the Cauchy stress T into an elastic component $\hat{T}$ and a viscous component σ both of which depend on the temperature, deformation gradient and local chemical composition. Moreover, we assume that the viscous part of the stress acts on the velocity gradient.

In the gas phase, it is best to adopt an Eulerian viewpoint. Consequently, we will consider the dissipation inequality resulting from the combination of the energy balance (2.61) with the localized Eulerian form of the entropy inequality. The latter can be stated as follows:

$$-\bar{\rho}\bar{\theta}\frac{d\bar{\eta}}{dt} - \nabla \cdot \bar{q} + \bar{Q} + \bar{q} \cdot \nabla_y(\ln\theta) \leq 0, \qquad (2.102)$$

where we define the mass-averaged density of entropy as follows:

$$\bar{\rho}\bar{\eta} \stackrel{def}{=} \sum_{k=1}^{N} \bar{\rho}_k \bar{\eta}_k + \bar{\eta}_{\text{mix}}, \tag{2.103}$$

with $\bar{\eta}_{\text{mix}}$ the density (per unit deformed volume) of the entropy of mixing. We thus have the following Eulerian dissipation inequality:

$$\begin{aligned} &\bar{\rho}^g \left(\frac{\partial \bar{\psi}^g}{\partial \theta} + \bar{\eta}\right)\frac{d\theta}{dt} + \left(\bar{\rho}^g \frac{\partial \bar{\psi}^g}{\partial F} F^T - \hat{T}\right) \cdot L - L \cdot \sigma[L] \\ &\quad + \sum_{k=1}^{N} \left(\frac{\partial \bar{\psi}}{\partial Y_k^g} - \bar{\mu}_k^g\right)\frac{d\bar{\rho}_k^g}{dt} + \sum_{k=1}^{N} \bar{\rho}_k^g \left(\frac{d\bar{\psi}^g}{dY^k} - \bar{\mu}_k^g\right) \nabla \cdot \bar{v} \\ &\quad + \sum_{k=1}^{N} \bar{\mu}_k^g \bar{R}_k^g + \sum_{k=1}^{N} \bar{h}_k^g \cdot \nabla_y \bar{\mu}_k^g + \bar{q} \cdot \nabla_y (\ln \theta) \leq 0, \end{aligned} \tag{2.104}$$

where we have made use of the following relations:

$$\begin{aligned} L \stackrel{def}{=} \nabla_y \bar{v} = \frac{dF}{dt} F^{-1} \quad &\Leftrightarrow \quad \frac{dF}{dt} = (\nabla \bar{v}) F, \qquad \text{and} \\ Y_k^g = \frac{\bar{\rho}_k^g}{\bar{\rho}} \quad &\Rightarrow \quad \frac{dY_k^g}{dt} = \frac{1}{\bar{\rho}^g}\frac{d\bar{\rho}_k^g}{dt} - \frac{\bar{\rho}_k^g}{\bar{\rho}^{g^2}}\frac{d\bar{\rho}^g}{dt} = \frac{1}{\bar{\rho}^g}\left(\frac{d\bar{\rho}_k^g}{dt} + \bar{\rho}_k^g \nabla_y \cdot \bar{v}\right). \end{aligned} \tag{2.105}$$

We postulate that the generalized Clausius-Duhem inequality be satisfied for all admissible thermodynamic processes. Following Coleman and Noll [CN], we define a thermodynamic process as the list of the following scalar, vector and tensor fields (defined as functions of the material point x and time t): the deformation mapping y, the temperature θ, the species mass densities $\{\bar{\rho}_k^g\}_{k=1}^N$, the Cauchy stress and the body force density, the external heat supply $\bar{Q}$, the internal energy $\bar{\epsilon}$, the species partial energies $\{\bar{\mu}_k^g\}_{k=1}^N$, the entropy $\bar{\eta}^g$, the heat flux $\bar{q}$, the species diffusive fluxes $\{\bar{h}_k^g\}_{k=1}^N$ and the species chemical production rates $\{\bar{R}_k^g\}_{k=1}^N$ that are *compatible* with the balance laws, i.e., that satisfy the species, linear and angular momenta, and energy equations. By *admissible* thermodynamic process, we mean one that is compatible with the constitutive relations (2.101).

If the dissipation inequality is not to be violated by any admissible thermodynamic process, then it clearly should hold for an admissible process such that the deformation, the temperature, and the mass fractions are homogeneous (i.e., depend only on time), and the various chemical species present in the system are diffusionless and do not react chemically with each other. For such a process, we have:

$$\nabla_y(\ln\theta) = 0 \quad \text{and} \quad \bar{h}_k^g = \bar{R}_k^g = 0, \qquad \forall\ k = 1, \ldots, N.$$

It follows that the dissipation inequality then reduces to:

$$\bar{\rho}^g\left(\frac{\partial\bar{\psi}^g}{\partial\theta} + \bar{\eta}^g\right)\frac{d\theta}{dt} + \left(\bar{\rho}^g\frac{\partial\bar{\psi}^g}{\partial F}F^T - \hat{T}\right)\cdot L - L\cdot\sigma[L] + \sum_{k=1}^{N}\left(\frac{\partial\bar{\psi}^g}{\partial Y_k^g} - \bar{\mu}_k^g\right)\frac{d\bar{\rho}_k^g}{dt} + \sum_{k=1}^{N}\bar{\rho}_k^g\left(\frac{d\bar{\psi}^g}{dY_k^g} - \bar{\mu}_k^g\right)\nabla_y\cdot\bar{v} \leq 0. \qquad (2.106)$$

As temporal fields, $\theta(t)$, $F(t)$ (and consequently $L(t)$), and $\{\bar{\rho}_k^g(t)\}_{k=1}^N$ can be chosen *arbitrarily*[4]. Consequently, at any time, $\frac{d\theta}{dt}$, L, and $\{\frac{d\bar{\rho}_k^g}{dt}\}_{k=1}^N$ can be assigned arbitrary values. In order for (2.106) to be satisfied at any time, the following relations should hold:

$$\begin{aligned}
\bar{\eta}^g &= -\frac{\partial\bar{\psi}^g}{\partial\theta}, \\
\bar{\mu}_k^g &= \frac{\partial\bar{\psi}^g}{\partial Y_k^g}, \qquad \forall\ k = 1, \ldots, N, \qquad (2.107)\\
\hat{T} &= \bar{\rho}^g\frac{\partial\bar{\psi}^g}{\partial F}F^T, \qquad \text{and} \\
\sigma[L]\cdot L &\geq 0. \qquad (2.108)
\end{aligned}$$

Note that from (2.107) it follows that the last term on the LHS of (2.106) is identically zero.

[4]This arbitrariness results from the requirement that *all* admissible thermodynamic processes be compatible with the dissipation inequality. An expert in Rational Mechanics will note that not all such admissible thermodynamic processes satisfy the species mass balances as stated above. However, this inconsistency is easily corrected by the introduction of external species supplies in the species equations and the corresonding energy supplies in the energy balance.

Next, we specialize to the case of a (linearly) *viscous fluid*, i.e.,

$$\bar{\psi}^g,\ \bar{\eta}^g,\ T,\ \bar{q},\ \{\bar{\mu}_k^g k\}_{k=1}^N,\ \{\bar{h}_k^g\}_{k=1}^N\},\ \text{and}\ \{\bar{R}_k^g\}_{k=1}^N$$

depend on F only through $\det F$ or equivalently through the specific volume $v \stackrel{def}{=} 1/\bar{\rho}^g$. We refer to Coleman and Noll [CN] who use a frame-indifference argument to obtain the following constitutive relation:

$$T \ = \ -pI + 2\mu D + \lambda(trD)I$$

where

$$p \ = \ -\frac{\partial \bar{\psi}^g}{\partial v}, \quad \text{and} \quad D \stackrel{def}{=} \frac{1}{2}(L + L^T)$$

are the hydrostatic pressure and the rate-of-deformation tensor respectively. The inequality (2.108) then yields the following constraints on the material parameters λ and μ:

$$\mu \ \geq \ 0 \text{ and } \lambda + \frac{2}{3}\mu \ \geq \ 0.$$

We can now rewrite the dissipation inequality as follows:

$$\sum_{k=1}^{N} \bar{\mu}_k^g \bar{R}_k^g + \sum_{k=1}^{N} \bar{h}_k^g \cdot \nabla_y \bar{\mu}_k^g + \bar{q} \cdot \nabla_y (\ln \theta) \leq 0. \tag{2.109}$$

Consider next an admissible thermodynamic process such that the various chemical species present in the system are not chemically reactive. The equation (2.109) then reduces to:

$$\sum_{k=1}^{N} \bar{h}_k^g \cdot \nabla_y \bar{\mu}_k^g + \bar{q} \cdot \nabla_y (\ln \theta) \leq 0. \tag{2.110}$$

We appeal to a lemma by Gurtin and Voorhees [GV1] to obtain the following consti-

tutive relations for the heat and species fluxes:

$$\bar{q} = -k^g \nabla_y(\ln\theta) - \sum_{i=1}^{N} k_i^g \nabla_y \bar{\mu}_i^g, \qquad \text{and} \tag{2.111}$$

$$\bar{h}_k^g = -D_k^g \nabla_y(\ln\theta) - \sum_{i=1}^{N} D_{ki}^g \nabla \bar{\mu}_i^g, \qquad \forall\ k = 1, \ldots, N, \tag{2.112}$$

where the matrix

$$\mathbf{K}^g = \mathbf{K}^g(\nabla_y(\ln\theta),\ \{\nabla_y \bar{\mu}_i^g\}_{i=1}^N,\ \theta,\ \bar{\rho}^g,\ \{Y_i^g\}_{i=1}^N) \stackrel{def}{=} \begin{bmatrix} k^g & k_1^g & \cdots & k_N^g \\ D_1^g & D_{11}^g & \cdots & D_{1N}^g \\ \vdots & \vdots & & \vdots \\ D_N^g & D_{N1}^g & \cdots & D_{NN}^g \end{bmatrix}$$

is such that $\mathbf{K}^g(0,\ 0,\ \theta,\ \bar{\rho}^g,\ \{Y_k^g\}_{k=1}^N)$ is positive semi-definite. The dependence of the diffusive species fluxes on the temperature gradient is known as the Soret effect, while the dependence of the heat flux on the concentration gradients of the various chemical species present is known as the Dufour effect. As mentioned above, in many CVD processes, the Soret effect is important because of the large temperature gradient in the gas phase, while the Dufour effect can often be neglected as the gas multi-species flows of interest are reasonably approximated as dilute mixtures.

Finally, consider an isothermal diffusionless admissible thermodynamic process. Consequently, the dissipation inequality assumes the form:

$$\sum_{i=1}^{N} \bar{\mu}_i^g \bar{R}_i^g \leq 0. \tag{2.113}$$

One would have to postulate constitutive relations of the form

$$\bar{R}_k^g \stackrel{def}{=} \bar{R}_k^g(\theta,\ \bar{\rho}^g,\ \{Y_i^g\}_{i=1}^N)$$

such that (2.113) is satisfied.

2.5.2 A remark on the special case of a multicomponent ideal gas

Consider now the case of a mixture of ideal gases. From Thermodynamics, we have the following relation between the chemical potential of the k^{th} species, the temperature field θ, and the partial pressure $\bar{p}_k$ associated with the species of interest: $\forall\ k = 1, \ldots, N$,

$$w_k \bar{\mu}_k^g \ = \ w_k \mu_k^{\circ}(\theta) + R\theta \ln \bar{p}_k^g, \tag{2.114}$$

where μ_k° is the standard chemical potential associated with the k^{th} species (per unit mass) and

$$\bar{p}_k^g \ = \ R_k \theta \bar{\rho}_k^g,$$

with $R_k \stackrel{def}{=} R/w_k$, R being the universal ideal-gas constant and w_k the molar weight of the k^{th} species. It follows that (2.114) can be rewritten as:

$$w_k \bar{\mu}_k^g \ = \ w_k \bar{\mu}_k^{\circ} + R\theta \ln \bar{\rho}_k^g, \tag{2.115}$$

where

$$w_k \bar{\mu}_k^{\circ} \stackrel{def}{=} w_k \mu_k^{\circ} + R\theta \ln(R_k \theta).$$

For illustrative purposes, consider the following simple reversible homogeneous chemical reaction taking place in the gas phase:

$$\mathcal{AB}(g) \rightleftharpoons \mathcal{A}(g) + \mathcal{B}(g), \tag{2.116}$$

with $k_f(\theta)$ and $k_b(\theta)$ its forward and backward reaction-rate constants respectively (both being positive functions of temperature). A thermodynamical-statistical cal-

culation[5] then yields the following expression for the reaction rate associated with (2.116):

$$\mathcal{R} = k_f(\theta)\frac{\bar{\rho}^g_{AB}}{w_{AB}} - k_b(\theta)\frac{\bar{\rho}^g_A}{w_A}\frac{\bar{\rho}^g_B}{w_B}. \tag{2.117}$$

Suppose for now that this is the only reaction taking place in the gas phase. It follows that the dissipation inequality (2.113) reduces to

$$\bar{\mu}^g_{AB}\bar{R}^g_{AB} + \bar{\mu}^g_A\bar{R}^g_A + \bar{\mu}^g_B\bar{R}^g_B \leq 0,$$

which can be rewritten as

$$(w_A\bar{\mu}^g_A + w_B\bar{\mu}^g_B - w_{AB}\bar{\mu}^g_{AB})\mathcal{R} \leq 0. \tag{2.118}$$

From (2.115) it follows that

$$\rho^g_i = \exp\left[\frac{w_i(\bar{\mu}^g_i - \bar{\mu}^\circ_i)}{R\theta}\right], \qquad \forall\, i = A, B, AB. \tag{2.119}$$

Consequently, (2.117) can be rewritten as

$$\begin{aligned}\mathcal{R} = {} & \frac{k_f(\theta)}{w_{AB}}\exp\left[\frac{w_{AB}(\bar{\mu}^g_{AB} - \bar{\mu}^\circ_{AB})}{R\theta}\right] \\ & - \frac{k_b(\theta)}{w_A w_B}\exp\left[\frac{w_A(\bar{\mu}^g_A - \bar{\mu}^\circ_A)}{R\theta}\right]\exp\left[\frac{w_B(\bar{\mu}^g_B - \bar{\mu}^\circ_B)}{R\theta}\right].\end{aligned} \tag{2.120}$$

From Thermodynamics, we know that chemical equilibrium is embodied in the following condition (cf. Callen [C]):

$$w_A\bar{\mu}^g_A|_{eq} + w_B\bar{\mu}^g_B|_{eq} = w_{AB}\bar{\mu}^g_{AB}|_{eq}. \tag{2.121}$$

Substituting (2.114) into (2.121), we can define the equilibrium constant associated

[5] E.g., cf. Hill [TH].

with (2.116) as follows:

$$k_{eq} \stackrel{def}{=} \frac{\bar{\rho}^g_A|_{eq}\bar{\rho}^g_B|_{eq}}{\bar{\rho}^g_{AB}|_{eq}} = \exp\left[\frac{w_{AB}\bar{\mu}^\circ_{AB} - w_A\bar{\mu}^\circ_A - w_B\bar{\mu}^\circ_B}{R\theta|_{eq}}\right], \tag{2.122}$$

where it should be noted that k_{eq} is a function of temperature only. Also, the reaction-rate constants are related to the equilibrium constant via the relation: (cf. [TH], p. 198)

$$\frac{k_f(\theta)}{k_b(\theta)} = \frac{w_{AB}}{w_A w_B}\, k_{eq}(\theta). \tag{2.123}$$

It can then easily be shown that:

$$\mathcal{R} = \frac{k_f(\theta)}{w_{AB}} \exp\left[\frac{w_{AB}(\bar{\mu}^g_{AB} - \bar{\mu}^\circ_{AB})}{R\theta}\right]\left[1 - \exp\left(\frac{\Delta\bar{\mu}^g}{R\theta}\right)\right], \tag{2.124}$$

where

$$\Delta\bar{\mu}^g \stackrel{def}{=} w_A\bar{\mu}^g_A + w_B\bar{\mu}^g_B - w_{AB}\bar{\mu}^g_{AB}.$$

Consequently, (2.118) reduces to

$$\frac{k_f(\theta)}{w_{AB}}\Delta\bar{\mu}^g \exp\left[\frac{w_{AB}(\bar{\mu}^g_{AB} - \bar{\mu}^\circ_{AB})}{R\theta}\right]\left[1 - \exp\left(\frac{\Delta\bar{\mu}^g}{R\theta}\right)\right] \leq 0, \tag{2.125}$$

which is trivially satisfied when $\Delta\bar{\mu}^g \leq 0$, i.e., when the forward reaction (decomposition of the $\mathcal{AB}$- molecules) is favored.

The preceeding case study was developed for pedagogical purposes. We are now in a position to generalize the above reasoning to the more relevant (and highly complex) case of a multicomponent system such that N_c chemical reactions (with $N_c \geq 2$) occur in the gas phase. As a starting point, consider the following generic reversible reaction labelled α:

$$\sum_{i=1}^{N_r^\alpha} \nu_i^\alpha \mathcal{I} \rightleftharpoons \sum_{k=1}^{N_p^\alpha} \nu_k^\alpha \mathcal{K}, \tag{2.126}$$

where N_r^α and N_p^α are the numbers of reactants and products (respectively) that contribute to (2.126), and $\{\nu_i^\alpha\}_{i=1}^{N_r^\alpha}$ and $\{\nu_k^\alpha\}_{k=1}^{N_p^\alpha}$ are the stochiometric coefficients associated with the reactants and products respectively (all stochiometric coefficients being positive integers by definition). The reaction rate associated with (2.126) is given by the following relation:

$$\mathcal{R}^\alpha = k_f^\alpha(\theta)\prod_{i=1}^{N_r^\alpha}\left(\frac{\bar{\rho}_i^g}{w_i}\right)^{\nu_i^\alpha} - k_b^\alpha(\theta)\prod_{k=1}^{N_p^\alpha}\left(\frac{\bar{\rho}_k^g}{w_k}\right)^{\nu_k^\alpha}, \tag{2.127}$$

with k_f^α and k_b^α the forward and backward reaction-rate constants (again positive functions of the temperature only). Making use of the definition of the chemical potential for an ideal gas (2.114), we can rewrite as:

$$\mathcal{R}^\alpha = k_f^\alpha(\theta)\prod_{i=1}^{N_r^\alpha}\frac{1}{w_i^{\nu_i^\alpha}}\exp\left[\frac{\nu_i^\alpha w_i(\bar{\mu}_i^g - \bar{\mu}_i^\circ)}{R\theta}\right] - k_b^\alpha(\theta)\prod_{k=1}^{N_p^\alpha}\frac{1}{w_k^{\nu_k^\alpha}}\exp\left[\frac{\nu_k^\alpha w_k(\bar{\mu}_k^g - \bar{\mu}_k^\circ)}{R\theta}\right]. \tag{2.128}$$

If (2.126) were to be the only homogeneous chemical reaction that takes place in the gas phase, the chemical equilibrium would be characterized by the following condition:

$$\sum_{i=1}^{N_r^\alpha}\nu_i^\alpha w_i\bar{\mu}_i^g|_{eq} = \sum_{k=1}^{N_p^\alpha}\nu_k^\alpha w_k\bar{\mu}_k^g|_{eq}, \tag{2.129}$$

from which we can define the equilibrium constant associated with the α-reaction:

$$k_{eq}^\alpha \stackrel{def}{=} \frac{\prod_{k=1}^{N_p^\alpha}\bar{\rho}_k^{g^{\nu_k^\alpha}}}{\prod_{i=1}^{N_r^\alpha}\bar{\rho}_i^{g^{\nu_i^\alpha}}} = \exp\left(-\frac{\Delta\bar{\mu}^\circ}{R\theta}\right), \tag{2.130}$$

where

$$\Delta\bar{\mu}^\circ \stackrel{def}{=} \sum_{k=1}^{N_p^\alpha}\nu_k^\alpha w_k\bar{\mu}_k^\circ - \sum_{i=1}^{N_r^\alpha}\nu_i^\alpha w_i\bar{\mu}_i^\circ.$$

It then follows that the reaction-rate constants are related via the relation:

$$\frac{k_f^\alpha(\theta)}{k_b^\alpha(\theta)} = \frac{\prod_{k=1}^{N_p^\alpha}\left(\frac{\bar{\rho}_k^g}{w_k}\right)^{\nu_k^\alpha}}{\prod_{i=1}^{N_r^\alpha}\left(\frac{\bar{\rho}_i^g}{w_i}\right)^{\nu_i^\alpha}} = \frac{\prod_{i=1}^{N_r^\alpha} w_i^{\nu_i^\alpha}}{\prod_{k=1}^{N_p^\alpha} w_k^{\nu_k^\alpha}} \exp\left(-\frac{\Delta\bar{\mu}^o}{R\theta}\right). \tag{2.131}$$

We can then show that the reaction rate associated with the α-reaction reduces to the following expression:

$$\mathcal{R}^\alpha = \frac{k_f^\alpha(\theta)}{\prod_{i=1}^{N_r^\alpha} w_i^{\nu_i^\alpha}} \prod_{i=1}^{N_r^\alpha} \exp\left[\frac{\nu_i^\alpha w_i(\bar{\mu}_i^g - \bar{\mu}_i^o)}{R\theta}\right]\left[1 - \exp\left(\frac{\Delta\bar{\mu}^g}{R\theta}\right)\right], \tag{2.132}$$

where

$$\Delta\bar{\mu}^g \stackrel{def}{=} \sum_{k=1}^{N_p^\alpha} \nu_k^\alpha w_k \bar{\mu}_k^g - \sum_{i=1}^{N_r^\alpha} \nu_i^\alpha w_i \bar{\mu}_i^g. \tag{2.133}$$

It can then easily be seen from (2.132) that if $\Delta\bar{\mu}^g \leq 0$, then $\mathcal{R}^\alpha \geq 0$, i.e., the forward reaction is favored.

Finally, when N_c homogeneous chemical reactions occur in the gas phase, each reaction α involving N_r^α reactants and N_p^α products, the dissipation inequality (2.113) reduces to the following:

$$\sum_{\alpha=1}^{N_c}\left(\sum_{m=1}^{N_p^\alpha} w_m \nu_m^\alpha \bar{\mu}_m^g - \sum_{m=1}^{N_r^\alpha} w_m \nu_m^\alpha \bar{\mu}_m^g\right)\mathcal{R}^\alpha \leq 0, \tag{2.134}$$

so that, if (2.133) is negative for each α ($1 \leq \alpha \leq N_c$), then (2.134) is satisfied, thus insuring that all such chemical reactions occurring in a mixture of ideal gases are compatible with the second law of Thermodynamics.

2.5.3 The solid phase

Consider the dissipation inequality in the bulk phase away from the surface (2.90). We make the constitutive assumption that the Helmholtz free energy density of the film phase depends on the state of strain in the bulk via the deformation gradient F,

the temperature field θ and the chemical composition of the film via the bulk species mass densities $\{\rho_k^f\}_{k=1}^N$:

$$\psi^f \stackrel{def}{=} \psi^f(\theta,\ F,\ \{\rho_k^f\}_{k=1}^N).$$

Using the Coleman-Noll procedure, we can then show that, in order for the dissipation inequality in the film not to be violated, i.e., for (2.90) to hold for all admissible thermodynamic processes (where an admissible thermodynamic process bears the same definition as was introduced within the context of the Eulerian study of a single phase viscous fluid), we can show that the following constitutive relations should be satisfied:

$$\eta^f = -\frac{\partial \psi^f}{\partial \theta},\ S^f = \frac{\partial \psi^f}{\partial F},\ \text{ and }\ \mu_k^f = \frac{\partial \psi^f}{\partial \rho_k^f},\ \forall\ k = 1, \ldots, N.$$

Consequently, the bulk dissipation inequality reduces to:

$$\sum_{k=1}^{N} h_k^f \cdot \nabla \mu_k^f + q^f \cdot \nabla(\ln \theta) \leq 0.$$

It can be then shown that the following constitutive relations are consistent with the bulk dissipation inequality (cf. [GV1]):

$$q^f = -k^f \nabla(\ln \theta) - \sum_{k=i}^{N} k_i^f \nabla \mu_i^f, \qquad \text{and} \tag{2.135}$$

$$h_k^f = -D_k^f \nabla(\ln \theta) - \sum_{i=1}^{N} D_{ki}^f \nabla \mu_i^f, \qquad \forall\ k = 1, \ldots, N, \tag{2.136}$$

if the matrix

$$\mathbf{K}^f = \mathbf{K}^f(\nabla(\ln \theta),\ \{\nabla \mu_i^f\}_{i=1}^N,\ \theta,\ F,\ \{\rho_i^f\}_{i=1}^N) \stackrel{def}{=} \begin{bmatrix} k^f & k_1^f & \cdots & k_N^f \\ D_1^f & D_{11}^f & \cdots & D_{1N}^f \\ \vdots & \vdots & & \vdots \\ D_N^f & D_{N1}^f & \cdots & D_{NN}^f \end{bmatrix}$$

is such that $\mathbf{K}^f(0,\ 0,\ \theta,\ F,\ \{\rho_k^f\}_{k=1}^N)$ is positive semi-definite.

2.5.4 The surface phase

Consider the dissipation inequality along the surface (2.92). If we make the constitutive assumption that the interfacial helmholtz free energy density is dependent on the temperature at the surface, the average deformation gradient, the local orientation of the surface (via its dependence on n_s), as well as the chemical composition of the surface via $\{\rho_k^s\}_{k=1}^N$, i.e., if

$$\psi^s \stackrel{def}{=} \psi(\theta, \{\rho_k^s\}_{k=1}^N, \langle F\rangle, n_s),$$

then, it follows from the Coleman-Noll procedure that the below constitutive relations should hold in order for (2.92) to be satisfied for all admissible thermodynamic processes:

$$\begin{aligned}
\eta^s &= -\frac{\partial \psi^s}{\partial \theta}, \\
\mu_k^s &= \frac{\partial \psi^s}{\partial \rho_k^s},\ \forall\ k = 1, \ldots, N, \\
S^s &= \frac{\partial \psi^s}{\partial \langle F\rangle}, \qquad \text{and} \\
c &= \frac{\partial \psi^s}{\partial n_s} - S^{sT}\langle F\rangle n_s.
\end{aligned}$$

Consequently, the surface dissipation inequality reduces to:

$$\sum_{k=1}^N h_k^s \cdot \nabla_s \mu_k^s + q^s \cdot \nabla_s(\ln\theta) + \sum_{k=1}^N \mu_k^s R_k^s + f v_s + \sum_{k=1}^N (\mu_k^g - \mu_k^s) J_k^g + \sum_{k=1}^N (\mu_f^g - \mu_k^s) J_k^f \leq 0. \tag{2.137}$$

Consider an admissible thermodynamic process such that the surface satisfies the condition of local equilibrium (i.e., the driving force at the surface f is nearly null and the species chemical potentials are continuous across the interface, that is, $\mu_k^g =$

$\mu_k^f = \mu_k^s,\ \forall\ k = 1, \ldots, N$). Assume in addition that the interfacial species are not chemically reactive. The dissipation inequality (2.92) reduces to:

$$\sum_{k=1}^{N} h_k^s \cdot \nabla_s \mu_k^s + q^s \cdot \nabla_s (\ln \theta) \leq 0,$$

from which we deduce that the following constitutive relations for the interfacial heat and species diffusive fluxes

$$h_k^s = -\sum_{i=1}^{N} D_{ki}^s \nabla_s \mu_i^s - D_k^s \nabla_s (\ln \theta), \qquad \text{and} \tag{2.138}$$

$$q^s = -\sum_{i=1}^{N} k_i^s \nabla_s \mu_i^s - k^s \nabla_s (\ln \theta) \tag{2.139}$$

are compatible with the dissipation inequality at the surface if

$$\mathbf{K}^s = \mathbf{K}^s(\nabla_s(\ln\theta),\ \{\nabla_s \mu_i^s\}_{i=1}^N,\ \theta,\ \{\rho_i^s\}_{i=1}^N) \stackrel{def}{=} \begin{bmatrix} k^s & k_1^s & \cdots & k_N^s \\ D_1^s & D_{11}^s & \cdots & D_{1N}^s \\ \vdots & \vdots & & \vdots \\ D_N^s & D_{N1}^s & \cdots & D_{NN}^s \end{bmatrix}$$

is such that $\mathbf{K}^s(0,\ 0,\ \theta,\ \{\rho_k^s\}_{k=1}^N)$ is positive semi-definite.

Consider now an admissible process such that the surface species are diffusionless as well as chemically reactionless and suppose there is no interfacial heat conduction. Assume in addition that the surface is stationary (i.e., $v_n \simeq 0$). The interfacial dissipation inequality then reduces to:

$$\sum_{k=1}^{N} (\mu_k^g - \mu_k^s) J_k^g + \sum_{k=1}^{N} (\mu_k^f - \mu_k^s) J_k^f \leq 0. \tag{2.140}$$

The following constitutive relations

$$J_k^\alpha = J_k^\alpha(\theta, \{\rho_i^\alpha, \rho_i^s\}_{i=1}^N) \tag{2.141}$$

are compatible with the dissipation inequality if

$$\sum_{k=1}^{N}(\mu_k^{\alpha} - \mu_k^{s})J_k^{\alpha}(\theta, \{\rho_i^g, \rho_i^s\}_{i=1}^N) \leq 0. \tag{2.142}$$

Typically, the deposition of the k^{th} species along the surface can be modeled as a reversible adsorption/desorption reaction of the following form:

$$\mathcal{K}(g) \rightleftharpoons \mathcal{K}(s) \tag{2.143}$$

where $\mathcal{K}(g)$ and $\mathcal{K}(s)$ denote the k^{th} species in the gas phase and along the surface respectively. Let $k_f(\theta)$ and $K_b(\theta)$ be the reaction-rate constants associated with the adsorption and desorption reactions respectively. The k^{th} deposition flux can then be written as

$$J_k^g = -(k_f(\theta)\rho_k^g - k_b(\theta)\rho_k^s), \tag{2.144}$$

where the first minus sign on the RHS of (2.144) accounts for the fact that more adsorption is assumed to be taking place than desorption. At equilibrium, the forward and backward reactions have identical rates, i.e.,

$$k_f(\theta)\rho_k^g|_{eq} = k_b(\theta)\rho_k^s.$$

It follows that the k^{th} deposition flux can be rewritten as

$$J_k^g = -k_f(\theta)(\rho_k^g - \rho_k^g|_{eq}). \tag{2.145}$$

Now suppose the k^{th} gaseous species behaves like an ideal gas. Consequently, its chemical potential is given by the following thermodynamic formula:

$$\mu_k^g = \mu_k^{g\circ}(\theta) + R_k\theta \ln \rho_k^g. \tag{2.146}$$

From (2.146) it follows that

$$\rho_k^g = \rho_k^g|_{eq} \exp\left(\frac{\mu_k^g - \mu_k^g|_{eq}}{R_k\theta}\right). \tag{2.147}$$

Again, at equilibrium, we have

$$\mu_k^s = \mu_k^g|_{eq}. \tag{2.148}$$

From (2.147) and (2.148), it follows that

$$J_k^g = -\Omega_k(\theta) \exp\left(\frac{\mu_k^g - \mu_k^s}{R_k\theta}\right), \tag{2.149}$$

where

$$\Omega_k(\theta) \stackrel{def}{=} k_f(\theta)\rho_k^g|_{eq} > 0,$$

so that (2.140) is satisfied when

$$\mu_k^g \geq \mu_k^s, \tag{2.150}$$

and

$$\sum_{k=1}^{N}(\mu_k^f - \mu_k^s)J_k^f \leq 0. \tag{2.151}$$

The condition (2.150) is in fact a necessary condition for deposition to take place and is assumed to be satisfied, so that (2.140) reduces to (2.151). Finally, we note that, for small deviations from equilibrium, (2.149) can be approximated by

$$J_k^g \cong \bar{\Omega}_k(\mu_k^g - \mu_k^s), \tag{2.152}$$

where

$$\bar{\Omega}_k \stackrel{def}{=} \frac{\Omega_k}{R_k \theta}.$$

Next consider an admissible *isothermal* thermodynamic process such that the surface is in equilibrium locally (as defined above), and the surface species are diffusionless. The interfacial dissipation inequality can then be written as:

$$\sum_{k=1}^{N} \mu_k^s R_s^k \ \leq \ 0$$

which would be satisfied by the following constitutive assumptions on the chemical production rates:

$$\forall \ k = 1, \ldots, N, \qquad R_k^s \stackrel{def}{=} R_k^s(\theta, \{\rho_i^s\}_{i=1}^N) \tag{2.153}$$

if

$$\sum_{k=1}^{N} \mu_k^s R_k^s(\theta, \{\rho_i^s\}_{i=1}^N) \leq 0. \tag{2.154}$$

We note here that, if one can treat the superficial species as ideal gases (a reasonable approximation in the limit of very low densities of adatoms along the surface), then a reasoning similar to the one developed in section (2.5.2) shows that the dissipation inequality along the interface (2.154) is not violated.

Finally, consider an evolving surface such that there is no interfacial heat conduction, species diffusion or adsorption-desorption between the bulk phases and the surface. (2.92) reduces to:

$$f v_n \leq 0,$$

from which we see that a *kinetic relation*[6] between the driving force and the normal

[6]The notion of kinetic relation was first introduced by Abeyaratne & Knowles, cf. [AK].

interfacial velocity of the form

$$f = -\beta(\theta)v_n \tag{2.155}$$

would not violate the interfacial dissipation inequality if $\beta(\theta)$ is a positive scalar function of temperature.

2.6 Formulation of the Free Boundary Problem

2.6.1 The fluid phase

In what follows, the bars and the y subscript are omitted in order to simplify an already quite cumbersome notation. The governing equations for the viscous fluid flow can be summarized as follows:

(i) The species equations:

$$\frac{\partial \rho_k^g}{\partial t} + \nabla \cdot (\rho_k^g v) = -\nabla \cdot h_k^g + R_k^g, \qquad \forall\ k = 1, \ldots, N. \tag{2.156}$$

(ii) The linear momentum equation:

$$\frac{\partial}{\partial t}(\rho^g v) + \nabla \cdot (\rho^g v \otimes v) = \nabla \cdot T + b, \tag{2.157}$$

where we have the following constitutive relations:

$$\begin{aligned} \psi^g &= \psi^g(\theta, \rho^g, \{Y_k^g\}_{k=1}^N), \\ p &= -\rho^{g2}\frac{\partial \psi^g}{\partial \rho^g}, \qquad \text{and} \\ T &= -(p - \frac{2}{3}\,\mu tr D)\mathbf{1} + 2\mu D, \end{aligned} \tag{2.158}$$

and b is the body force density (e.g., gravity in the case of vertical CVD reactors).

(iii) The energy equation:

$$\rho^g \frac{d\epsilon^g}{dt} - T \cdot D + \nabla \cdot q^g - Q^g + \sum_{k=1}^{N} \nabla \cdot (\mu_k^g h_k^g) = 0, \tag{2.159}$$

with the following constitutive relations:

$$\begin{aligned}
\epsilon^g =& \psi^g - \theta \frac{\partial \psi^g}{\partial \theta}, \\
\mu_k^g =& \frac{\partial \psi^g}{\partial Y_k^g}, \qquad \forall\ k = 1, \ldots, N, \\
q^g =& -k^g(\theta) \nabla(\ln \theta) - \sum_{i=1}^{N} k_i^g(\theta, \{\rho_m^g\}_{m=1}^N) \nabla \mu_i^g, \\
h_k^g =& -D_k^g(\theta, \{\rho_m^g\}_{m=1}^N) \nabla(\ln \theta) - \sum_{i=1}^{N} D_{ki}^g(\theta) \nabla \mu_i^g, \quad \forall\ k = 1, \ldots, N, \text{ and} \\
R_k^g =& R_k^g(\theta, \{\mu_i^g\}_{i=1}^N), \qquad \forall\ k = 1, \ldots, N,
\end{aligned} \tag{2.160}$$

where

$$\mathbf{K}^g = \mathbf{K}^g(\theta,\ \{\rho_i^g\}_{i=1}^N) \stackrel{def}{=} \begin{bmatrix} k^g & k_1^g & \cdots & k_N^g \\ D_1^g & D_{11}^g & \cdots & D_{1N}^g \\ \vdots & \vdots & & \vdots \\ D_N^g & D_{N1}^g & \cdots & D_{NN}^g \end{bmatrix}$$

is positive-definite, and

$$\sum_{k=1}^{N} \mu_k^g R_k^g(\theta, \{\mu_i^g\}_{i=1}^N) \leq 0.$$

It should be noted that we have $N + 5$ unknown scalar variables: the N species densities $\{\rho_k^g\}_{k=1}^N$, the three components of the velocity field v, the pressure p and the temperature θ. We also have $N + 5$ scalar equations: the N species equations, the three projections of the linear momentum equation along a given set of coordinate axes, the energy balance, as well as the constitutive relation (2.158) which gives the pressure if a well suited constitutive relation for the Helmohltz free energy of the gas

phase is postulated. So that, a priori, and given an appropriate set of initial and boundary conditions, the problem is well-posed in the fluid flow phase.

2.6.2 Specialization to the case of a multicomponent ideal gas

Assume the gas mixture behaves like an ideal gas. Consequently, we have:

$$\epsilon^g = c_v^g \theta,$$

where $c_v^g \stackrel{def}{=} \sum_{i=1}^{N} Y_i^g c_{v,i}^g$ is a constant.

Now, the flow being viscous, and making use of the continuity equation, we can rewrite the energy balance as:

$$\rho^g c_v^g \frac{d\theta}{dt} + \nabla \cdot q^g - Q^g - R\theta \frac{d\rho^g}{dt} - \tau \cdot D + \sum_{k=1}^{N} \nabla \cdot (\mu_k^g h_k^g) = 0, \tag{2.161}$$

where we have also made use of the ideal-gas equation of state[7]:

$$p = \rho^g R\theta. \tag{2.162}$$

Adding and subtracting the term $R\rho^g \frac{d\theta}{dt}$ to (2.161), and making use of (2.162) as well as the relation between specific heat at constant pressure and specific heat at constant volume for an ideal gas, i.e., $c_p^g = c_v^g + R$, we obtain the following energy balance for a multicomponent ideal gas:

$$\rho^g c_p^g \frac{d\theta}{dt} - \frac{dp}{dt} - \tau \cdot D + \nabla \cdot q^g - Q^g + \sum_{k=1}^{N} \nabla \cdot (\mu_k^g h_k^g) = 0. \tag{2.163}$$

[7]which is to be viewed as a specialization of (2.158) to the case of an ideal gas

2.6.3 The bulk of the thin solid film

We confine ourselves to the (physically relevant) quasi-static case and assume in addition that the thin film behaves like a linearly elastic solid. Consequently, the formulation is based on the dispacement field rather than the deformation field (linear elasticity) and inertia will be neglected. In the context of linear elasticity, there is no formal distinction between the reference and current configurations, so that differentiation in the equations to follow is with respect to spatial coordinates, thus yielding a set of equations compatible with those governing the behavior of the gas phase. The governing equations in the bulk can then be listed as follows:

(i) The species equations[8]:

$$\frac{\partial \rho_k^f}{\partial t} + \nabla \cdot h_k^f = 0, \qquad \forall\ k = 1, \ldots, N, \tag{2.164}$$

with:

$$\begin{aligned} \psi^f &= \psi^f(\theta, \{\rho_k^f\}_{k=1}^N, E), \\ \mu_k^f &= \frac{\partial \psi^f}{\partial \rho_k^f}, \qquad \forall\ k = 1, \ldots, N, \qquad \text{and} \\ h_k^f &= -D_k^f(\theta, \{\rho_k^f\}_{k=1}^N)\nabla(\ln\theta) - \sum_{i=1}^{N} D_{ki}^f(\theta)\nabla\mu_i^f, \ \forall\ k = 1, \ldots, N, \end{aligned} \tag{2.165}$$

where $E \stackrel{def}{=} \frac{1}{2}(\nabla u + \nabla u^T)$ is the infinitesimal strain tensor.

(ii) The balance of forces[9]:

$$\nabla \cdot T = 0,$$

where:

$$T \stackrel{def}{=} \mathbf{C}^f(\theta, \{\rho_k^f\}_{k=1}^N)E. \tag{2.166}$$

[8] in the absence of homogeneous chemical reactions in the solid phase

[9] in the absence of body forces

Notice that the tensor of elastic moduli is not only a function of the temperature but also of the local chemical composition of the thin solid film.

(iii) The energy balance:

$$\frac{\partial \epsilon^f}{\partial t} - T \cdot \dot{E} + \nabla \cdot q^f - Q^f + \sum_{k=1}^{N} \nabla \cdot (\mu_k^f h_k^f) = 0,$$

where:

$$\begin{aligned} \epsilon^f &= \psi^f - \theta \frac{\partial \psi^f}{\partial \theta}, \\ q^f &= -k^f(\theta) \nabla (\ln \theta) - \sum_{i=1}^{N} k_i^f(\theta, \{\rho_k^f\}_{k=1}^N) \nabla \mu_i^f, \end{aligned}$$

with T given by (2.166), and the matrix

$$\mathbf{K}^f = \mathbf{K}^f(\theta,\ \{\rho_i^f\}_{i=1}^N) \stackrel{def}{=} \begin{bmatrix} k^f & k_1^f & \cdots & k_N^f \\ D_1^f & D_{11}^f & \cdots & D_{1N}^f \\ \vdots & \vdots & & \vdots \\ D_N^f & D_{N1}^f & \cdots & D_{NN}^f \end{bmatrix}$$

is positive-definite.

Again, it should be noted that we have as many scalar unknowns as we have scalar equations (the unknowns being the N species densities $\{\rho_k^f\}_{k=1}^N$, the three components of the displacement field and the temperature field, the equations being the N species equations, the three components of the force balance and the energy balance.

2.6.4 The equations governing the evolution of the interface

We consider a structured surface endowed with a surface energy and interfacial species densities, i.e., the surface can sustain mass and we account for its anisotropy via the dependence of the surface energy density on the outer unit normal field. Moreover, we neglect the superficial elastic stresses. In addition, we confine ourselves to the

quasi-static situation, and consequently inertia will be neglected along the surface[10]. Finally, we assume that there is no slip along the interface, i.e., the tangential component of the velocity jump across the interface is identically zero. This, in addition to the requirement that the surface be coherent, i.e., the normal component of the velocity jump is null, yields the continuity of the material velocity across the evolving film-gas interface. But the bulk phase being quasi-static, this continuity condition reduces to a zero gas-phase velocity at the surface. It then follows that the governing equations at the surface reduce to:

(i) The species equations:

$$\overset{\circ}{\rho}{}^s_k - ([[\rho_k]] + \rho^s_k \kappa) v_n + [[h_k]] \cdot n_s + \nabla_s \cdot h^s_k - R^s_k = 0, \tag{2.167}$$

where the superficial species diffusive fluxes are given by:

$$h^s_k = -D^s_k(\theta, \{\rho^s_k\}_{k=1}^N) \nabla_s (\ln \theta) - \sum_{i=1}^{N} D^s_{ki}(\theta) \nabla(\mu^s_i), \qquad \forall\ k = 1, \ldots, N,$$

where the chemical production rates are given by (2.153).

(ii) The species flux-matching conditions: $\forall\ k = 1, \ldots, N$,

$$\begin{aligned} -\rho^g_k v_n &= -\, h^g_k \cdot n_s + J^g_k, \qquad \text{and} \\ \rho^f_k v_n &= h^f_k \cdot n_s + J^f_k, \end{aligned} \tag{2.168}$$

where the gas and film species diffusive fluxes are given by (2.160) and (2.165) respectively, and the adsorption-desorption species fluxes are given by (2.141).

Consider the single-species case (so that there are no chemical reactions taking place along the surface), in the absence of surface diffusion and such that the super-

[10]Neglecting inertia at the surface would have also been a physically reasonable approximation in the limit where the interfacial species densitites can be ignored, i.e., if they are negligible with respect to, say, the bulk species densities.

ficial mass density is negligible with respect to the bulk mass density. Consequently, (2.167) reduces to

$$[[\rho]]v_n = [[h]] \cdot n_s.$$

Adding the two equations (2.168), we obtain:

$$[[\rho]]v_n = [[h]] \cdot n_s + J^f + J^g.$$

Now, combining the above two equations yields the following relation:

$$J^f = -J^g.$$

Next, we note that there is no bulk diffusion in a single-species film, so that the second equation in (2.168) reduces to

$$v_n = -\frac{1}{\rho^f} J^g,$$

which, for small deviations away from equilibrium, can be rewritten as

$$v_n = \frac{\bar{\Omega}}{\rho^f}(\mu^g - \mu^s). \tag{2.169}$$

The linear growth law (2.169) is often known as the Hertz-Knudsen formula (cf. Saito [S]).

(iii) The continuity-of-traction condition:

$$T^f n_s = 0, \tag{2.170}$$

where we have assumed that the gas-phase stresses are negligible when compared to those of the bulk along the surface.

(iv) The surface energy equation:

$$\overset{\circ}{\epsilon}^s - f v_n + c \cdot \overset{\circ}{n}_s + [[q]] \cdot n_s + \nabla_s \cdot q^s - Q^s + \sum_{k=1}^{N} \nabla_s \cdot (\mu_k^s h_k^s) + \sum_{k=1}^{N} [[\mu_k h_k]] \cdot n_s = 0, \tag{2.171}$$

where:

$$\begin{aligned}
\psi^s &= \psi^s(\theta, n_s, \{\, \rho_i^s \}_{i=1}^N), \\
\epsilon^s &= \psi^s - \theta \frac{\partial \psi^s}{\partial \theta}, \\
c &= -\frac{\partial \psi^s}{\partial n_s}, \\
\mu_k^s &= \frac{\partial \psi^s}{\partial \rho_k^s}, \forall\ k = 1, \ldots, N, \\
q^s &= -k^s(\theta) \nabla_s (\ln \theta) - \sum_{i=1}^{N} k_i^s(\theta, \{\rho_k^s\}_{k=1}^N) \nabla_s \mu_i^s, \qquad \text{and} \\
f &= [[G]] + G^s \kappa + \nabla_s \cdot c.
\end{aligned} \tag{2.172}$$

In the absence of interfacial structure (i.e., in the absence of superficial mass), the RHS of (2.172) includes the additional term $-n_s \cdot [[F^T S]] n_s$. The no-slip condition (i.e., the requirement that the material velocity be continuous across the interface) reduces this additional contribution to $-[[F]] n_s \cdot \langle S \rangle n_s$. In the context of linear elasticity, this is equivalent to $-[[\nabla u]] n_s \cdot \langle T \rangle n_s$ (cf., e.g., [GV2] or [LS]). Moreover, if the approximation of negligible gas-phase stresses at the surface is made, then (2.170) cancels this last term, thus yielding the expression (2.172) for the driving force at the interface (cf. [GV]). By contrast, in the case of an interface separating two *solid* bulk phases, this supplementary term cannot be neglected.

(v) The kinetic relation:

$$f = \beta(\theta) v_n, \tag{2.173}$$

where β is a positive function of temperature.

The unknown variables along the surface are the N superficial species densities $\{\rho_k^s\}_{k=1}^N$ and the normal velocity of the interface v_n. The corresponding $N+1$ equations are the surface species equations and the kinetic relation. Thus, the problem seems a priori to be well-posed at the surface, and the explicit determination of those unknowns (given appropriate initial and boundary conditions) would allow us to account for the morphological evolution of the interface (i.e., the growth of the thin solid film). The species flux-matching conditions provide boundary conditions for the species equations in the gas and bulk phases. The interfacial energy balance (2.171) combined with the requirement that the temperature be continuous across the interface constitute the boundary conditions needed to determine the temperature profiles in the bulk phases. Finally, the jump condition (2.170) combined with the requirement that there be no slip along the coherent surface represent the necessary boundary conditions at the evolving surface needed to solve for the velocity field in the gas phase and the dispacement field in the bulk of the thin film.

2.7 Special Cases

2.7.1 The case of local equilibrium

In what follows, local equilibrium means a vanishingly small driving force along the evolving interface whose normal velocity is taken to be finite. In addition to local equilibrium, a number of assumptions will be made. We believe that these assumptions constitute physically reasonable approximations to the conditions under which some growth processes are operated. Begin by considering the case of a structured surface (in the sense of a moving surface endowed with a surface energy density) that cannot sustain mass, i.e., $\forall\ k = 1, \ldots, N$,

$$\rho_k^s \simeq 0. \tag{2.174}$$

By a surface which cannot sustain mass we mean that the superficial species densities are very small if compared to, say, the bulk species densities. Consequently,

these interfacial species density fields can be neglected in the equations describing the morphological evolution of the surface, thus the approximations (2.174). But the superficial chemical potentials cannot be neglected. We also assume that the superficial diffusive flux associated with a given species along the interface is proportional to the surface gradient of the chemical potential of the species in question. This last assumption is consistent with the fact that the surface species are very dilute. We can thus write the species equations (2.167) as follows:

$$[[\rho_k]]v_n \;=\; [[h_k]] \cdot n_s - \nabla_s \cdot h_k^s + R_k^s. \tag{2.175}$$

Moreover, we consider only small departures from chemical equilibrium along the gas-surface interface, i.e., for any chemical species, its deposition flux (from the gas phase) is proportional to the jump in its chemical potential across the interface separating the gas phase from the superficial one. In addition, we restrict ourselves to the isothermal case, a reasonable approximation when the substrate on top of which the film is growing is maintained at a fixed constant temperature and the film is of negligible thickness so that temperature variations across its height can be reasonably ignored. It follows that the surface species diffusivities, which in the dilute limit are functions of the temperature only, are constant. Consequently, (2.175) reduces to:

$$-[[\rho_k]]v_n \;=\; -[[h_k]] \cdot n_s + D_k^s \Delta_s \mu_k^s + R_k^s(\{\mu_i^s\}_{i=1}^N). \tag{2.176}$$

Also, if we assume the continuity of the chemical potential across the film-surface interface, i.e., if $\mu_k^f \;=\; \mu_k^s$, then the equation (2.28), the definition (2.91), and the constitutive assumption (2.152) yield the following result: $\forall\; k = 1, \ldots, N$,

$$h_k^f \cdot n_s \;=\; 0.$$

Making use of (2.27), it then follows that (2.176) reduces to:

$$\rho_k^f v_n \;=\; -J_k^g + D_k^s \Delta_s \mu_k^s + R_k^s(\{\mu_i^s\}_{i=1}^N),$$

which, having assumed small departures from chemical equilibrium at the gas-surface interface, can be rewritten as:

$$\rho_k^f v_n = \lambda_k^g(\mu_k^g - \mu_k^s) + D_k^s \Delta_s \mu_k^s + R_k^s(\{\mu_i^s\}_{i=1}^N). \tag{2.177}$$

If we consider now the case of a growing film of fixed chemical composition, i.e., ρ_k^f is constant, and treat the gas phase as a resevoir, i.e., μ_k^g is constant, we obtain the following equations: $\forall\ k = 1, \ldots, N$,

$$v_n = A_k + B_k \mu_k^s + C_k \Delta_s \mu_k^s + \frac{1}{\rho_k^f} R_k^s(\{\mu_i^s\}_{i=1}^N), \tag{2.178}$$

with

$$A_k = \frac{\lambda_k^g}{\rho_k^f}\mu_k^g, \quad B_k = -\frac{\lambda_k^g}{\rho_k^f}, \quad \text{and} \quad C_k = \frac{D_k^s}{\rho_k^f}.$$

If we now restrict our attention to *isotropic* surfaces, i.e., the surface shear c is identically zero, the local equilibrium condition, i.e., the zero-driving-traction condition, reduces to:

$$\sum_{k=1}^{N} \rho_k^f \mu_k^s = \psi^f - \psi^g + \sum_{k=1}^{N} \rho_k^g \mu_k^g - \sigma\kappa, \tag{2.179}$$

where, because of the assumptions of constant temperature, fixed chemical composition of the film, isotropic surface which cannot sustain mass, and the approximation of the gas phase as a reservoir, ψ^g, $\{\rho_k^g\}_{k=1}^N$ and $\sigma = \psi^s$ are all constant.

It follows that (2.178)-(2.179) represent a set of $N+1$ partial differential equations for the $N+1$ scalar variables $\{\mu_k^s\}_{k=1}^N$ and v_n.

2.7.2 Specialization of the local equilibrium case to single-species systems

We now specialize to the case of a single-species system. Consequently, there are no chemical reactions occurring at the surface. It follows that (2.179) yields the following standard relation between the surface chemical potential and the interfacial curvature (cf. Herring [H1] and Mullins [M]):

$$\mu^s = a + b\kappa, \tag{2.180}$$

where:

$$a = \frac{\psi^f - \psi^g + \mu^g \rho^g}{\rho^f}, \qquad \text{and} \qquad b = -\frac{\sigma}{\rho^f}.$$

Finally, (2.178) yields the following relation between the growth velocity and the curvature of the surface (cf. Mullins [M], Davi and Gurtin [DG] and Spencer et al. [SVD]):

$$v_n = c_1 + c_2\kappa + c_3\Delta_s(\psi^f - \sigma\kappa), \tag{2.181}$$

with:

$$\begin{aligned} c_1 &= \frac{\lambda^g}{\rho^{f^2}}\{\psi^g - \psi^f + (\rho^f - \rho^g)\mu^g\}, \\ c_2 &= -\frac{\lambda^g \sigma}{\rho^{g^2}}, \qquad \text{and} \\ c_3 &= \frac{D^s}{\rho^{f^2}}, \end{aligned}$$

where it is important to notice that the influence of the stress in the bulk of the film on the morphological evolution of the moving surface is 'buried' in the dependence of the bulk Helmholtz free energy ψ^f on the infinitesimal strain tensor E.

2.8 Discussion

We conclude by briefly comparing our approach to that developed in the more classical continuum treatments of mixtures in an attempt to justify a posteriori our methodological choices. In the classical treatment of mixtures, a fundamental postulate of the theory is that, for a mixture of N constituents ($N \geq 2$), each constituent be modeled as a distinct continuum. The superposition of these N separate continua then forms the mixture of interest. More specifically, in the material space, there would be as many reference configurations as there are constituents present in the mixture. To each distinct reference configuration Ω_k, there corresponds an independent motion y_k mapping the reference configuration in question into the *unique* current configuration (i.e., the time-dependent region in the physical space occupied by the mixture which is 'visible' to the experimental observer). The constituent (or partial) velocities are then defined as the time detivatives of the various mappings introduced above. In addition, one would define partial stresses to account for the contact forces on a given constituent resulting from contact with all the other constituents. Moreover, one would need to introduce two additional fields that do not appear in the theory for single continua: the local forces acting on a given constituent and the local energy supply to that constituent, both due to the presence of the other constituents and the need to account for the interactions among different constituents (for an extensive discussion of the classical mixture theory, we refer the reader to [BD]). One would also have to formulate, in the current configuration, the fundamental balances laws (i.e., the conservation of mass, the linear and angular momenta equations, and the energy balance) for each of the constituents present in the mixture. Finally, an adequate version of the Clausius-Duhem inequality would then impose restrictions on the constitutive assumptions one can make on the various fields introduced above.

As is obvious from the discussion above, the classical mixture theory requires a large number of constitutive relations (and the more constituents we have, the larger the number of constitutive assumptions we would have to make). By introducing the notions of a *single* stress tensor and a *single* velocity field, we have chosen to approach

the issue of the presence of many constituents differently, in part to avoid making a large number of constitutive assumptions. But our main motivation for doing so can be stated as follows: when one writes balance laws for each of the constituents present in the mixture, one is implicitly treating each constituent as a separate phase. This formualtion is best suited for *immiscible* mixtures, i.e., those mixtures whose 'constituents remain physically separate on a scale which is large in comparison with molecular dimensions' (Drumheller). Typical examples of immiscible mixtures are bubbly liquids (e.g., a nonreacting mixture of a Newtonian fluid and a gas with a single temperature), fluid-saturated porous media, etc. The gas mixtures used in chemical vapor deposition processes cannot be treated as immiscible mixtures, precisely because the mixing is such that the various chemical species present are not separable at the macroscopic level. Consequently, the gas-mixture flow is best modeled as a single phase (with a single temperature field), thus requiring one set of balance laws rather than as many as there are species present.

Chapter 3 Multicomponent Gas Flow in a Vertical Axisymmetric CVD Reactor

3.1 Formulation of the Problem

3.1.1 Framework

In the present chapter, we investigate the flow of a multicomponent gas in a vertical axisymmetric stagnation-point flow CVD reactor. The physical setting is that shown in Figure 2.1 of chapter 2. Our goal is to examine the conditions under which the similarity solution first introduced by von Kármán [K] holds. The similarity solution is of interest to the practitioners of CVD of compound thin films mainly because it insures the uniformity of the chemical composition of the growing thin film. Our procedure consists of an asymptotic analysis of the flow equations in the limit of small Mach number and small aspect ratio (defined here as the ratio of the height of the reactor channel to the radius of the substrate on which the deposition takes place). This approach was applied first by Hariharan et al. [YHC] to a vertical reactor of a different geometry in the context of a dilute single-species flow.

The axisymmetric geometry leads to the choice of a cylindrical system of coordinates within which to express the equations that govern the gaseous flow. The multispecies viscous flow enters the chamber via a horizontal showerhead, which can, for simplicity, be modeled as a porous plate and its entrance velocity is assumed to be vertical (downward-oriented) and spatially uniform. The heated substrate on top of which the deposition of the thin solid film takes place is located below the showerhead at a distance L and is modeled as a thick horizontal plate whose radius r_s is the same as that of the showerhead. Typically, the substrate is undergoing a rotational motion whose purpose is to ensure a better uniformity of the deposited film, but for

the sake of simplicity, we shall assume (without loss of much generality since the main features of the flow will still be identified) that the substrate is fixed. Consequently, the circumferential component of the velocity field is identically zero (and the circumferential momentum balance is thus trivially satisfied). Also, the axial symmetry of the reactor implies that none of the flow fields of interest depends on the angular coordinate ϕ.

We limit our investigation to the case of a very dilute mixture, i.e., the various chemical reactants are assumed to be highly diluted in a single carrier *inert* gas (usually hydrogen or nitrogen). Such a limiting case is arguably a physically reasonable approximation of many CVD processes, in particular, the growth of superconducting $YBa_2Cu_3O_{7-\delta}$ thin films by MOCVD, where the metallorganic precursors carrying the species to be deposited are typically very diluted in nitrogen. As a consequence of the dilute-mixture approximation, we can make the following assumptions:

(i) The material properties of the gas mixture (e.g., the shear viscosity coefficient μ, the heat conductivity k^g, etc.) are assumed to be identical to those of the carrier gas. Consequently, these material properties will be functions of the temperature exclusively (rather than being also dependent on the chemical composition of the mixture in question). Moreover, the Dufour effect (i.e., the heat conduction resulting from the presence of species concentration gradients) is negligible if compared to the heat convection and conduction. It then follows that the heat flux obeys the simplest form of Fourier's law, i.e., it is proportional to the temperature gradient, where the 'constant' of proportionality is the temperature-dependent conductivity of the carrier gas.

(ii) The diffusion of each species is treated as a simple binary diffusion process in the carrier gas. That is, the diffusive mass flux of a given species k ($k = 1, \ldots, N-1$, the N^{th} species being assumed here to be the carrier gas) is proportional to the temperature gradient (the Soret effect) and the density gradient of the species in question to the exclusion of all the other species density gradients. It should be noted here that the Soret effect cannot be neglected as the difference in the temperature between the showerhead and the independently heated substrate can be quite significant (typically

of the order of a few hundred degrees Celsius). More specifically, the diffusive flux of the k^{th} species is given by

$$h_k^g = D_k^c \nabla \rho_k^g + D_k^t \nabla \theta,$$

where the thermal diffusion coefficient has the following functional dependence:

$$D_k^t(\theta, \rho_k^g) = \rho_k^g a_{kc}(\theta, \rho_k^g) D_k^c(\theta),$$

with D_k^t and D_k^c the thermal and 'effective' diffusion coefficients (respectively), a_{kc} the Soret coefficient (where the subscript c denotes the carrier gas), ρ_k^g the partial mass density field of the k^{th} species present in the mixture, and θ the temperature field. In addition, we assume that the diluted species are heavier than the carrier gas, i.e., $\forall\ k = 1, \ldots, N-1$,

$$\rho_k^g \ll \rho^g, \quad w_k > w_c, \quad \sigma_k > \sigma_c,$$

where the subscript c refers to the carrier gas, w_k and w_c are the molar weights of the k^{th} species and the carrier gas (respectively), and σ_k and σ_c are the collision diameters of the molecules of the k^{th} species and the carrier gas (respectively). Moreover, if we assume that the molecules of the various species behave like rigid elastic spheres, then, from the kinetic theory of gases, it can be shown that the Soret coefficients $\{a_{kc}\}_{k=1}^{N-1}$ can be approximated by *constants* (cf. [K] and the references therein).

We will first consider the general case, i.e., the unsteady flow of a chemically reacting multicomponent gas. When solving analytically the first order approximative equations (obtained by expanding asymptotically the flow fields about the Mach number and the aspect ratio), we shall specialize to the case of a steady flow. The steady-state assumption is motivated by the observation that the time scales for convection and diffusion of gaseous species are much smaller than the time scale of growth by deposition of the thin solid film, so that it is reasonable to assume that the equations governing the behavior of the flow are time-independent.

Finally, the gas mixture is assumed to behave like a multicomponent ideal gas, and the flow is modeled as a viscous Newtonian one.

3.1.2 Terminology

Let (r, ϕ, z) be a cylindrical coordinate system in the Euclidean (physical) space, such that the z-axis coincides with the axis of symmetry of the vertical CVD reactor (cf. Figure 2.1). As mentioned above, the geometry of the reactor being axisymmetric, the flow fields depend only on the radial and axial coordinates r and z.

Let ρ^g be the total mass density (per unit current volume) of the gas mixture, and let ρ_k^g be the partial mass density of the k^{th} chemical species present in the gas mixture (we consider the general case of a multicomponent system with N constituents where $N \geq 2$).

Let v be the radial (scalar) velocity field, w the circumferential (scalar) velocity field (identically zero), and u the axial (scalar) velocity field. p denotes the pressure and g is the gravity constant (the only body force of interest, which cannot be neglected in the case of a vertical reactor). Finally, let θ denote the temperature field.

It should be noted that a purely Eulerian approach is adopted here, so that all of the fields defined above are spatial ones. Also, the flow being viscous, the stress tensor can be decomposed into an isotropic elastic component $-p\mathbf{1}$ and a viscous component τ such that $\tau = 2\mu D + \lambda(\nabla \cdot \mathbf{v})\mathbf{1}$, where $\mathbf{v}$ is the (vectorial) velocity field, D is the rate-of-deformation gradient ($D \stackrel{def}{=} \frac{1}{2}(\nabla \mathbf{v} + \nabla \mathbf{v}^T)$), and μ and λ are the shear and bulk viscosities (respectively) and are assumed to be temperature-dependent. Moreover, we make Stoke's hypothesis, i.e., we assume that $\lambda = -\frac{2}{3}\mu$.

The gas mixture being a multicomponent ideal gas, its enthalpy is a function of temperature only and its specific heat at constant pressure C_p^g is a constant. Finally, k^g denotes the thermal conductivity (as it appears in Fourier's law), and it is to be distinguished in what follows from the thermal diffusivity k.

3.1.3 The governing equations

We can now state the equations that determine the behavior of the flow as follows:

(i) The total mass balance (Continuity equation):

$$\frac{\partial \rho^g}{\partial t} + \frac{1}{r}\frac{\partial}{\partial r}(\rho^g v r) + \frac{\partial}{\partial z}(\rho^g u) = 0. \tag{3.1}$$

(ii) The radial momentum equation:

$$\begin{aligned}\rho^g \frac{\partial v}{\partial t} + \rho^g \left(v\frac{\partial v}{\partial r} + u\frac{\partial v}{\partial z} \right) &= -\frac{\partial p}{\partial r} + \frac{2}{r}\frac{\partial}{\partial r}\left[\mu r \left(\frac{\partial v}{\partial r} - \frac{1}{3}\nabla \cdot \mathbf{v} \right) \right] \\ &\quad -\frac{2\mu}{r}\left(\frac{v}{r} - \frac{1}{3}\nabla \cdot \mathbf{v} \right) + \frac{\partial}{\partial z}\left[\mu \left(\frac{\partial u}{\partial r} + \frac{\partial v}{\partial z} \right) \right], \end{aligned} \tag{3.2}$$

where:

$$\nabla \cdot \mathbf{v} \stackrel{def}{=} \frac{\partial v}{\partial r} + \frac{v}{r} + \frac{\partial u}{\partial z}.$$

(iii) The axial momentum equation:

$$\begin{aligned}\rho^g \frac{\partial u}{\partial t} + \rho^g \left(v\frac{\partial u}{\partial r} + u\frac{\partial u}{\partial z} \right) &= -\frac{\partial p}{\partial z} - \rho^g g \\ &\quad + \frac{1}{r}\frac{\partial}{\partial r}\left[\mu r \left(\frac{\partial u}{\partial r} + \frac{\partial v}{\partial z} \right) \right] + 2\frac{\partial}{\partial z}\left[\mu \left(\frac{\partial u}{\partial z} - \frac{1}{3}\nabla \cdot \mathbf{v} \right) \right]. \end{aligned} \tag{3.3}$$

(iv) The energy balance:

$$\begin{aligned}&\rho^g C_p^g \frac{\partial \theta}{\partial t} + \rho^g C_p^g \left(v\frac{\partial \theta}{\partial r} + u\frac{\partial \theta}{\partial z} \right) = \\ &\quad v\frac{\partial p}{\partial r} + u\frac{\partial p}{\partial z} + \frac{1}{r}\frac{\partial}{\partial r}\left(r k^g \frac{\partial \theta}{\partial r} \right) + \frac{\partial}{\partial z}\left(k^g \frac{\partial \theta}{\partial z} \right) + \tau \cdot D, \end{aligned} \tag{3.4}$$

where the viscous dissipation is given by:

$$\begin{aligned}\tau \cdot D = \mu &\left\{ 2\frac{\partial v}{\partial r}\left(\frac{\partial v}{\partial r} - \frac{1}{3}\nabla \cdot \mathbf{v} \right) + 2\frac{v}{r}\left(\frac{v}{r} - \frac{1}{3}\nabla \cdot \mathbf{v} \right) \right\} \\ &+2\mu \left\{ \frac{\partial u}{\partial z}\left(\frac{\partial u}{\partial z} - \frac{1}{3}\nabla \cdot \mathbf{v} \right) + \frac{\partial v}{\partial z}\left(\frac{\partial u}{\partial r} + \frac{\partial v}{\partial z} \right) \right\}. \end{aligned}$$

It should be noted here that we have assumed that there is no heat transfer by radiation. Also, having made the dilute-mixture approximation, we neglect the energy supply due to the homogeneous chemical reactions that occur in the gas flow. Finally, we have assumed that the specific heats (at constant pressure) associated with the various species present in the mixture are roughly equal (an approximation valid when the various molecules are of comparable size). When combined to the requirement that the total diffusive flux (defined as the sum over all species of the partial diffusive fluxes) be null, the latter assumption results in neglecting the energy supply associated with the species diffusion.

(v) The species equations: $\forall\ k = 1, \ldots, N-1$,

$$\frac{\partial \rho_k^g}{\partial t} + \frac{1}{r}\frac{\partial}{\partial r}(r\rho_k^g v) + \frac{\partial}{\partial z}(\rho_k^g u) = \frac{1}{r}\frac{\partial}{\partial r}\left[r\left(D_k^c\frac{\partial \rho_k^g}{\partial r} + \frac{D_k^t}{\theta}\frac{\partial \theta}{\partial r}\right)\right] + \frac{\partial}{\partial z}\left(D_k^c\frac{\partial \rho_k^g}{\partial z} + \frac{D_k^t}{\theta}\frac{\partial \theta}{\partial z}\right) + R_k, \quad (3.5)$$

where D_k^c is the effective diffusion coefficient, D_k^t is the thermal diffusion coefficient for the k^{th} species, and R_k is the rate of production of particles of the k^{th} species by all the homogeneous chemical reactions involving the species of interest.

(vi) Finally, the ideal-gas equation of state:

$$p = \bar{R}\rho^g\theta \quad (3.6)$$

with $\bar{R} \stackrel{def}{=} \frac{R}{W^g}$, where R is the universal gas constant and W^g is the molecular weight of the gas mixture.

Notice that the circumferential momentum equation was omitted from the list of governing equations as it is trivially satisfied when the circumferential velocity field is identically zero. It should also be noted that only $N-1$ species equations have been included in the above list of governing equations. Indeed, the total mass density being defined as the sum over all the species present in the gas mixture of the partial mass densities, if it is included in the list of independent variables, then we are only left with $N-1$ species densities as independent variables, the last species density

being determined from the relation $\rho^g \stackrel{def}{=} \sum_{k=1}^{N} \rho_k^g$. Consequently, the corresponding governing equations are the continuity equation (3.1) and the $N-1$ species equations (3.5). This is consistent with the fact that the continuity equation can be obtained by summing the N species equations under the assumption that the total diffusive mass flux vanishes.

3.1.4 The boundary conditions

The variables of the problem are the following: the total mass density ρ^g, the $N-1$ independent species densitites $\{\rho_k^g\}_{k=1}^{N-1}$, the radial and axial velocities v and u, the temperature θ, and finally the pressure p, that is a total of $N+4$ scalar variables. The equations of the problem are: the continuity equation (3.1), the two linear momentum equations (3.2) and (3.3), the energy balance (3.4), the $N-1$ species equations (3.5), and finally the ideal-gas equation of state (3.6), that is $N+4$ scalar equations. Consequently, the problem is formally well-posed, granted an adequate set of boundary conditions.

Along the showerhead ($z = L$), the following boundary conditions hold: $\forall\ r \in [0, r_s]$, $\forall\ t \in [0, \infty)$,

$$\text{the temperature is prescribed: } \theta(r, L, t) = \theta_i, \tag{3.7}$$

$$\text{the axial velocity is known: } u(r, L, t) = u_i, \tag{3.8}$$

$$\text{the radial velocity is identically zero: } v(r, L, t) = 0, \tag{3.9}$$

and the species inflow fluxes are known: $\forall\ k = 1, \ldots, N-1$,

$$\rho_k^g(r, L, t)u_i + D_k \left(\frac{\partial \rho_k^g}{\partial z}(r, L, t) + \frac{\alpha_k^g \rho_k^g(r, L, t)}{\theta_i} \frac{\partial \theta}{\partial z}(r, L, t) \right) = -\dot{m}_k, \tag{3.10}$$

where the subscript i designates the inlet (prescribed) quantities, $\dot{m}_k$ is the flow rate of the k^{th} species into the reactor chamber, D_k its effective diffusion coefficient and α_k^g is its Soret coefficient (constant).

The microstructural features of the surface morphology are much smaller than the thickness of the growing thin film. Consequently, we can approximate the evolving

interface separating the bulk of the film from the gaseous phase as a *flat* moving surface. Moreover, the height of the growing thin film is itself negligible[1] when compared to any of the other characteristic dimensions of the problem at hand (whether the height of the channel L, or the radius of the showerhead r_s, or even the thickness of the substrate on which the deposition and the subsequent growth take place). It is then reasonable to assume that the gas-film interface is stationary, i.e., the gas mixture only 'sees' a flat surface[2] located at $z = 0$ (where we have chosen the origin of the system of cylindrical coordinates to coincide with the center of the circular substrate).

We can now list the boundary conditions that hold along the film surface ($z = 0$): $\forall\ r \in [0, r_s]$, $\forall\ t \in [0, \infty)$,

$$\text{the film temperature is constant:}\quad \theta(r, 0, t) = \theta_f, \tag{3.11}$$

$$\text{the axial velocity is equal to the growth velocity:}\quad u(r, 0, t) = v_s, \tag{3.12}$$

$$\text{the radial velocity is identically zero:}\quad v(r, 0, t) = 0, \tag{3.13}$$

and the species flux-matching conditions are: $\forall\ k = 1, \ldots, N-1$,

$$\rho_k^g(r, 0, t) v_s - D_k \left(\frac{\partial \rho_k^g}{\partial z}(r, 0, t) + \frac{\alpha_k \rho_k^g(r, 0, t)}{\theta_f} \frac{\partial \theta}{\partial z}(r, 0, t) \right) = J_k^g, \tag{3.14}$$

where the subscript f designates the film (prescribed) quantities. The film height is so small that temperature variations across the film thickness can be neglected, and the film temperature is assumed to be constant and equal to the fixed temperature of the substrate. In a continuum model that couples the gas phase to the thin solid film via the equations governing the morphological evolution of the surface, the growth velocity (i.e., the normal component of the interfacial velocity) is one of the fundamental unknown variables of the formulation. Here, we consider this growth velocity to be given, and this provides one of the two boundary conditions needed to explicitly determine the profile of the axial velocity in the gas phase. Finally, the

[1] Or, equivalently, the growth velocity of the thin film is much smaller than any of the other characteristic gas-phase velocities, whether diffusive or convective.

[2] E.g., cf. [YHC] or [GG] or [MKD].

term J_k^g represents the adsorption flux or flux into the surface (or, in the absence of surface structure, flux into the bulk of the film) of the k^{th} species. We assume that the adsorption of a molecule takes place via an elementary irreversible adsorption reaction, i.e., we make the following constitutive assumptions on the adsorption fluxes along the vapor-film interface:

$$J_k^g \stackrel{def}{=} \lambda_k^g \rho_k^g, \qquad \forall\ k = 1, \ldots, N-1 \tag{3.15}$$

where the reaction-rate constant λ_k^g is a function of temperature only. The constitutive relation (3.15) is chosen for simplicity. In chapter 4 we show that the deposition flux associated with the k^{th} species can depend on the chemical composition of the gas flow as well as on the morphological features of the film-gas interface. But having approximated the interface by a flat surface, (3.15) is to be thought of as an averaged deposition flux over the microstructure of the interface.

Finally, we assume that the mean pressure in the reactor chamber is a prescribed constant $\hat{p}_a$.

The integral continuity condition

For future use, we derive the following equation by integrating the continuity equation (3.20):

$$\int_{z=0}^{z=L} r\frac{\partial \rho^g}{\partial t}\, dz + \int_{z=0}^{z=L} \frac{\partial}{\partial r}(r\rho^g v)\, dz + \int_{z=0}^{z=L} \frac{\partial}{\partial z}(r\rho^g u)\, dz = 0. \tag{3.16}$$

Making use of the boundary conditions (3.8) and (3.12), and assuming that the growth velocity v_s can be neglected with respect to the inlet axial velocity u_i, we can rewrite the above equation as:

$$r\frac{\partial}{\partial t}\left(\int_{z=0}^{z=L} \rho^g\, dz\right) + \frac{\partial}{\partial r}\left(r\int_{z=0}^{z=L} \rho^g v\, dz\right) + r\rho_i^g u_i \;=\; 0. \tag{3.17}$$

Integrating with respect to r, we obtain the following integral version of the continuity equation:

$$\int_{z=0}^{z=L} \rho^g v \, dz \;=\; -\frac{1}{2}\rho_i^g u_i r - \frac{1}{r}\,\frac{\partial}{\partial t}\left(\int_{z=0}^{z=L}\int_{\xi=0}^{\xi=r} \xi\rho^g(\xi,z,t)\, d\xi dz\right). \tag{3.18}$$

3.1.5 Scaling

Let θ_i and θ_f be the temperatures at the inlet showerhead and the heated substrate respectively. The typical height of the grown film being much smaller than the thickness of the substrate, it is reasonable to assume that the variation in temperature along the thickness of the thin film is negligible, i.e., we shall assume that the film is at constant temperature θ_f. We now define the reference temperature as the average of the above two temperatures: $\theta_r \stackrel{def}{=} \frac{1}{2}(\theta_i + \theta_f)$. All the reference quantities are evaluated at the reference temperature θ_r and at some prescribed reference pressure $\bar{p}_r$.

In order to nondimensionalize the set of governing equations, we now introduce the following characteristic scalings:

(1) The time is scaled as follows: $t = t_r\bar{t}$, with $t_r \stackrel{def}{=} L/v_s^r$, where L is the height of the channel and v_s^r is the typical growth rate of the thin solid film at the reference temperature θ_r (and at the reference pressure $\bar{p}_r$).

(2) The total mass density ρ^g is scaled by the reference density $\rho_r^g = \frac{\bar{p}_r}{R\theta_r}$ giving the nondimensional total mass density $\bar{\rho} \stackrel{def}{=} \frac{\rho^g}{\rho_r^g}$.

(3) The temperature θ is scaled using the reference temperature θ_r, thus introducing a nondimensional temperature $\bar{\theta} \stackrel{def}{=} \frac{\theta}{\theta_r}$.

(4) The radial coordinate r is scaled by the radius of the showerhead r_s giving the nondimensional radial coordinate $\bar{r} \stackrel{def}{=} \frac{r}{r_s}$; identically, the axial coordinate is scaled by the height of the channel L yielding the nondimensional axial coordinate $\bar{z} \stackrel{def}{=} \frac{z}{L}$.

(5) The nondimensional pressure $\bar{p}$ is defined via the relation $p = p_r\bar{p}$ where $p_r \stackrel{def}{=} \rho_r^g \frac{k_r^2}{L^2}$ is the reference dynamical pressure and $k_r \stackrel{def}{=} k(\theta_r)$ is the reference thermal diffusivity of the gas mixture.

(6) The $N-1$ independent species densities are scaled using the (known) inlet species densities $\{\rho^g_{k,i}\}_{k=1}^{N-1}$, thus introducing the nondimensional species densities $\bar{\rho}_k \stackrel{def}{=} \frac{\rho^g_k}{\rho^g_{k,i}}$, $\forall\ k = 1, \ldots, N-1$.

(7) Finally, the radial and axial components of the velocity field are scaled as follows: $\bar{v} = \frac{v}{v_r}$ and $\bar{u} = \frac{u}{u_r}$, where the reference velocities are given by $v_r \stackrel{def}{=} \frac{k_r}{L}$ and $u_r \stackrel{def}{=} \frac{k_r}{r_s}$.

3.1.6 Non-dimensionalization

The non-dimensional governing equations

Having introduced the above scalings, we can now rewrite the governing equations (3.1)-(3.6) in their non-dimensional form. In doing so, we will introduce a number of dimensionless parameters (e.g., Prandlt's number, Froude's number, etc.) which we shall interpret as being 'measures' of the relative 'magnitudes' of the various competing physical mechanisms at play in the gas phase (the convective and diffusive transport of species, the homogeneous and heterogeneous chemical kinetics, the conduction of heat and the effect of gravity and viscosity, etc.).

(i) The continuity equation:

$$\frac{\rho^g_r v^r_s}{L}\frac{\partial \bar{\rho}}{\partial \bar{t}} + \frac{\rho^g_r k_r}{r_s L}\left(\frac{1}{\bar{r}}\frac{\partial}{\partial \bar{r}}(\bar{r}\bar{\rho}\bar{v}) + \frac{\partial}{\partial \bar{z}}(\bar{\rho}\bar{u})\right) = 0. \tag{3.19}$$

Omitting the bars, we can rewrite the nondimensional continuity equation as follows:

$$\Xi\frac{\partial \bar{\rho}}{\partial \bar{t}} + \frac{1}{r}\frac{\partial}{\partial r}(r\rho v) + \frac{\partial}{\partial z}(\rho u) = 0, \tag{3.20}$$

where

$$\Xi \stackrel{def}{=} \frac{r_s v^r_s}{k_r}$$

is a 'measure' of the time scale for convection in the flow vs. the time scale for the

growth of the film.

(ii) The radial momentum equation:

First, rewrite (3.2) as follows:

$$\rho^g \frac{\partial v}{\partial t} + \rho^g \left(v \frac{\partial v}{\partial r} + u \frac{\partial v}{\partial z} \right) = - \frac{\partial p}{\partial r} + \frac{2}{3r} \frac{\partial}{\partial r} \left[\mu r \left(2 \frac{\partial v}{\partial r} - \frac{v}{r} - \frac{\partial u}{\partial z} \right) \right] - \frac{2\mu}{3r} \left(2 \frac{v}{r} - \frac{\partial v}{\partial r} - \frac{\partial u}{\partial z} \right) + \frac{2}{3r} \frac{\partial}{\partial z} \left[\mu \left(\frac{\partial u}{\partial r} + \frac{\partial v}{\partial z} \right) \right].$$

It follows that:

$$\begin{aligned} \frac{\rho_r^g k_r v_s^r}{L^2} \bar{\rho} \frac{\partial \bar{v}}{\partial \bar{t}} + \frac{\rho_r^g k_r^2}{r_s L^2} \bar{\rho} \left(\bar{v} \frac{\partial \bar{v}}{\partial \bar{r}} + \bar{u} \frac{\partial \bar{v}}{\partial \bar{z}} \right) &= - \frac{\rho_r^g k_r^2}{r_s L^2} \frac{\partial \bar{p}}{\partial \bar{r}} \\ + \frac{k_r \mu_r}{r_s^2 L} \frac{2}{3\bar{r}} \left\{ \frac{\partial}{\partial \bar{r}} \left[\bar{\mu} \bar{r} \left(2 \frac{\partial \bar{v}}{\partial \bar{r}} - \frac{\bar{v}}{\bar{r}} - \frac{\partial \bar{u}}{\partial \bar{z}} \right) \right] - \bar{\mu} \left(2 \frac{\bar{v}}{\partial \bar{r}} - \frac{\partial \bar{v}}{\partial \bar{r}} - \frac{\partial \bar{u}}{\partial \bar{z}} \right) \right\} \\ + \frac{k_r \mu_r}{r_s^2 L} \frac{\partial}{\partial \bar{z}} \left(\bar{\mu} \frac{\partial \bar{u}}{\partial \bar{r}} \right) + \frac{k_r \mu_r}{L^3} \frac{\partial}{\partial \bar{z}} \left(\bar{\mu} \frac{\partial \bar{v}}{\partial \bar{z}} \right), \end{aligned}$$

where $\mu_r = \mu(\theta_r)$ and $\bar{\mu}$ is the dimensionless viscosity coefficient of the gas mixture.

For the purpose of simplifying the notation, we drop the bars, and we rewrite the dimensionless radial momentum equation as:

$$\begin{aligned} \epsilon \Xi \rho \frac{\partial v}{\partial t} + \epsilon \rho \left(v \frac{\partial v}{\partial r} + u \frac{\partial v}{\partial z} \right) &= - \epsilon \frac{\partial p}{\partial r} + \mathcal{P} \frac{\partial}{\partial z} \left(\mu \frac{\partial v}{\partial z} \right) \\ &+ \epsilon^2 \mathcal{P} \frac{2}{3r} \frac{\partial}{\partial r} \left[\mu r \left(2 \frac{\partial v}{\partial r} - \frac{v}{r} - \frac{\partial u}{\partial z} \right) \right] \\ &- \mu \epsilon^2 \mathcal{P} \left(2 \frac{v}{r} - \frac{\partial v}{\partial r} - \frac{\partial u}{\partial z} \right) \\ &+ \epsilon^2 \mathcal{P} \frac{\partial}{\partial z} \left(\mu \frac{\partial u}{\partial r} \right), \end{aligned} \tag{3.21}$$

where ϵ is the aspect ratio

$$\epsilon \stackrel{def}{=} \frac{L}{r_s}, \tag{3.22}$$

and $\mathcal{P}$ is Prandlt's number

$$\mathcal{P} \stackrel{def}{=} \frac{\mu_r}{\rho_r^g k_r} = \frac{\nu_r}{k_r}, \tag{3.23}$$

with $\nu_r = \frac{\mu_r}{\rho_r^g}$ the kinematic viscosity. Prandlt's number is a 'measure' of the relative 'magnitudes' of viscous effects vs. heat conduction effects.

(iii) The axial momentum equation:

First, rewrite (3.3) as follows:

$$\begin{aligned}\rho^g \frac{\partial u}{\partial t} + \rho^g \left(v\frac{\partial u}{\partial r} + u\frac{\partial u}{\partial z} \right) = & -\frac{\partial p}{\partial z} - \rho^g g \\ & + \frac{1}{r}\frac{\partial}{\partial r}\left[\mu r \left(\frac{\partial u}{\partial r} + \frac{\partial v}{\partial z} \right) \right] + \frac{2}{3}\frac{\partial}{\partial z}\left[\mu \left(2\frac{\partial u}{\partial z} - \frac{\partial v}{\partial r} - \frac{v}{r} \right) \right].\end{aligned} \tag{3.24}$$

Next, using the scalings introduced above, we rewrite the above equation as:

$$\begin{aligned}\frac{\rho_r^g k_r v_s^r}{r_s L}\bar{\rho}\frac{\partial \bar{u}}{\partial \bar{t}} + \frac{\rho_r^g k_r^2}{r_s^2 L}\bar{\rho}\left(\bar{v}\frac{\partial \bar{u}}{\partial \bar{r}} + \bar{u}\frac{\partial \bar{u}}{\partial \bar{z}} \right) = & -\frac{\rho_r^g k_r^2}{L^3}\frac{\partial \bar{p}}{\partial \bar{z}} - \rho_r^g g\bar{\rho} \\ & + \frac{k_r \mu_r}{r_s^3}\frac{1}{\bar{r}}\frac{\partial}{\partial \bar{r}}\left(\bar{\mu}\bar{r}\frac{\partial \bar{u}}{\partial \bar{r}} \right) + \frac{k_r \mu_r}{r_s L^2}\frac{1}{\bar{r}}\frac{\partial}{\partial \bar{r}}\left(\bar{\mu}\bar{r}\frac{\partial \bar{v}}{\partial \bar{z}} \right) \\ & + \frac{2}{3}\frac{k_r \mu_r}{r_s L^2}\frac{\partial}{\partial \bar{z}}\left[\bar{\mu}\left(2\frac{\partial \bar{u}}{\partial \bar{z}} - \frac{\partial \bar{v}}{\partial \bar{r}} - \frac{\bar{v}}{\bar{r}} \right) \right].\end{aligned}$$

Finally, dropping the bars, we can write the dimensionless axial momentum equation in the following form:

$$\begin{aligned}\epsilon \Xi \rho \frac{\partial u}{\partial t} + \epsilon^2 \rho \left(v\frac{\partial u}{\partial r} + u\frac{\partial u}{\partial z} \right) = & -\frac{\partial p}{\partial z} - \frac{1}{\mathcal{F}}\rho + \epsilon^3 \mathcal{P}\frac{1}{r}\frac{\partial}{\partial r}\left(\mu r \frac{\partial u}{\partial r} \right) \\ & + \epsilon \mathcal{P}\left\{ \frac{1}{r}\frac{\partial}{\partial r}\left(\mu r \frac{\partial v}{\partial z} \right) + \frac{2}{3}\frac{\partial}{\partial z}\left[\mu\left(2\frac{\partial u}{\partial z} - \frac{\partial v}{\partial r} - \frac{v}{r} \right) \right] \right\},\end{aligned} \tag{3.25}$$

where Froude's number is given by

$$\mathcal{F} \stackrel{def}{=} \frac{k_r^2}{gL^3}$$

and can be regarded as the 'ratio' of inertia effects to gravity effects.

(iv) The energy conservation equation:

Begin by writing the viscous dissipation term as follows:

$$\tau \cdot D = \frac{2\mu}{3}\frac{\partial v}{\partial r}\left(2\frac{\partial v}{\partial r} - \frac{v}{r} - \frac{\partial u}{\partial z}\right) + \mu\left\{\frac{2}{3}\left[\frac{v}{r}\left(2\frac{v}{r} - \frac{\partial v}{\partial r} - \frac{\partial u}{\partial z}\right) + \frac{\partial u}{\partial z}\left(2\frac{\partial u}{\partial z} - \frac{\partial v}{\partial r} - \frac{v}{r}\right)\right] + \frac{\partial v}{\partial z}\left(\frac{\partial u}{\partial r} + \frac{\partial v}{\partial z}\right)\right\}.$$

It then follows that the energy balance (3.4) can be rewritten as:

$$\begin{aligned}
&\frac{\rho_r^g C_p^g \theta_r v_s^r}{L}\bar{\rho}\frac{\partial \bar{\theta}}{\partial \bar{t}} + \frac{\rho_r^g C_p^g k_r \theta_r}{r_s L}\bar{\rho}\left(\bar{v}\frac{\partial \bar{\theta}}{\partial \bar{r}} + \bar{u}\frac{\partial \bar{\theta}}{\partial \bar{z}}\right) = \\
&\quad \frac{\rho_r^g k_r^3}{r_s L^3}\left(\bar{v}\frac{\partial \bar{p}}{\partial \bar{r}} + \bar{u}\frac{\partial \bar{p}}{\partial \bar{z}}\right) + \frac{\rho_r^g C_p^g k_r \theta_r}{r_s^2}\frac{1}{\bar{r}}\frac{\partial}{\partial \bar{r}}\left(\bar{r}\bar{k}\frac{\partial \bar{\theta}}{\partial \bar{r}}\right) + \frac{\rho_r^g C_p^g k_r \theta_r}{L^2}\frac{\partial}{\partial \bar{z}}\left(\bar{k}\frac{\partial \bar{\theta}}{\partial \bar{z}}\right) \\
&\quad + \frac{2\mu_r k_r^2}{3 r_s^2 L^2}\bar{\mu}\left\{\frac{\partial \bar{v}}{\partial \bar{r}}\left(2\frac{\partial \bar{v}}{\partial \bar{r}} - \frac{\bar{v}}{\bar{r}} - \frac{\partial \bar{u}}{\partial \bar{z}}\right) + \frac{\bar{v}}{\bar{r}}\left(2\frac{\bar{v}}{\bar{r}} - \frac{\partial \bar{v}}{\partial \bar{r}} - \frac{\partial \bar{u}}{\partial \bar{z}}\right) + \frac{\partial \bar{u}}{\partial \bar{z}}\left(2\frac{\partial \bar{u}}{\partial \bar{z}} - \frac{\partial \bar{v}}{\partial \bar{r}} - \frac{\bar{v}}{\bar{r}}\right)\right\} \\
&\qquad + \frac{\mu_r k_r^2}{r_s^2 L^2}\bar{\mu}\frac{\partial \bar{v}}{\partial \bar{z}}\frac{\partial \bar{u}}{\partial \bar{r}} + \frac{\mu_r k_r^2}{L^4}\bar{\mu}\left(\frac{\partial \bar{v}}{\partial \bar{z}}\right)^2.
\end{aligned}$$

Dropping the bars, we can rewrite the above equation as:

$$\begin{aligned}
&\Xi\rho\frac{\partial \theta}{\partial t} + \rho\left(v\frac{\partial \theta}{\partial r} + u\frac{\partial \theta}{\partial z}\right) = \\
&\quad \frac{k_r^2}{C_p^g L^2 \theta_r}\left(v\frac{\partial p}{\partial r} + u\frac{\partial p}{\partial z}\right) + \epsilon\frac{1}{r}\frac{\partial}{\partial r}\left(rk\frac{\partial \theta}{\partial r}\right) + \frac{1}{\epsilon}\frac{\partial}{\partial z}\left(k\frac{\partial \theta}{\partial z}\right) \\
&\quad + \frac{2\mu_r k_r}{r_s L \rho_r^g C_p^g \theta_r}\mu\left\{\frac{\partial v}{\partial r}\left(2\frac{\partial v}{\partial r} - \frac{v}{r} - \frac{\partial u}{\partial z}\right) + \frac{v}{r}\left(2\frac{v}{r} - \frac{\partial v}{\partial r} - \frac{\partial u}{\partial z}\right)\right\} \\
&\quad + \frac{2\mu_r k_r}{r_s L \rho_r^g C_p^g \theta_r}\mu\frac{\partial u}{\partial z}\left(2\frac{\partial u}{\partial z} - \frac{\partial v}{\partial r} - \frac{v}{r}\right) + \frac{\mu_r k_r}{r_s L \rho_r^g C_p^g \theta_r}\mu\frac{\partial v}{\partial z}\frac{\partial u}{\partial r} + \frac{\mu_r k_r r_s}{L^3 \rho_r^g C_p^g \theta_r}\mu\left(\frac{\partial v}{\partial z}\right)^2.
\end{aligned}$$

Now, by definition, the speed of sound (denoted in what follows by a) is the speed at which small disturbances (i.e., waves) are propagated through the compressible fluid in question:

$$a^2 \stackrel{def}{=} \left(\frac{\partial p}{\partial \rho^g}\right)_\eta,$$

where the disturbances produced in the fluid by a sound wave, i.e., the induced temperature and velocity gradients, are so small that it is reasonable to assume that each fluid particle undergoes a nearly isentropic process (cf. [LR]). For an ideal gas undergoing an isentropic process, it can be shown that the following relation holds:

$$a^2 = \gamma \bar{R}\theta,$$

with γ the ratio of the specific heats at constant pressure and volume defined below. Consequently, we choose as a nominal (or characteristic) speed of sound for the multicomponent ideal gas at hand the following:

$$a_r \stackrel{def}{=} (\bar{R}\theta_r)^{1/2}.$$

We can now define Mach's number as:

$$M \stackrel{def}{=} \frac{v_r}{a_r} = \frac{k_r}{L(\bar{R}\theta)^{1/2}}, \tag{3.26}$$

which, as the 'ratio' of the characteristic speed of the flow to the speed of sound in the gas mixture at hand, is a 'measure' of the effects of compressibility in the *moving* fluid.

Also, introduce the ratio of the specific heat at constant pressure to that at constant volume for the multicomponent ideal gas:

$$\gamma \stackrel{def}{=} \frac{C_p^g}{C_v^g},$$

which implies that the following relation holds:

$$\frac{\gamma - 1}{\gamma} = \frac{C_p^g - C_v^g}{C_p^g}.$$

The gas mixture being ideal, we obtain:

$$\bar{R} = \frac{\gamma - 1}{\gamma} C_p^g,$$

where we have used the ideal-gas identity $C_p^g - C_v^g = \bar{R}$.

Consequently, we have the following relation:

$$\frac{k_r^2}{C_p^g L^2 \theta_r} = \frac{\gamma - 1}{\gamma} M^2.$$

Similarily, and making use of the definition of Prandlt's number (3.23), we can show that the following realtions hold:

$$\begin{aligned} \frac{\mu_r k_r}{r_s L \rho_r^g C_p^g \theta_r} &= \frac{\gamma - 1}{\gamma} \epsilon M^2 \mathcal{P}, \qquad \text{and} \\ \frac{\mu_r k_r r_s}{L^3 \rho_r^g C_p^g \theta_r} &= \frac{\gamma - 1}{\gamma} \frac{1}{\epsilon} M^2 \mathcal{P}. \end{aligned}$$

It then follows that the nondimensional energy balance equation can be written as:

$$\begin{aligned} \epsilon \Xi \rho \frac{\partial \theta}{\partial t} + \epsilon \rho \left(v \frac{\partial \theta}{\partial r} + u \frac{\partial \theta}{\partial z} \right) &= \epsilon^2 \frac{1}{r} \frac{\partial}{\partial r} \left(r k \frac{\partial \theta}{\partial r} \right) + \frac{\partial}{\partial z} \left(k \frac{\partial \theta}{\partial z} \right) + \frac{\gamma - 1}{\gamma} M^2 \mathcal{P} \mu \left(\frac{\partial v}{\partial z} \right)^2 \\ &+ \frac{2}{3} \frac{\gamma - 1}{\gamma} \epsilon^2 M^2 \mathcal{P} \mu \left[\frac{\partial v}{\partial r} \left(2 \frac{\partial v}{\partial r} - \frac{v}{r} - \frac{\partial u}{\partial z} \right) + \frac{v}{r} \left(2 \frac{v}{r} - \frac{\partial v}{\partial r} - \frac{\partial u}{\partial z} \right) \right] \\ &+ \frac{\gamma - 1}{\gamma} \epsilon^2 M^2 \mathcal{P} \mu \left[\frac{2}{3} \frac{\partial u}{\partial z} \left(2 \frac{\partial u}{\partial z} - \frac{\partial v}{\partial r} - \frac{v}{r} \right) + \mu \frac{\partial v}{\partial z} \frac{\partial u}{\partial r} \right] \\ &+ \frac{\gamma - 1}{\gamma} \epsilon M^2 \left(v \frac{\partial p}{\partial r} + u \frac{\partial p}{\partial z} \right), \end{aligned} \tag{3.27}$$

with Mach's number given by (3.26).

(v) The species equations:

Recall the definition of the Soret coefficient associated with the thermal diffusion of each of the chemical species present in the system:

$$D_k^t(\theta, \rho_k^g) \stackrel{def}{=} \alpha_k \rho_k^g D_k^c(\theta), \qquad \forall\ k = 1, \ldots, N,$$

and introduce, for each species k, the change in terminology $D_k = D_k^c$.

The species equations then become: $\forall\ k = 1, \ldots, N-1$,

$$\frac{\partial \rho_k^g}{\partial t} + \frac{1}{r}\frac{\partial}{\partial r}(r\rho_k^g v) + \frac{\partial}{\partial z}(\rho_k^g u) = \frac{1}{r}\frac{\partial}{\partial r}\left[rD_k\left(\frac{\partial \rho_k^g}{\partial r} + \frac{\alpha_k \rho_k^g}{\theta}\frac{\partial \theta}{\partial r}\right)\right] + \frac{\partial}{\partial z}\left[D_k\left(\frac{\partial \rho_k^g}{\partial z} + \frac{\alpha_k \rho_k^g}{\theta}\frac{\partial \theta}{\partial z}\right)\right] + R_k. \quad (3.28)$$

Consider now the following generic reversible reaction labelled α:

$$\sum_{i=1}^{N_r^\alpha} \nu_i^\alpha \mathcal{I} \rightleftharpoons \sum_{k=1}^{N_p^\alpha} \nu_k^\alpha \mathcal{K}, \quad (3.29)$$

where N_r^α and N_p^α are the numbers of reactants and products (respectively) that contribute to (3.29), and $\{\nu_i^\alpha\}_{i=1}^{N_r^\alpha}$ and $\{\nu_k^\alpha\}_{k=1}^{N_p^\alpha}$ are the stochiometric coefficients associated with the reactants and products respectively (all stochiometric coefficients being positive integers by definition). The reaction rate associated with (3.29) is given by the following relation:

$$\mathcal{R}^\alpha = k_f^\alpha(\theta)\prod_{i=1}^{N_r^\alpha}\left(\frac{\bar{\rho}_i^g}{w_i}\right)^{\nu_i^\alpha} - k_b^\alpha(\theta)\prod_{k=1}^{N_p^\alpha}\left(\frac{\bar{\rho}_k^g}{w_k}\right)^{\nu_k^\alpha}, \quad (3.30)$$

with k_f^α and k_b^α the forward and backward reaction-rate constants (again positive functions of the temperature only). It follows that:

$$R_k = w_k \sum_{\alpha=1}^{N_c}\left\{k_f^\alpha(\theta)\prod_{i=1}^{N_r^\alpha}\left(\frac{\bar{\rho}_i^g}{w_i}\right)^{\nu_i^\alpha} - k_b^\alpha(\theta)\prod_{k=1}^{N_p^\alpha}\left(\frac{\bar{\rho}_k^g}{w_k}\right)^{\nu_k^\alpha}\right\}, \quad (3.31)$$

where N_c is the total number of homogeneous chemical reactions that involve the k^{th} species as either a reactant or a product. (3.31) can be rewritten as:

$$R_k = w_k \sum_{\alpha=1}^{N_c}\left[k_{f,r}^\alpha \prod_{m=1}^{N_r^\alpha}\left(\frac{\bar{\rho}_{m,i}^g}{w_m}\right)^{\nu_m^\alpha}\right]\bar{k}_f^\alpha(\bar{\theta})\prod_{m=1}^{N_\alpha^r}\bar{\rho}^{\nu_m^\alpha} - w_k \sum_{\alpha=1}^{N_c}\left[k_{b,r}^\alpha \prod_{n=1}^{N_p^\alpha}\left(\frac{\bar{\rho}_{n,i}^g}{w_n}\right)^{\nu_n^\alpha}\right]\bar{k}_b^\alpha(\bar{\theta})\prod_{n=1}^{N_p^\alpha}\bar{\rho}^{\nu_n^\alpha}, \quad (3.32)$$

with $k_{f,r}^{\alpha} \stackrel{def}{=} k_f^{\alpha}(\theta_r)$ and $k_{b,r}^{\alpha} \stackrel{def}{=} k_b^{\alpha}(\theta_r)$. It then follows that (3.28) can be rewritten as:

$$\frac{\rho_{k,i}^g v_s^r}{L}\frac{\partial \bar{\rho}_k}{\partial \bar{t}} + \frac{\rho_{k,i}^g k_r}{r_s L}\left[\frac{1}{\bar{r}}\frac{\partial}{\partial \bar{r}}(\bar{r}\bar{\rho}_k\bar{v}) + \frac{\partial}{\partial \bar{z}}(\bar{\rho}_k\bar{u})\right] =$$
$$\frac{D_{k,r}\rho_{k,i}^g}{r_s^2}\frac{1}{\bar{r}}\frac{\partial}{\partial \bar{r}}\left[\bar{r}\bar{D}_k\left(\frac{\partial \bar{\rho}_k}{\partial \bar{r}} + \frac{\alpha_k\bar{\rho}_k}{\bar{\theta}}\frac{\partial \bar{\theta}}{\partial \bar{r}}\right)\right] + \frac{D_{k,r}\rho_{k,i}^g}{L^2}\frac{\partial}{\partial \bar{z}}\left[\bar{D}_k\left(\frac{\partial \bar{\rho}_k}{\partial \bar{z}} + \frac{\alpha_k\bar{\rho}_k}{\bar{\theta}}\frac{\partial \bar{\theta}}{\partial \bar{z}}\right)\right]$$
$$+\sum_{\alpha=1}^{N_c}\left(a_k^{\alpha}\bar{k}_f^{\alpha}(\bar{\theta})\prod_{m=1}^{N_r^{\alpha}}\bar{\rho}^{\nu_m^{\alpha}} - b_k^{\alpha}\bar{k}_b^{\alpha}(\bar{\theta})\prod_{n=1}^{N_p^{\alpha}}\bar{\rho}^{\nu_n^{\alpha}}\right),$$

with

$$a_k^{\alpha} \stackrel{def}{=} w_k\left[k_{f,r}^{\alpha}\prod_{m=1}^{N_r^{\alpha}}\left(\frac{\bar{\rho}_{m,i}^g}{w_m}\right)^{\nu_m^{\alpha}}\right], \qquad \text{and}$$
$$b_k^{\alpha} \stackrel{def}{=} w_k\left[k_{b,r}^{\alpha}\prod_{n=1}^{N_p^{\alpha}}\left(\frac{\bar{\rho}_{n,i}^g}{w_n}\right)^{\nu_n^{\alpha}}\right],$$

and where we have scaled the species diffusion coefficients as follows:

$$D_k = D_{k,r}\bar{D}_k, \qquad \text{where } D_{k,r} \stackrel{def}{=} D_k^c(\theta_r). \tag{3.33}$$

Dropping the bars, we state the dimensionless species equations as follows:

$$\epsilon\Xi\mathcal{P}_k\frac{\partial \rho_k}{\partial t} + \epsilon\mathcal{P}_k\left[\frac{1}{r}\frac{\partial}{\partial r}(r\rho_k v) + \frac{\partial}{\partial z}(\rho_k u)\right] =$$
$$\epsilon^2\frac{1}{r}\frac{\partial}{\partial r}\left[rD_k\left(\frac{\partial \rho_k}{\partial r} + \frac{\alpha_k\rho_k}{\theta}\frac{\partial \theta}{\partial r}\right)\right] + \frac{\partial}{\partial z}\left[D_k\left(\frac{\partial \rho_k}{\partial z} + \frac{\alpha_k\rho_k}{\theta}\frac{\partial \theta}{\partial z}\right)\right]$$
$$+\sum_{\alpha=1}^{N_c}\left(\epsilon\mathcal{D}_k^{\alpha,f}\bar{k}_f^{\alpha}(\bar{\theta})\prod_{m=1}^{N_r^{\alpha}}\bar{\rho}^{\nu_m^{\alpha}} - \epsilon\mathcal{D}_k^{\alpha,b}\bar{k}_b^{\alpha}(\bar{\theta})\prod_{n=1}^{N_p^{\alpha}}\bar{\rho}^{\nu_n^{\alpha}}\right), \tag{3.34}$$

where the Péclet number associated with the k^{th} species is defined as follows:

$$\mathcal{P}_k \stackrel{def}{=} \frac{k_r}{D_{k,r}}$$

is to be regarded as an indication of the relative 'magnitudes' of convective mass

transport vs. diffusive mass transport associated with the k^{th} species, and

$$\mathcal{D}_k^{\alpha,f} \stackrel{def}{=} \frac{a_k^\alpha L r_s}{\rho_{k,i}^g D_{k,r}}, \qquad \text{and}$$
$$\mathcal{D}_k^{\alpha,b} \stackrel{def}{=} \frac{b_k^\alpha L r_s}{\rho_{k,i}^g D_{k,r}}$$

are the gas-phase Damköhler numbers associated with the forward and backward α-reactions (respectively) and are 'measures' of the typical time scale of diffusion of the k^{th} species vs. the typical time scale of the forward and backward reactions of interest.

We note here that we have implicitly assumed that the time scales for convection and diffusion of species are comparable. In the diffusion-limited regime, i.e., when the time scale for species diffusion is much larger than the time scale for convection, the above Damköhler numbers would have to be defined as

$$\mathcal{D}_k^{\alpha,f} \stackrel{def}{=} \frac{a_k^\alpha r_s^2}{\rho_{k,i}^g D_{k,r}}, \qquad \text{and}$$
$$\mathcal{D}_k^{\alpha,b} \stackrel{def}{=} \frac{b_k^\alpha r_s^2}{\rho_{k,i}^g D_{k,r}},$$

and the last two terms in (3.34), i.e., those terms accounting for the net production (or destruction) of k-particles by homogeneous reactions, would have the factor ϵ^2 rather than ϵ. Both regimes will lead to the same approximate equations in the limit of vanishingly small aspect ratio, as terms of order $O(\epsilon)$ or higher order will drop out (see equations (3.118)).

(vi) The ideal-gas equation of state:

Finally, we rewrite the equation of state (3.6) as:

$$\rho_r^g \frac{k_r^2}{L^2} \bar{p} \;=\; \bar{R} \rho_r^g \theta_r \bar{\rho} \bar{\theta}$$

which yields the dimensionless ideal-gas equation of state:

$$M^2 p = \rho\theta, \tag{3.35}$$

where we have dropped the bars in order to simplify the notation which is already quite cumbersome.

The non-dimensional boundary conditions

Along the showerhead ($\bar{z} = 1$), we have the following non-dimensional boundary conditions, where for simplicity we have once again dropped the bars: $\forall\ r \in [0,1]$, $\forall\ t \in [0,\infty)$,

$$\theta(r,1,t) = \tilde{\theta}_i, \qquad \text{where} \quad \tilde{\theta}_i \stackrel{def}{=} \frac{2\theta_i}{\theta_i + \theta_f}, \tag{3.36}$$

$$u(r,1,t) = \tilde{u}_i, \qquad \text{where} \quad \tilde{u}_i \stackrel{def}{=} \frac{r_s u_i}{k_r}, \tag{3.37}$$

$$v(r,1,t) = 0, \tag{3.38}$$

$$\tag{3.39}$$

and $\forall\ k = 1, \ldots, N-1$,

$$\epsilon \mathcal{P}_k \tilde{u}_i \rho_k(r,1,t) + D_k \left(\frac{\partial \rho_k}{\partial z}(r,1,t) + \frac{\alpha_k \rho_k(r,1,t)}{\tilde{\theta}_i} \frac{\partial \theta}{\partial z}(r,1,t) \right) = -\tilde{m}_k, \tag{3.40}$$

where:

$$\tilde{m}_k \stackrel{def}{=} \frac{\dot{m}_k L}{\rho_k^g D_{k,r}}.$$

Recall the following constitutive relation linking the adsorption flux of the k^{th} species to its density at the gas-film interface:

$$J_k^g \stackrel{def}{=} \lambda_k^g(\theta) \rho_k^g(r, z=0), \quad \forall\ k = 1, \ldots, N-1, \tag{3.41}$$

where $\lambda_k^g(\theta)$ is the temperature-dependent sticking coefficient accounting for the ad-

sorption of the k^{th}. For each species k, we scale the 'sticking coefficient' λ_k^g as follows:

$$\lambda_k^g = \lambda_{k,r}^g \bar{\lambda}_k, \qquad \text{where } \lambda_{k,r}^g \stackrel{def}{=} \lambda_k^g(\theta_r). \tag{3.42}$$

Consequently, along the gas-film interface ($\bar{z} = 0$), the non-dimensional boundary conditions can be written as: $\forall\ r \in [0,1]$, $\forall\ t \in [0,\infty)$,

$$\theta(r,0),t = \tilde{\theta}_f, \qquad \text{where} \quad \tilde{\theta}_f \stackrel{def}{=} \frac{2\theta_f}{\theta_i + \theta_f}, \tag{3.43}$$

$$u(r,0,t) = \tilde{v}_s, \qquad \text{where} \quad \tilde{v}_s \stackrel{def}{=} \frac{r_s v_s}{k_r}, \tag{3.44}$$

$$v(r,0,t) = 0, \tag{3.45}$$

and $\forall\ k = 1,\ldots,N-1$,

$$\epsilon \mathcal{P}_k \tilde{v}_s \rho_k(r,0,t) - D_k \left(\frac{\partial \rho_k}{\partial z}(r,0,t) + \frac{\alpha_k \rho_k(r,0,t)}{\tilde{\theta}_f} \frac{\partial \theta}{\partial z}(r,0,t) \right) = \epsilon \mathcal{D}_k^s \lambda_k(\tilde{\theta}_f) \rho_k(r,0,t), \tag{3.46}$$

where:

$$\mathcal{D}_k^s \stackrel{def}{=} \frac{\lambda_{k,r} r_s}{D_{k,r}} \tag{3.47}$$

is the surface Damköhler number associated with the k^{th} species and is a 'ratio' of the adsorption velocity to the diffusive velocity of the k^{th} species (or, in other words, it is the ratio of the typical time needed for the k-particles to diffuse in the gas phase towards the interface to the characteristic time it takes to incorporate these k-particles into the surface).

Finally, the prescribed background pressure can be written in its non-dimensional form as follows:

$$\tilde{p}_a \stackrel{def}{=} \frac{\hat{p}_a}{\bar{p}_r}. \tag{3.48}$$

The non-dimensional integral continuity equation

Using the scalings introduced above, we write the nondimensional integral continuity equation (3.18) as follows:

$$\int_{z=0}^{z=1} \rho v \, dz \;=\; -\frac{1}{2}\rho_i u_i r - \frac{\Xi}{r}\,\frac{\partial}{\partial t}\left(\int_{z=0}^{z=1}\int_{\xi=0}^{\xi=r} \xi\rho(\xi,z,t)\, d\xi dz\right), \tag{3.49}$$

where we have dropped the bars for simplicity.

Before proceeding with the asymptotic analysis, we briefly summarize the problem at hand by listing the non-dimensional governing equations and the corresponding non-dimensional boundary conditions. The continuity equation is given by (3.20), the radial and axial momentum equations are given by (3.21) and (3.25) respectively, the energy balance by (3.27), the $N-1$ species equations by (3.34), and the ideal-gas equation of state by (3.35). The corresponding non-dimensional boundary conditions at the inlet are given by (3.36)–(3.40). The non-dimensional boundary conditions at the film-gas interface reduce to (3.43)–(3.46). Finally, the non-dimensional prescribed background pressure is given by (3.48).

3.2 The Asymptotic Analysis

3.2.1 Asymptotic expansions of the flow fields

We are interested in investigating the behavior of the low-Mach-number flow in an axisymmetric reactor whose geometry is characterized by a small aspect ratio ϵ, i.e., a reactor such that the inlet showerhead and substrate have a very large common radius r_s in comparison to the height of the channel L. In the limit of infinite radius, the gas flow behaves like a stagnation-point flow, i.e., it can be fully described by a similarity solution (first established by von Kármán, cf. [K]. See also Pollard and Newman [PN]). This similarity solution results in a uniform film thickness and chemical composition, which is why this design is of so much interest to experimentalists who have investigated the operational conditions under which the

similarity solution is a valid approximation over most of the substrate. It is precisely the question of what is a good approximation and under which assumptions (on the geometry as well as the flow regime) that we attempt to study. Also, typical CVD flows are characterized by Mach numbers much smaller than one (usually $M < 10^{-2}$). Consequently, we shall work in the limit of vanishingly small aspect ratio ϵ and Mach number M, with the assumption that $\epsilon \gg M^2$. By using two-parameter asymptotic expansions of the various flow fields, we can obtain an analytical solution of the set of governing equations up to the leading order.

Consider the scaled equation of state (3.35). For this equation to reduce to the incompressible limit as $M \to 0$, it suffices to expand the pressure p asymptotically in powers of M^2 in the following fashion (cf. Hariharan et al. and the references therein [YHC]):

$$p = \frac{\tilde{p}}{M^2} + p_0 + M^2 p_1 + \cdots \tag{3.50}$$

Now, consider the scaled radial momentum equation (3.21). In order for the pressure gradient term not to vanish as the aspect ratio becomes infinitely small, it suffices to expand p_0 asymptotically in ϵ as follows:

$$p_0 = \frac{\hat{p}}{\epsilon} + \hat{p}_0 + \epsilon \hat{p}_1 + \cdots \tag{3.51}$$

It follows that the two-parameter asymptotic expansion of the pressure is:

$$p = \frac{\tilde{p}}{M^2} + \left(\frac{\hat{p}}{\epsilon} + \hat{p}_0 + \epsilon \hat{p}_1 + \cdots \right) + M^2 p_1 + \cdots \tag{3.52}$$

Similarly, we asymptotically expand all the other field variables as follows:

$$\rho = \rho_0 + M^2\rho_1 + \cdots, \tag{3.53}$$

$$\theta = \theta_0 + M^2\theta_1 + \cdots, \tag{3.54}$$

$$v = v_0 + M^2 v_1 + \cdots, \tag{3.55}$$

$$u = u_0 + M^2 u_1 + \cdots, \tag{3.56}$$

and $\forall\ k = 1, \ldots, N-1$,

$$\rho_k = \hat{\rho}_k + M^2\rho_{k,1} + \cdots, \tag{3.57}$$

where

$$\rho_0 = \hat{\rho}_0 + \epsilon\hat{\rho}_1 + \cdots \tag{3.58}$$

$$\theta_0 = \hat{\theta}_0 + \epsilon\hat{\theta}_1 + \cdots \tag{3.59}$$

$$v_0 = \hat{v}_0 + \epsilon\hat{v}_1 + \cdots \tag{3.60}$$

$$u_0 = \hat{u}_0 + \epsilon\hat{u}_1 + \cdots \tag{3.61}$$

and $\forall\ k = 1, \ldots, N-1$,

$$\hat{\rho}_k = \hat{\rho}_{k,0} + \epsilon\hat{\rho}_{k,1} + \cdots \tag{3.62}$$

The (scaled) heat conduction coefficient is a function of the (scaled) temperature. Consequently, we have:

$$k(\theta) = k(\hat{\theta}_0) + \epsilon k'(\hat{\theta}_0)\hat{\theta}_1 + \cdots + M^2 k'(\hat{\theta})\theta_1 + \cdots \tag{3.63}$$

Identically, we can expand the other temperature-dependent (scaled) parameters

as follows:

$$\mu(\theta) = \mu(\hat{\theta}_0) + \epsilon\mu'(\hat{\theta}_0)\hat{\theta}_1 + \cdots + M^2\mu'(\hat{\theta})\theta_1 + \cdots \tag{3.64}$$

and $\forall\ k = 1, \ldots, N-1$,

$$D_k(\theta) \;=\; D_k(\hat{\theta}_0) + \epsilon D_k^{'}(\hat{\theta}_0)\hat{\theta}_1 + \cdots + M^2 D_k^{'}(\hat{\theta})\theta_1 + \cdots \tag{3.65}$$

Finally, the sticking coefficient associated with the adsorption of the k^{th} species at the gas-film interface, as well as the forward and backward reaction-rate constants associated with the homogeneous reaction α can be expanded as follows: $\forall\ k = 1, \ldots, N$, and $\forall\ \alpha = 1, \ldots, N_c$,

$$\begin{aligned}
\lambda_k(\theta) &= \lambda_k(\hat{\theta}_0) + \epsilon\lambda_k^{'}(\hat{\theta}_0)\hat{\theta}_1 + \cdots + M^2\lambda_k^{'}(\hat{\theta})\theta_1 + \cdots, \\
k_f^{\alpha}(\theta) &= k_f^{\alpha}(\hat{\theta}_0) + \epsilon k_f^{\alpha'}(\hat{\theta}_0)\hat{\theta}_1 + \cdots + M^2 k_f^{\alpha'}(\hat{\theta})\theta_1 + \cdots, \qquad \text{and} \\
k_b^{\alpha}(\theta) &= k_b^{\alpha}(\hat{\theta}_0) + \epsilon k_b^{\alpha'}(\hat{\theta}_0)\hat{\theta}_1 + \cdots + M^2 k_b^{\alpha'}(\hat{\theta})\theta_1 + \cdots
\end{aligned} \tag{3.66}$$

The continuity, momentum, energy equations and the ideal-gas equation of state can be solved separately, i.e., as a set of coupled equations for the total density, velocity, energy and pressure variables. Once the temperature and velocity fields are explicitly determined, it becomes possible to solve the $N-1$ species equations for the $N-1$ species densities.

We shall then begin by solving the flow equations, and only then do we solve the species equations. We will proceed as follows: we first expand the variable fields in power series of M^2 (as done above), substitute these expansions into the governing equations and keep all the terms up to the first order in M^2 (an approximation valid in the limit of vanishingly small Mach numbers). We then expand these terms in power series of ϵ (again as done above) and throw away terms of first and higher order in ϵ (a procedure justifiable in the limit of very small aspect ratios). We finally

solve the remaining approximate equations analytically.

3.2.2 The asymptotic equations

We begin by substituting the asymptotic expansions of the flow fields in terms of M^2 in the non-dimensional equations and boundary conditions listed above.

The flow equations

Consider first the scaled continuity equation. The substitution of the expansions (3.53), (3.55) and (3.56) into (3.20) yields the following $O(1)$ equation:

$$\Xi\frac{\partial\rho_0}{\partial t}+\frac{1}{r}\frac{\partial}{\partial r}(r\rho_0 v_0)+\frac{\partial}{\partial z}(\rho_0 u_0) \;=\; 0. \tag{3.67}$$

Next, consider the scaled radial momentum equation. The substitution of the expansions (3.50), (3.53)-(3.56) and (3.64) into (3.21) leads to the following $O(1/M^2)$ equation:

$$\epsilon\frac{\partial\tilde{p}}{\partial r} \;=\; 0, \tag{3.68}$$

and the following $O(1)$ equation:

$$\begin{aligned}\epsilon\Xi\rho_0\frac{\partial v_0}{\partial t}+\epsilon\rho_0\left(v_0\frac{\partial v_0}{\partial r}+u_0\frac{\partial v_0}{\partial z}\right) &= -\epsilon\frac{\partial p_0}{\partial r}+\mathcal{P}\frac{\partial}{\partial z}\left(\mu(\theta_0)\frac{\partial v_0}{\partial z}\right)\\ &+\epsilon^2\mathcal{P}\left\{\frac{\partial}{\partial z}\left(\mu(\theta_0)\frac{\partial v_0}{\partial z}\right)+\frac{2}{3r}\frac{\partial}{\partial r}\left[r\mu(\theta_0)\left(2\frac{\partial v_0}{\partial r}-\frac{v_0}{r}-\frac{\partial u_0}{\partial z}\right)\right]\right\}\\ &-\epsilon^2\mathcal{P}\mu(\theta_0)\left(2\frac{v_0}{r}-\frac{\partial v_0}{\partial r}-\frac{\partial u_0}{\partial z}\right).\end{aligned} \tag{3.69}$$

A similar procedure applied to the scaled axial momentum equation (3.25) yields the following $O(1/M^2)$ equation:

$$\frac{\partial\tilde{p}}{\partial z} \;=\; 0, \tag{3.70}$$

and the $O(1)$ equation below:

$$\epsilon\Xi\rho_0\frac{\partial u_0}{\partial t}+\epsilon^2\rho_0\left(v_0\frac{\partial u_0}{\partial r}+\frac{\partial u_0}{\partial z}\right)=-\frac{\partial p_0}{\partial z}-\frac{1}{\mathcal{F}}\rho_0+\epsilon^3\mathcal{P}\frac{1}{r}\frac{\partial}{\partial r}\left(r\mu(\theta_0)\frac{\partial u_0}{\partial r}\right)$$
$$+\epsilon\mathcal{P}\left\{\frac{1}{r}\frac{\partial}{\partial r}\left(r\mu(\theta_0)\frac{\partial v_0}{\partial r}\right)+\frac{2}{3}\left[\mu(\theta_0)\left(2\frac{\partial u_0}{\partial z}-\frac{\partial v_0}{\partial r}-\frac{v_0}{r}\right)\right]\right\}. \quad (3.71)$$

Identically, the same procedure applied to the scaled energy balance (3.27) gives the following $O(1)$ equation:

$$\epsilon\Xi\rho_0\frac{\partial\theta_0}{\partial t}+\epsilon\rho_0\left(v_0\frac{\partial\theta_0}{\partial r}+u_0\frac{\partial\theta_0}{\partial z}\right)=\epsilon^2\frac{1}{r}\frac{\partial}{\partial r}\left(rk(\theta_0)\frac{\partial\theta_0}{\partial r}\right)$$
$$+\frac{\partial}{\partial z}\left(k(\theta_0)\frac{\partial\theta_0}{\partial z}\right)+\frac{\gamma-1}{\gamma}\epsilon\left(v_0\frac{\partial\tilde{p}}{\partial r}+u_0\frac{\partial\tilde{p}}{\partial z}\right). \quad (3.72)$$

Finally, the scaled ideal-gas equation of state (3.35) yields the following $O(1)$ equation:

$$\tilde{p} = \rho_0\theta_0. \quad (3.73)$$

The corresponding boundary conditions

We also substitute the asymptotic expansions of the flow variables in power series of M^2 (3.53)-(3.56) into the scaled boundary conditions along the showerhead (3.36)-(3.38) and along the gas-film interface (3.43)-(3.45), thus obtaining the following $O(1)$ in M^2 boundary conditions:

$$\theta_0(r,z=1) = \tilde{\theta}_i, \quad (3.74)$$
$$u_0(r,z=1) = \tilde{u}_i, \quad \text{and} \quad (3.75)$$
$$v_0(r,z=1) = 0, \quad (3.76)$$

and

$$\theta_0(r, z = 0) = \tilde{\theta}_f, \tag{3.77}$$

$$u_0(r, z = 0) = \tilde{v}_s, \qquad \text{and} \tag{3.78}$$

$$v_0(r, z = 0) = 0. \tag{3.79}$$

The integral continuity equation

Substituting (3.53) and (3.55) into (3.49), we obtain the following $O(1)$ equation in M^2:

$$\int_{z=0}^{z=1} \rho_0 v_0 \, dz = -\frac{1}{2}\rho_i u_i r - \frac{\Xi}{r}\frac{\partial}{\partial t}\left(\int_{z=0}^{z=1}\int_{\xi=0}^{\xi=r} \xi\rho_0(\xi, z, t)\, d\xi dz\right). \tag{3.80}$$

Next, we substitute the expansions of the flow fields in terms of power series of ϵ into the governing equations and boundary conditions derived above and then truncate all the terms of order ϵ or higher, thus obtaining the desired approximate equations and their corresponding boundary conditions.

The flow equations

We now consider the equations (3.67)-(3.73) which are $O(1)$ in M^2. Substituting the expansions in power series of ϵ (3.51), (3.58)-(3.61) and (3.63) into these equations, we obtain the following equations:

(i) The $O(1)$ continuity equation:

$$\Xi\frac{\partial\hat{\rho}_0}{\partial t} + \frac{1}{r}\frac{\partial}{\partial r}(r\hat{\rho}_0\hat{v}_0) + \frac{\partial}{\partial z}(\hat{\rho}_0\hat{u}_0) = 0. \tag{3.81}$$

(ii) The $O(1)$ radial momentum equation:

$$-\frac{\partial\hat{p}}{\partial r} + \mathcal{P}\frac{\partial}{\partial z}\left(\mu(\hat{\theta}_0)\frac{\partial\hat{v}_0}{\partial z}\right) = 0. \tag{3.82}$$

As will become obvious when we solve the $O(1)$ equations, we will also need the

$O(\epsilon/M^2)$ radial momentum equation:

$$\frac{\partial \tilde{p}}{\partial r} = 0. \tag{3.83}$$

(iii) The $O(1)$ axial momentum equation:

$$\frac{\partial \hat{p}_0}{\partial z} - \mathcal{F}\hat{\rho}_0 = 0. \tag{3.84}$$

We also need the $O(1/M^2)$ axial momentum equation

$$\frac{\partial \tilde{p}}{\partial z} = 0, \tag{3.85}$$

and the $O(1/\epsilon)$ axial momentum equation

$$\frac{\partial \hat{p}}{\partial z} = 0. \tag{3.86}$$

(iv) The energy balance:

$$\frac{\partial}{\partial z}\left(k(\hat{\theta}_0)\frac{\partial \hat{\theta}_0}{\partial z}\right) = 0. \tag{3.87}$$

(v) The $O(1)$ ideal-gas equation of state:

$$\tilde{p} = \hat{\rho}_0\hat{\theta}_0. \tag{3.88}$$

The corresponding boundary conditions

Substituting the expansions of the flow variables in power series of ϵ into the inlet boundary conditions (3.74)-(3.75) and those at surface separating the gaseous flow from the solid film (3.77)-(3.79), we obtain the following $O(1)$ in ϵ boundary

conditions:

$$\hat{\theta}_0(r, z = 1) = \tilde{\theta}_i, \tag{3.89}$$

$$\hat{u}_0(r, z = 1) = \tilde{u}_i, \quad \text{and} \tag{3.90}$$

$$\hat{v}_0(r, z = 1) = 0, \tag{3.91}$$

$$\tag{3.92}$$

and

$$\hat{\theta}_0(r, z = 0) = \tilde{\theta}_f, \tag{3.93}$$

$$\hat{u}_0(r, z = 0) = \tilde{v}_s, \quad \text{and} \tag{3.94}$$

$$\hat{v}_0(r, z = 0) = 0. \tag{3.95}$$

The integral continuity equation

Substituting (3.58) and (3.60) into (3.80), we obtain the following integral mass balance which is $O(1)$ in ϵ:

$$\int_{z=0}^{z=1} \hat{\rho}_0 \hat{v}_0 \, dz = -\frac{1}{2}\rho_i u_i r - \frac{\Xi}{r}\frac{\partial}{\partial t}\left(\int_{z=0}^{z=1}\int_{\xi=0}^{\xi=r} \xi \hat{\rho}_0(\xi, z, t) \, d\xi dz\right). \tag{3.96}$$

3.2.3 The solution procedure for the steady-state case

We now specialize to the case of a vanishingly small Ξ, i.e., as mentioned above, we assume that the typical time scale for the growth of the thin solid film is much larger than the convective and species diffusive characteristic time scales in the gaseous flow. Consequently, we shall solve the approximate steady-state equations (3.82)-(3.88) and the corresponding approximate boundary conditions (3.89)-(3.95), in addition to the steady-state continuuity equation

$$\frac{1}{r}\frac{\partial}{\partial r}(r\hat{\rho}_0\hat{v}_0) + \frac{\partial}{\partial z}(\hat{\rho}_0\hat{u}_0) = 0, \tag{3.97}$$

and its integral form

$$\int_{z=0}^{z=1} \hat{\rho}_0 \hat{v}_0 \, dz \;=\; -\frac{1}{2} r \rho_i u_i. \tag{3.98}$$

The temperature field

We begin by making constitutive assumptions on the temperature-dependence of the viscosity and heat conduction coefficients. More specifically, we shall assume the following 'generalized' Sutherland laws:

$$\mu(\theta) \stackrel{def}{=} \theta^{\alpha}, \qquad \text{and} \tag{3.99}$$

$$k(\theta) \stackrel{def}{=} \theta^{\beta}, \tag{3.100}$$

where α and β are real numbers $(0 < \alpha,\ \beta < 1)$.

Now, substituting (3.100) into the energy balance (3.87) and integrating with respect to z, we obtain the following relation:

$$\frac{1}{\beta+1} \frac{\partial}{\partial z} (\hat{\theta}_0^{\beta+1}) \;=\; \alpha(r),$$

where $\alpha(r)$ is yet to be determined.

Integrating a second time with respect to z yields the following relation:

$$\hat{\theta}_0(r,z) \;=\; (a(r)z + b(r))^{\frac{1}{\beta+1}}, \tag{3.101}$$

where $a(r) \stackrel{def}{=} (\beta+1)\alpha(r)$ and $b(r)$ can be explicitly determined using the boundary conditions (3.89) and (3.93). We find that $a(r)$ and $b(r)$ are constant and given by following relations:

$$b \;=\; \tilde{\theta}_f^{\beta+1}, \qquad \text{and} \tag{3.102}$$

$$a \;=\; \tilde{\theta}_i^{\beta+1} - \tilde{\theta}_f^{\beta+1}. \tag{3.103}$$

The total mass density profile

From (3.83) and (3.85), we conclude that $\tilde{p}$ is constant:

$$\tilde{p} \;=\; \tilde{p}_a \;=\; \text{constant.} \tag{3.104}$$

It then follows from (3.88) that the total mass density field $\hat{\rho}_0$ is inversely proportional to the temperature field $\hat{\theta}_0$ (and consequently is independent of r):

$$\hat{\rho}_0(z) \;=\; \frac{\tilde{p}_a}{\hat{\theta}(z)}. \tag{3.105}$$

The radial velocity field

First, from (3.86) we conclude that $\hat{p}$ is a function only of r. Consequently, we can rewrite the radial momentum equation (3.82) as follows:

$$\frac{\partial}{\partial z}\left(\mu(\hat{\theta}_0)\frac{\partial \hat{v}_0}{\partial z}\right) \;=\; \frac{1}{\mathcal{P}}\hat{p}'(r).$$

Integrating twice with respect to z, we obtain the following relation:

$$\hat{v}_0(r,z) \;=\; \frac{\hat{p}'(r)}{\mathcal{P}}\int_{\xi=0}^{\xi=z}\frac{\xi}{\mu(\hat{\theta}_0(\xi))}\,d\xi + c(r)\int_{\xi=0}^{\xi=z}\frac{1}{\mu(\hat{\theta}_0(\xi))}\,d\xi + d(r),$$

where $c(r)$ and $d(r)$ are yet to be determined.

Making use of the boundary conditions (3.91) and (3.95), we find that:

$$\begin{aligned} d(r) \;&=\; 0, \qquad \text{and} \\ c(r) \;&=\; \frac{c}{\mathcal{P}}\hat{p}'(r), \end{aligned}$$

where

$$c \;\stackrel{def}{=}\; -\frac{\int_{\xi=0}^{\xi=1}\frac{\xi}{\mu(\hat{\theta}_0(\xi))}\,d\xi}{\int_{\xi=0}^{\xi=1}\frac{1}{\mu(\hat{\theta}_0(\xi))}\,d\xi}.$$

This allows us to rewrite the radial velocity as a product of two functions, one of r and the other of z:

$$\hat{v}_0 \;=\; R(r)Z(z), \tag{3.106}$$

where:

$$R(r) \;\stackrel{def}{=}\; \frac{1}{\mathcal{P}}\hat{p}^{'}(r), \qquad \text{and} \tag{3.107}$$

$$Z(z) \;\stackrel{def}{=}\; \int_{\xi=0}^{\xi=z} \frac{\xi}{\mu(\hat{\theta}_0(\xi))}\, d\xi + c\int_{\xi=0}^{\xi=z} \frac{1}{\mu(\hat{\theta}_0(\xi))}\, d\xi. \tag{3.108}$$

Now, substituting the constitutive relation (3.99) into (3.108), we have:

$$Z(z) \;=\; \int_{\xi=0}^{\xi=z} \xi\hat{\theta}_0^{-\alpha}(\xi)\, d\xi + c\int_{\xi=0}^{\xi=z} \hat{\theta}_0^{-\alpha}(\xi)\, d\xi. \tag{3.109}$$

Integrating the first term on the RHS of (3.109) by parts, and then making a change of variables $\eta \rightarrow a\xi + b$, where a and b are given by (3.102) and (3.103), and after some tedious but straightforward algebra, we obtain the following relation for the radial velocity field as a function of the temperature field:

$$\begin{aligned} Z(z) \;=\; \frac{1}{1-\alpha} z\hat{\theta}_0^{1-\alpha}(z) \;&-\; \frac{1+\beta}{a(1-\alpha)(2+\beta-\alpha)}\left(\hat{\theta}_0^{2+\beta-\alpha}(z) - \tilde{\theta}_f^{2+\beta-\alpha}\right) \\ &+\; \frac{c(1+\beta)}{a(1+\beta-\alpha)}\left(\hat{\theta}_0^{1+\beta-\alpha}(z) - \tilde{\theta}_f^{1+\beta-\alpha}\right). \end{aligned} \tag{3.110}$$

Next, we substitute (3.106) and (3.104) into the integral continuity equation (3.98) and solve for $R(r)$. This yields the following relation:

$$R(r) \;=\; Dr, \tag{3.111}$$

where D is a constant given by:

$$D \;\stackrel{def}{=}\; -\frac{\tilde{\theta}_i\tilde{u}_i}{2\int_{\xi=0}^{\xi=1} \frac{Z(\xi)}{\hat{\theta}_0(\xi)}\, d\xi}, \tag{3.112}$$

where we have used the ideal-gas equation of state as it applies at the inlet:

$$\tilde{\rho}_i \stackrel{def}{=} \frac{\tilde{p}_a}{\tilde{\theta}_i}.$$

Consequently, the leading term of the radial velocity profile is of the form

$$\hat{v}_0 \propto rZ(z), \tag{3.113}$$

the constant of proportionality being D and where $Z(z)$ is given by (3.110).

The axial velocity profile

Finally, we use the continuity equation (3.97) to determine the axial velocity field. Substituting (3.106), (3.111) and (3.105) into (3.97), and then integrating with respect to z, we obtain the following relation:

$$\hat{u}_0(r,z) = -2D\hat{\theta}_0(z)\int_{\xi=0}^{\xi=z}\frac{Z(\xi)}{\hat{\theta}_0(\xi)}\,d\xi + f(r)\hat{\theta}_0(z), \tag{3.114}$$

where $f(r)$ is yet to be determined.

Substituting (3.114) into the inlet boundary condition (3.90) yields the following relation:

$$f(r) = \text{constant} = f = 2D\int_{\xi=0}^{\xi=1}\frac{Z(\xi)}{\hat{\theta}_0(\xi)}\,d\xi + \frac{\tilde{u}_i}{\tilde{\theta}_i},$$

and we can rewrite (3.114) as follows:

$$\hat{u}_0(z) = E(z)\hat{\theta}_0(z), \tag{3.115}$$

where

$$E(z) \stackrel{def}{=} -2D\int_{\xi=0}^{\xi=z}\frac{Z(\xi)}{\hat{\theta}_0(\xi)}\,d\xi + f. \tag{3.116}$$

Remark

We note here that the growth velocity need not be prescribed as it is not needed to explicitly determine the $O(1)$ flow fields (nor is it needed to determine the species density profiles as will be seen below). This is due to the fact that, in the integral continuity equation, the term containing this growth velocity $\rho_f^g v_s$ is neglected on the basis that the growth velocity v_s is much smaller than the inlet velocity u_i. Underlying such an approximation is the assumption that the gas densities ρ_i^g and ρ_f^g are of the same order of magnitude. If this were not to be the case, then we cannot make the approximation mentioned above and consequently the growth velocity will need to be prescribed if one is to explicitly determine the $O(1)$ radial velocity profile.

The species density fields

We are now in a position to determine explicitly the $O(1)$ species density profiles. In order to do so, we proceed in a fashion analogous to the procedure applied above to the flow fields. That is, we begin by substituting the expansions of the species densities in power series of M^2 (3.57) into the scaled species equations (3.34), keeping only those terms that are $O(1)$ in M^2. We thus obtain the following $O(1)$ species equations in M^2: $\forall\ k = 1, \ldots, N-1$,

$$\epsilon \Xi \mathcal{P}_k \frac{\partial \hat{\rho}_k}{\partial t} + \epsilon \mathcal{P}_k \left[\frac{1}{r} \frac{\partial}{\partial r} (r \hat{\rho}_k v_0) + \frac{\partial}{\partial z} (\hat{\rho}_k u_0) \right] =$$
$$\epsilon^2 \frac{1}{r} \frac{\partial}{\partial r} \left[r D_k(\theta_0) \left(\frac{\partial \hat{\rho}_k}{\partial r} + \frac{\alpha_k \hat{\rho}_k}{\theta_0} \frac{\partial \theta_0}{\partial r} \right) \right] + \frac{\partial}{\partial z} \left[D_k(\theta_0) \left(\frac{\partial \hat{\rho}_k}{\partial z} + \frac{\alpha_k \hat{\rho}_k}{\theta_0} \frac{\partial \theta_0}{\partial z} \right) \right]$$
$$+ \sum_{\alpha=1}^{N_c} \left(\epsilon \mathcal{D}_k^{\alpha,f} \bar{k}_f^{\alpha}(\theta_0) \prod_{m=1}^{N_\alpha^r} \hat{\rho}^{\nu_m^\alpha} - \epsilon \mathcal{D}_k^{\alpha,b} \bar{k}_b^{\alpha}(\theta_0) \prod_{n=1}^{N_p^\alpha} \hat{\rho}^{\nu_n^\alpha} \right). \tag{3.117}$$

Next, we substitute the expansions of the species density fields in power series of ϵ (3.62) into the above equations (3.117) and we neglect $O(\epsilon)$ and higher order terms,

thus obtaining the following $O(1)$ species equations: $\forall\ k = 1, \ldots, N-1$,

$$\frac{\partial}{\partial z}\left[D_k(\hat{\theta}_0)\left(\frac{\partial \hat{\rho}_{k,0}}{\partial z} + \frac{\alpha_k \hat{\rho}_{k,0}}{\hat{\theta}_0}\frac{\partial \hat{\theta}_0}{\partial z}\right)\right] \;=\; 0. \tag{3.118}$$

Integrating with respect to z, we obtain the following relations: $\forall\ k = 1, \ldots, N-1$,

$$D_k(\hat{\theta}_0)\left[\frac{\partial \hat{\rho}_{k,0}}{\partial z} + \left(\frac{\alpha_k}{\hat{\theta}_0}\frac{\partial \hat{\theta}_0}{\partial z}\right)\hat{\rho}_{k,0}\right] \;=\; M_k(r), \tag{3.119}$$

where the $M_k(r)$ are yet to be determined.

Consider now the inlet boundary conditions (3.40). Substituting first the expansions in power series of M^2 and then those in power series of ϵ of the species densities (3.117) and (3.118) (respectively) into (3.40), we obtain the following boundary conditions which will be $O(1)$ in both M^2 and ϵ: $\forall\ k = 1, \ldots, N-1$,

$$D_k(\tilde{\theta}_i)\left(\frac{\partial \hat{\rho}_{k,0}}{\partial z}(r, z=1) + \frac{\alpha_k \hat{\rho}_k(r, z=1)}{\tilde{\theta}_i}\frac{\partial \hat{\theta}_0}{\partial z}(r, z=1)\right) \;=\; \tilde{m}_k. \tag{3.120}$$

We expect (3.119) to hold everywhere in the domain of integration, in particular along the showerhead. Consequently, substituting (3.119) into (3.120) yields the following result: $\forall\ k = 1, \ldots, N-1$,

$$M_k(r) \;=\; M_k \;=\; \tilde{m}_k.$$

Next, we rewrite (3.119) as follows:

$$\frac{\partial \hat{\rho}_{k,0}}{\partial z} + F(z)\hat{\rho}_{k,0} \;=\; \frac{M_k}{D_k(\hat{\theta}_0(z))}, \tag{3.121}$$

where

$$F(z) \stackrel{def}{=} \alpha_k \frac{d}{dz}(\ln \hat{\theta}_0(z)).$$

Consider the homogeneous equation associated with (3.121). It can easily be

shown that the general solution of this homogeneous equation is of the form:

$$\hat{\rho}_{k,0}(r,z) \;=\; b_k(r)\exp f(z), \tag{3.122}$$

with

$$f(z) \stackrel{def}{=} -\int_{\xi=0}^{\xi=z} F(\xi)\, d\xi.$$

Substituting (3.122) where b_k is now taken to be a function of both coordinates r and z into (3.121), we obtain the equation:

$$\frac{\partial b_k}{\partial z}(r,z) \;=\; M_k \frac{\exp(-f(z))}{D_k(\hat{\theta}_0(z))}$$

whose solution is given by:

$$b_k(r,z) \;=\; M_k \int_{\xi=0}^{\xi=z} \frac{\exp(-f(\xi))}{D_k(\hat{\theta}_0(\xi))}\, d\xi + N_k(r), \tag{3.123}$$

where $N_k(r)$ is yet to be determined.

Applying to the boundary conditions (3.46) along the gas-film interface a, procedure identical to that applied to (3.40) along the showerhead yields the following $O(1)$ (in M^2 and ϵ) equations: $\forall\ k = 1, \ldots, N-1$,

$$D_k(\tilde{\theta}_f)\left(\frac{\partial \hat{\rho}_{k,0}}{\partial z}(r,0) + \frac{\alpha_k \hat{\rho}_{k,0}(r,0)}{\tilde{\theta}_f}\frac{\partial \hat{\theta}_0}{\partial z}(r,0)\right) \;=\; \tilde{\mathcal{D}}_k^s \lambda_k(\tilde{\theta}_f)\hat{\rho}_{k,0}(r,0), \tag{3.124}$$

where $\tilde{\mathcal{D}}_k^s \stackrel{def}{=} \epsilon \mathcal{D}_k^s = \lambda_k L/D_{k,r}$ has been assumed to be $O(1)$, i.e., $\mathcal{D}_k^s = O(1/\epsilon)$, so that the deposition is governed by the diffusion of the reactants rather than by the surface kinetics. Now, substituting (3.120), (3.122) and (3.123) into the equation (3.124) leads to the following relation: $\forall\ k = 1, \ldots, N-1$,

$$N_k(r) \;=\; N_k \;=\; \frac{1}{\tilde{\mathcal{D}}_k^s}\frac{D_k(\tilde{\theta}_i)}{\lambda_k(\tilde{\theta}_f)}\,\tilde{m}_k.$$

Consequently, we can rewrite the $O(1)$ species density profiles as:

$$\hat{\rho}_{k,0}(r,z) \;=\; b_k(z)\left(\frac{\hat{\theta}_0(z)}{\tilde{\theta}_f}\right)^{-\alpha_k}, \tag{3.125}$$

where

$$b_k(z) \;=\; \frac{\tilde{m}_k}{\tilde{\theta}_f^{\alpha_k}}\left(\int_{\xi=0}^{\xi=z}\frac{\hat{\theta}_0^{\alpha_k}(\xi)}{D_k(\hat{\theta}_0(\xi))}\,d\xi + \frac{1}{\tilde{\mathcal{D}}_k^s}\frac{D_k(\tilde{\theta}_i)}{\lambda_k(\tilde{\theta}_f)}\tilde{\theta}_f^{\alpha_k}\right). \tag{3.126}$$

3.3 Summary

We have developed a model for the viscous and heat conducting flow of a chemically reactive multicomponent gas mixture in the channel of an axisymmetric vertical chemical vapor deposition reactor such as are widely used for industrial applications. The gas mixture is assumed to be very dilute and the precursors are taken to be much heavier than the carrier gas. The flowing vapor is also assumed to behave like an ideal gas and the various material parameters (e.g., viscosity, heat conduction coefficient, species diffusivities, etc.) are assumed to be dependent on the temperature. The Soret effects are taken into account as the temperature gradients are typically very large in CVD processes, but heat radiation is ignored. An asymptotic analysis is performed in the limits of small aspect ratio (i.e., a reactor geometry characterized by a substrate radius much larger than the channel height) and small Mach numbers (a reasonable approximation for many CVD flows).

It is found that the temperature profile is given by (3.101), (3.102) and (3.103). The total mass density profile is given by (3.105). The radial velocity profile is given by (3.113), (3.112) and (3.110), while the axial velocity profile is described by (3.115) and (3.116). Finally, the species density profiles are given by (3.125) and (3.126). The leading order solutions listed above are of the *similarity* type, i.e., they reduce the level of complexity of the system (by making the flow fields depend only on the vertical coordinate rather than both the radial and axial ones). Most importantly, they indicate that for such limits, the *uniformity* of the temperature and

species densities along the substrate can be approached, thus justifying a posteriori the interest in CVD reactors characterized by a geometry like the one described above and operating under experimental conditions insuring a low Mach number.

Chapter 4 A Mesoscopic Step-Flow Model for the Growth of Multispecies Films

4.1 Introduction

The growth of epitaxially deposited thin solid films often proceeds by the "terrace and ledge" mechanism. The surface of the growing film is characterized by large terraces separated by steps, which are often of multi-atom height. Atoms adsorb at the terraces from the gas phase, then diffuse along those terraces and finally attach to the ledges where they react to form the compound as shown in Figure 4.1. The study of the terrace-and-ledge mechanism was pioneered by the seminal work of Burton, Cabrera and Frank [BCF] (see also Zangwill [Z] and Pimpinelli and Villain [VP] and the references therein for more recent studies). As mentioned in the introduction, these studies have focused on the growth of films of a single chemical species or element.

There is currently a growing interest in perovskite thin films for their ferroelectric (such as in $PbTiO_3$) and superconducting (such as in $YBa_2Cu_3O_{7-\delta}$) properties. The role of heterogeneous chemistry, i.e., the chemical reactions that occur along the surface separating the solid phase from the vapor, during the growth of these films is of great importance. The models describing the growth of thin films by chemical vapor deposition (CVD) deal extensively with the surface chemistry (cf., e.g., [CK]). However, with the exception of Mountziaris and Jensen [JM], these models often assume that the surface of the growing film is flat.

The morphological evolution of mulispecies films has been investigated and macroscopic continuum models have been proposed in the setting of alloys, i.e., of substitu-

tional thin solid films (e.g., see Spencer et al. [SVD] and Guyer and Voorhees [GV]). A significant difference between alloys and compounds is that compounds have to satisfy the constraint of stochiometry while alloys are not subject to such requirements. Consequently, alloys can readily absorb excess quantities of deposited species, but compounds do not have this ability. Thus, during the growth of *compound* thin films, the presence of chemical species in excess leads to a build-up that could result in (i) a nonlinear dependence of the growth rate on the concentrations of gas-phase species, and (ii) the nucleation of undesired secondary phases (such as islands of CuO or BaO in the case of $YBa_2Cu_3O_{7-\delta}$).

In this chapter, we present a simple attempt to model the growth of a multispecies compound thin film by a terrace-and-ledge mechanism. We consider a *model* system with N chemical species (where $N \geq 2$), and postulate a series of mechanisms for the adsorption/desorption of species along the terraces as well as a sequence of incorporation chemical reactions at the steps. This work was motivated by the desire to gain a better understanding of the growth of high-temperature superconducting $YBa_2Cu_3O_{7-\delta}$ thin films by metal-organic CVD (MOCVD). Unfortunately, many of the exact physical and chemical mechanisms by which the growth occurs at the atomistic or molecular scale are not completely understood nor experimentally fully characterized for such complex systems as $YBa_2Cu_3O_{7-\delta}$. However, we believe that the mechanisms postulated here are quite general and realistic, and reflect the nonlinear interactions that are inherent to multispecies physical systems.

We describe the adsorption-desorption, terrace diffusion and attachment mechanisms in detail and write down the corresponding governing equations in section 4.2. We note here that we have restricted ourselves to the isothermal situation, since the terraces are much smaller than the length-scale on which significant temperature variations occur in the film. Consequently, the temperature-dependent material parameters that enter our model (e.g., the diffusion coefficients, the reaction-rate constants, etc.) will be constant.

We then study in section 4.3 the growth of the film by the motion of a one-dimensional train of equidistant steps. Clearly, the exact morphology of growth of

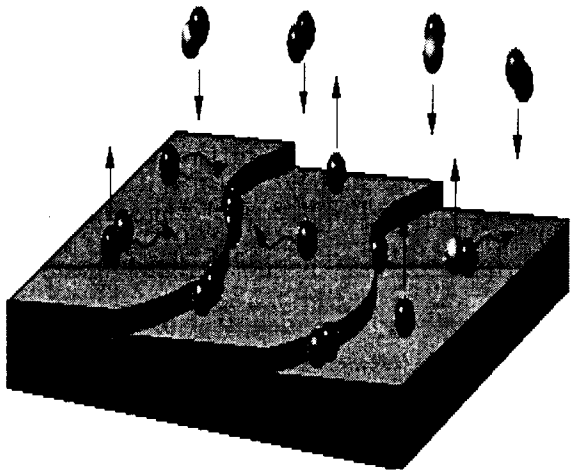

Figure 4.1: Schematic of the surface microstructure and growth mechanisms. The gas-phase precursors are symbolically shown as diatomic molecules. Along the terraces, adatoms diffuse until they reach the upper step where compound formation occurs via chemical reaction.

various thin films is more complicated (for example, $YBa_2Cu_3O_{7-\delta}$ grows by the motion of steps which *spiral* around screw dislocations). It is our belief, however, that this simplified setting of step-flow correctly demonstrates the interesting features resulting from the interactions between the multiple species. We then calculate the overall growth rate of the film, and its dependence on the gas-phase concentrations and the terrace widths.

In sections 4.4 and 4.5, we illustrate the complex dependence of the averaged growth rate on the gas-phase chemical composition and the surface morphology by specializing to the case of two species. We finally fit the results to simple constitutive relations.

4.2 The Multispecies Terrace-and-Ledge Model

4.2.1 The general framework

Consider the growth of a thin solid film of a multicomponent compound (denoted C) made up of N chemical species (denoted $S_1, S_2, \ldots S_N$) by chemical vapor deposition (CVD). Here, a chemically reacting gas is introduced into a reactor where it flows past a heated substrate and deposits a film on the substrate. The gas phase consists of metallorganic precursors diluted in a neutral carrier gas. The precursors are organic molecules to which the species of interest are bound. As they approach

the heated substrate, the precursors undergo a series of reactions, leading ulimately to the adsorption of the species of interest on the terraces.

We are interested in the growth of the film, and hence concentrate on the part of the vapor directly above the film. This region consists of precursors of the form X_kS_k, where X_k is the organic ligand bound to S_k, mixed with the inert gas. We assume that the concentration of X_kS_k is given (constant). This is reasonable since the terrace widths are much smaller than the mean-free paths of the molecules in the gas. Each compound X_kS_k is adsorbed to the terrace where it decomposes into X_k which is released to the gas and the species S_k which attaches to an adsorption site. The various adsorbed species diffuse around the terrace, a small fraction is desorbed back into the vapor while the remaining particles reach the step, where they undergo a series of chemical reactions, leading to the formation of the compound which is then incorporated into the film, thus causing the step to move.

4.2.2 Adsorption-Desorption

The mechanisms by which the adsorption and desorption of species along the terraces take place can be formalized as follows: $\forall\ k = 1, \ldots, N$,

$$X_kS_k(g) + O(t) \xrightarrow{\lambda^k_{ads}} S_k(t) + X_k(g), \qquad \text{and} \tag{4.1}$$

$$S_k(t) \xrightarrow{\lambda^k_{des}} S_k(g), \tag{4.2}$$

where g denotes the gaseous species and t the species along the terrace. $O(t)$ represents an open adsorption site, and λ^k_{ads} and λ^k_{des} denote the reaction-rate constants associated with the adsorption and desorption (respectively) of the k^{th} species. Note that in the above proposed chemical formalism, we have implicitly assumed that there is only one type of adsorption sites, i.e., any open adsorption site is capable of hosting an adsorbed molecule regardless of which species it belongs to. This is obviously not the only mechanism possible, as there are situations in which different species adsorb on distinct sites. Consequently, for such a deposition mechanism, one would need to introduce as many types of open sites (denoted $\{O_k(t)\}_{k=1}^N$) as there are species

present in the system of interest.

The rate of production of k-adatoms (along the terraces) by the reactions (4.1) and (4.2) can be expressed as follows:

$$R_k = w_k \left\{ \lambda^k_{ads}[X_k S_k]_g \left(\Gamma - \sum_{i=1}^{N} \frac{\rho_i}{w_i} \right) - \lambda^k_{des} \frac{\rho_k}{w_k} \right\}, \tag{4.3}$$

where ρ_k is the terrace density of k-adatoms, w_k is the molar weight of the k^{th} species, Γ is the total molar density of sites along an individual terrace and $[X_k S_k]_g$ is the molar concentration of the precursor carrying the k^{th} species in the gas phase (assumed to be constant). It follows that $\Gamma - \sum_{i=1}^{N} \rho_i/w_i$ is the terrace density of open sites, i.e., those that are not already hosting an adatom. Now, if $\sum_{i=1}^{N} \rho_i/w_i$ is much smaller than Γ, i.e., if the adatoms are very dilute along the terraces, then the production rate of k-particles can be approximated by the following expression:

$$R_k = w_k \left(\tilde{\lambda}^k_{ads}[X_k S_k]_g - \lambda^k_{des} \frac{\rho_k}{w_k} \right), \tag{4.4}$$

where $\tilde{\lambda}^k_{ads} \stackrel{def}{=} \Gamma \lambda^k_{ads}$.

Note that in the presence of N distinct types of open site, the reaction rate is identical to that given by (4.3) except that $\Gamma - \sum_{i=1}^{N} \frac{\rho_i}{w_i}$ is replaced by $\Gamma_k - \frac{\rho_k}{w_k}$, where the latter is the terrace density of open sites of the k^{th} type (i.e., those sites that can still adsorb k-particles). Consequently, we obtain an expression for the rate of adsorption-desorption of k-adatoms analogous to (4.4):

$$R_k = w_k \left(\hat{\lambda}^k_{ads}[X_k S_k]_g - \hat{\lambda}^k_{des} \frac{\rho_k}{w_k} \right), \tag{4.5}$$

where $\hat{\lambda}^k_{ads} \stackrel{def}{=} \Gamma_k \lambda^k_{ads}$ and $\hat{\lambda}^k_{des} \stackrel{def}{=} \lambda^k_{ads}[X_k S_k]_g + \lambda^k_{des}$.

As will become clear from sections 4.4 and 4.5, the form of R_k (i.e., whether it is expressed by (4.3) or (4.4)) makes a significant difference in terms of the dependence of the growth rate of the film on the chemical composition of the gas phase. We shall call (4.3) the production rate of k-particles corresponding to the deposition

scenario *with competition*, while (4.4) corresponds to the case of deposition *without competition*.

4.2.3 Diffusion

Along an individual terrace, the equation governing the evolution of the terrace density of adatoms of the k^{th} species is given by: $\forall\ k = 1, \ldots, N$,

$$\frac{\partial \rho_k}{\partial t} = D_k \nabla^2 \rho_k + R_k, \tag{4.6}$$

where ρ_k is the mass density of adatoms of the k^{th} species along the terrace, D_k its diffusion coefficient, and R_k is the mass production rate of k-adatoms due to adsorption and desorption along the terrace.

The reaction-diffusion equations (4.6) obviously require boundary conditions at the upper and lower steps that delimit the terrace of interest. These boundary conditions will be discussed in the next subsection.

4.2.4 Incorporation

It is at the steps that the different species react to form the compound of interest which is then incorporated into the film. Typically, at any given step, the incorporation of the particles from the upper terrace is much *smaller* than the incorporation of the species from the lower terrace in view of the Ehlrich-Schwoebel barrier (e.g., see Elkinani and Villain [VE]). We take this to an extreme, and assume that there is no incorporation from the upper terrace (the so-called infinite Ehlrich-Schwoebel barrier). Thus, we have the following boundary conditions:

$$-D_k(\nabla \rho_k)^- \cdot n_s^- = \rho_k^- \mathbf{v}_s^- \cdot n_s^- \quad \text{at the lower step, and} \tag{4.7}$$

$$-D_k(\nabla \rho_k)^+ \cdot n_s^+ = \rho_k^+ \mathbf{v}_s^+ \cdot n_s^+ - R_{inc}^k \quad \text{at the upper step,} \tag{4.8}$$

where R_{inc}^k is the rate of production (or destruction) of k-particles associated with the formation of the compound at the upper step.

The incorporation from the lower terrace proceeds by a series of reactions. We describe this series of reactions for a model case of a compound AB_2C_3 of three species A, B and C. We assume that the step is of unit cell height and that the unit cell consists of layers ordered $CBCACB$ and repeated periodically $CBCACBCBCACB\ldots$. A complete step provides a site $O(s)$ where a C-atom can attach to form $C(s)$. A B-atom can now attach to form $CB(s)$ to which another C-atom can attach to form $CBC(s)$ and so forth till the final B-atom attaches to form a complete step and thus generate a new site $O(s)$. We thus propose the following chemical formalism at the upper step:

$$\begin{aligned}
O(s) + C(t) &\xrightarrow{\lambda_1} C(s) \\
C(s) + B(t) &\xrightarrow{\lambda_2} CB(s) \\
CB(s) + C(t) &\xrightarrow{\lambda_3} CBC(s) \\
CBC(s) + A(t) &\xrightarrow{\lambda_4} CBCA(s) \\
CBCA(s) + C(t) &\xrightarrow{\lambda_5} CBCAC(s) \\
CBCAC(s) + B(t) &\xrightarrow{\lambda_6} CBCACB(s) + O(s),
\end{aligned} \tag{4.9}$$

where s denotes particles at the upper step. The reaction rates associated with the above chemical reactions are:

$$\begin{aligned}
R_1 =& k_1\rho_c\{\Gamma_s - [C]_s - [CB]_s - [CBC]_s - [CBCA]_s - [CBCAC]_s\}, \\
R_2 =& k_2\rho_b[C]_s, \\
R_3 =& k_3\rho_c[CB]_s, \\
R_4 =& k_4\rho_a[CBC]_s, \\
R_5 =& k_5\rho_c[CBCA]_s, \qquad \text{and} \\
R_6 =& k_6\rho_b[CBCAC]_s,
\end{aligned} \tag{4.10}$$

where Γ_s is the total molar concentration of incorporation sites along the upper step, and $[S_k]_s$ is the molar concentration of incorporation sites occupied by particles of

the k^{th} species, so that $\Gamma_s - [C]_s - [CB]_s - [CBC]_s - [CBCA]_s - [CBCAC]_s$ is the molar concentration of open incorporation sites (i.e., those sites along the upper step capable of hosting C-atoms). Also, ρ_k is the terrace density of S_k-atoms at the upper step, and $\{k_i\}_{i=1}^{6}$ are the reaction-rate constants associated with the incorporation reactions listed above.

It then follows that:

$$\begin{aligned} \frac{\partial \rho_a}{\partial t} &= R^a_{inc} = -\, w_a R_4, \\ \frac{\partial \rho_b}{\partial t} &= R^b_{inc} = -\, w_b (R_2 + R_6), \qquad \text{and} \\ \frac{\partial \rho_c}{\partial t} &= R^c_{inc} = -\, w_c (R_1 + R_3 + R_5), \end{aligned} \tag{4.11}$$

which are then substituted into the boundary conditions (4.8).

We now make the following simplifying assumption. We assume that these reactions occur much faster than the diffusion of adatoms along the terraces, so that we can assume that the step formation reaches a steady state. In other words, we assume that each of the reactions above proceeds at the same rate, i.e., $R_1 = R_2 = \cdots = R_6$. It then follows that

$$\begin{aligned} R^a_{inc} &= -\, w_a R_{inc}, \\ R^b_{inc} &= -\, 2 w_b R_{inc}, \qquad \text{and} \\ R^c_{inc} &= -\, 3 w_c R_{inc}, \end{aligned}$$

where

$$R_{inc} \;=\; \frac{k_1 \Gamma_s \rho_c}{1 + \frac{k_1}{k_3} + \frac{k_1}{k_5} + \frac{k_1}{k_2}\frac{\rho_c}{\rho_b} + \frac{k_1}{k_4}\frac{\rho_c}{\rho_a} + \frac{k_1}{k_6}\frac{\rho_c}{\rho_b}},$$

or equivalently,

$$R_{inc} = \frac{\Gamma_s}{\left(\frac{1}{k_1}+\frac{1}{k_3}+\frac{1}{k_5}\right)\frac{1}{\rho_c}+\left(\frac{1}{k_2}+\frac{1}{k_6}\right)\frac{1}{\rho_b}+\frac{1}{k_4}\frac{1}{\rho_a}}. \tag{4.12}$$

We note here that R_{inc} is proportional to the inverse of the "harmonic mean" of the reaction-rate constants corrected by the adatom terrace densities. Suppose now that one of the reaction-rate constants is much smaller than the others, say, $k_1 \ll k_2, \ldots, k_6$, i.e., the first reaction in the incorporation sequence (4.9) is much slower than the others. Consequently, the following approximation holds:

$$R_{inc} \cong k_1 \Gamma_s \rho_c,$$

i.e., the first reaction of the incorporation sequence (4.9) is the "rate-limiting reaction," and R_{inc} has a simple linear dependence on the terrace density of C-adatoms at the upper step. If, however, the reaction-rate constants are of comparable magnitudes, then one is forced to recourse to the nonlinear form of R_{inc} given by (4.12).

It can be seen from the above calculation that for any compound, the rate of incorporation can be explicitly determined following a procedure which generalizes the one described above, assuming that the exact sequence of incorporation reactions at the upper step is known and under the approximation of steady-state step formation.

4.3 The Step-Flow Model

4.3.1 The steady one-dimensional flow of steps

We now specialize to the one-dimensional case, where all the steps point in the same direction (this is the so-called 1+1 dimension with one dimension being the lateral one and the other being the height– cf. Figure 4.2). It follows that (4.6)

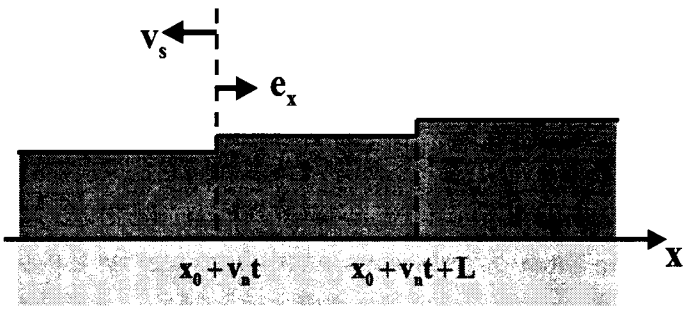

Figure 4.2: Schematic of the one-dimensional train of equidistant steps, where all the steps are pointing in the same direction.

reduces to the one-dimensional reaction-diffusion equation:

$$\frac{\partial \rho_k}{\partial t} = D_k \frac{\partial^2 \rho_k}{\partial x^2} + R_k, \tag{4.13}$$

and the boundary conditions (4.7) and (4.8) reduce to:

$$D_k \left(\frac{\partial \rho_k}{\partial x} \right)^- = \rho_k^- v_s^- \qquad \text{at the lower step, and} \tag{4.14}$$

$$D_k \left(\frac{\partial \rho_k}{\partial x} \right)^+ = -\rho_k^+ v_s^+ - w_k R_{inc} \qquad \text{at the upper step,} \tag{4.15}$$

where $v_s^{\pm} \stackrel{def}{=} \mathbf{v}_s^{\pm} \cdot (-\mathbf{e}_x)$ is positive, and $\mathbf{e}_x$ is the unit vector along the x-axis.

We now introduce the following dimensionless variables:

$$\begin{aligned} \bar{x} &= \frac{x}{\mathcal{L}}, \\ \bar{v}_s &= \frac{v_s}{v_n}, \\ \bar{t} &= \frac{v_n t}{\mathcal{L}}, \\ \bar{\rho}_k &= \frac{\rho_k}{\rho_{k,r}}, \\ \bar{R}_k &= \frac{R_k}{\lambda_{k,r} \rho_{k,r}}, \qquad \text{and} \\ \bar{R}_{inc} &= \frac{R_{inc}}{R_{inc}^r}, \end{aligned}$$

where the subscript and superscript r denote a reference quantity. Here, $\mathcal{L}$ is a

characteristic terrace width, v_n a characteristic step velocity, $\lambda_{k,r}$ a characteristic reaction-rate constant associated with the adsorption of the k^{th} species along the terrace, $\rho_{k,r} \stackrel{def}{=} w_k \Gamma_r$, with Γ_r a characteristic molar density of adsorption sites along an individual terrace, and $R^r_{inc} \stackrel{def}{=} \frac{\rho^r_f}{w_f} v_n$, with ρ^r_f the characteristic bulk density and w_f the molar weight of the compound. All of the above characteristic quantities are either evaluated or measured at some characteristic temperature of growth θ_r, and v_n can be deduced from growth-rate measurements.

It follows that the dimensionless diffusion equation can be written as:

$$\mathcal{P}_k \frac{\partial \bar{\rho}_k}{\partial \bar{t}} = \frac{\partial^2 \bar{\rho}_k}{\partial \bar{x}^2} + \mathcal{D}_k \bar{R}_k, \tag{4.16}$$

where the terrace Péclet number associated with the k^{th} species

$$\mathcal{P}_k \stackrel{def}{=} \frac{v_n \mathcal{L}}{D^r_k},$$

with $D^r_k = D_k(\theta_r)$, is the ratio of the typical time for the diffusion of k-particles along the terrace to the characteristic time associated with the motion of the step, and the terrace Damköhler number associated with the k^{th} species

$$\mathcal{D}_k \stackrel{def}{=} \frac{\lambda_{k,r} [X_k S_k]^r_g \mathcal{L}^2}{D^r_k},$$

where $[X_k S_k]^r_g$ is the gas-phase molar concentration of the precursor carrying the k^{th} species at the reference temperature, measures the typical time for adatoms to diffuse along the terrace vs. the characteristic time needed for them to adsorb.

Also, the dimensionless boundary conditions at the lower and upper steps can be expressed as follows:

$$\left(\frac{\partial \bar{\rho}_k}{\partial \bar{x}} \right)^- = -\mathcal{P}_k \bar{\rho}^-_k \bar{v}^-_s, \qquad \text{and} \tag{4.17}$$

$$\left(\frac{\partial \bar{\rho}_k}{\partial \bar{x}} \right)^+ = -\mathcal{P}_k \bar{\rho}^+_k \bar{v}^+_s + \mathcal{P}_k \frac{\rho^r_f}{\rho_{k,r}} \bar{R}_{inc}. \tag{4.18}$$

When the motion of the steps is much slower than the diffusion of adatoms along the terraces, the Péclet numbers associated with the various species become vanishingly small and the transient term in the LHS of (4.16) as well as the the 'convective' terms in the boundary conditions at the lower and upper steps (i.e., the first terms on the RHS of (4.17) and (4.18) respectively) can be neglected. Notice that the ratio $\rho_f^r/\rho_{k,r}$ is sufficiently large for the last term on the RHS of (4.18) not to be negligible.

In what follows, we restrict ourselves to the case of a train of equidistant steps. As mentioned above, this is consistent with the steady-state approximation assuming that the initial state is such that all the terraces are of equal width $\mathcal{L}$. At any instant in time t, an arbitrary terrace then consists of the domain $[x_0 + v_n t, x_0 + v_n t + \mathcal{L}]$ along the x-axis, where x_0 is arbitrary (x_0 is the initial position of the lower step of the arbitrary terrace of interest– cf. Figure 4.2) and v_n is the step velocity (which is now identical for all steps as the train of steps is steady). After the change of variables $x \longrightarrow x - x_0 - v_n t$, the approximate governing equations reduce to steady diffusion-reaction equations: $\forall\ k = 1, \ldots, N$,

$$D_k \frac{\partial^2 \rho_k}{\partial x^2} + R_k = 0, \qquad \forall\ x \in [0, \mathcal{L}] \tag{4.19}$$

complemented by the following boundary conditions:

$$\frac{\partial \rho_k}{\partial x}(x = 0) = 0, \qquad \text{and} \tag{4.20}$$

$$D_k \frac{\partial \rho_k}{\partial x}(x = \mathcal{L}) = -w_k R_{inc}. \tag{4.21}$$

4.3.2 The overall growth rate

We are interested in determining the net deposition fluxes of the various species from the gas phase into the terraces as they are an indication of the growth rate of the solid thin film. For the individual terrace under consideration ($x \in [0, \mathcal{L}]$), the average flux of the k^{th} species (i.e., the total flux of k-mass to the terrace divided by

the terrace width) is given by the following integral:

$$\langle R_k \rangle \;=\; \frac{1}{\mathcal{L}} \int_{x=0}^{x=\mathcal{L}} R_k(x)\; dx, \tag{4.22}$$

and making use of (4.19) and (4.20), we obtain the following relation

$$\langle R_k \rangle \;=\; -\frac{D_k}{\mathcal{L}} \frac{\partial \rho_k}{\partial x}(x = \mathcal{L}),$$

which, in turn, and with the help of (4.21), reduces to

$$\langle R_k \rangle \;=\; \frac{w_k}{\mathcal{L}} R_{inc}(\{\rho_k(x = \mathcal{L})\}_{k=1}^{N}). \tag{4.23}$$

Consequently, our task consists of solving the set of equations (4.19) combined with the boundary conditions (4.20) and (4.21) listed above in order to determine the values of the species densities at the upper step $\rho_k(x = \mathcal{L})$ for all $k = 1, \ldots, N$. The species net deposition fluxes then follow from (4.23).

Consider a film with a large number of steps growing according to the mechanism described earlier (i.e., a steady step-flow growth such that the terraces are of equal width). Let h describe the average thickness of the film. By average we mean that we model the film at a sufficiently large lengthscale that the details of an individual terrace or step are not visible. Thus, at any point along the interface separating the film from the vapor, $\nabla h = a/\mathcal{L}$ where a is the step height and $\mathcal{L}$ the terrace width.

The model described in the previous sections gives us the net deposition flux (4.23), and the growth of the film is then described by the equation:

$$\rho_f \frac{\partial h}{\partial t} = w_f \mathbf{G}(\mathcal{L}, \{\rho_k^g\}_{k=1}^{N}),$$

where N is the total number of species present along the surface, ρ_f the bulk (nominal) mass density, and the partial time-derivative of the average height h is nothing but the vertical component of the growth velocity. $\mathbf{G}$ is a measure of the growth rate of

the thin solid film and is defined as follows:

$$\mathbf{G} \stackrel{def}{=} \frac{1}{\mathcal{L}} R_{inc}(\{\rho_k(x=\mathcal{L})\}_{k=1}^{N}).$$

It should be noted here that we are interested in the functional dependence of the growth rate on the surface morphology (via its dependence on the terrace width $\mathcal{L}$) and the molar concentrations of the precursors in the vapor $\{[X_k S_k]\}_{k=1}^{N}$.

In what follows, we shall specialize the formalism laid out above to systems characterized by the presence of two chemical species A and B (more specifically, the precursors $X_A A$ and $X_B B$, the ligands X_A and X_B, and the desorbed molecules A and B in the gas phase; the adatoms A and B along the terraced surface; and the compound AB in the bulk of the solid thin film). As mentioned above, we will examine the two mechanisms by which species deposition takes place: in section 4.4, we deal with the noncompetitive mechanism, and in section 4.5, we consider the case in which the adsorption of adatoms is accompanied by a competition for open sites.

4.4 The Two-species Noncompetitive Case

Consider the i^{th} species. In the absence of competition for open adsorption sites, the equation governing the distribution of i-adatoms along an individual terrace is given by: $\forall\ S_i = A, B$,

$$D_i \frac{d^2\rho_i}{dx^2}(x) + k_{ads}^i \rho_{X_i S_i}^g - k_{des}^i \rho_i(x) = 0, \qquad \forall\ x \in [0, \mathcal{L}], \tag{4.24}$$

where $\rho_{X_i S_i}^g$ denotes the mass density of the precursor $X_i S_i$ in the gas phase, with X_i the organic molecule shielding the particle S_i to be deposited at the surface of the thin film.

We rewrite (4.24) as follows:

$$\frac{d^2\rho_i}{dx^2}(x) - \pi_i^2 \rho_i(x) = -\frac{k_{ads}^i}{D_i} \rho_{X_i S_i}^g, \tag{4.25}$$

where

$$\pi_i \stackrel{def}{=} \left(\frac{k^i_{des}}{D_i}\right)^{1/2}.$$

Making use of the infinite-Schwoebel-barrier boundary condition at the lower step

$$\frac{d\rho_i}{dx}(x=0) \;=\; 0, \qquad \forall\; S_i = A, B,$$

we can write the solution to (4.25) in the following form

$$\rho_i(x) = c_i \cosh(\pi_i x) + \frac{k^i_{ads}}{k^i_{des}}\rho^g_{X_i S_i}, \qquad \forall\; x \in [0, \mathcal{L}], \tag{4.26}$$

where the constant of integration c_i is yet to be determined.

At the upper step, the boundary conditions can be expressed as follows:

$$-D_A\frac{d\rho_A}{dx}(x=\mathcal{L}) \;=\; \frac{k_{inc}}{w_B}\rho_A(x=\mathcal{L})\rho_B(x=\mathcal{L}), \text{ and} \tag{4.27}$$

$$-D_B\frac{d\rho_B}{dx}(x=\mathcal{L}) \;=\; \frac{k_{inc}}{w_A}\rho_A(x=\mathcal{L})\rho_B(x=\mathcal{L}). \tag{4.28}$$

Combining (4.27) and (4.28), we obtain

$$\frac{d\rho_B}{dx}(x=\mathcal{L}) \;=\; \frac{D_A}{D_B}\frac{w_B}{w_A}\frac{d\rho_A}{dx}(x=\mathcal{L}). \tag{4.29}$$

This proportionality of the diffusive mass fluxes of adatoms A and B at the upper steps is dictated by the fact that only the formation of the stochiometric compound is allowed.

Taking the derivative of (4.26) w.r.t. x and substituting into (4.29), we obtain the following relation between c_A and c_B:

$$c_B \;=\; \alpha c_A,$$

where

$$\alpha \stackrel{def}{=} \frac{D_A}{D_B}\frac{w_B}{w_A}\frac{\pi_A}{\pi_B}\frac{\sinh(\pi_A\mathcal{L})}{\sinh(\pi_B\mathcal{L})}. \tag{4.30}$$

Consequently, in order to explicitly determine the density profiles of both species along the terrace, we only have to solve (4.27) for the unknown c_A. For simplicity, we change notation: c_A will be replaced in what follows by c. After some straightforward algebra, we can rewrite (4.27) in the form of a quadratic in c:

$$\mathcal{A}c^2 + \mathcal{B}c + \mathcal{D} = 0, \tag{4.31}$$

where:

$$\begin{aligned}
\mathcal{A} &= \frac{k_{inc}}{w_B}\alpha\cosh(\pi_A\mathcal{L})\cosh(\pi_B\mathcal{L}),\\
\mathcal{B} &= \frac{k_{inc}}{w_B}\left(\frac{k^B_{ads}}{k^B_{des}}\rho^g_{X_BB}\cosh(\pi_B\mathcal{L}) + \alpha\frac{k^A_{ads}}{k^A_{des}}\rho_{X_AA}\cosh(\pi_A\mathcal{L})\right) + D_A\pi_A\sinh(\pi_A\mathcal{L}),\\
\mathcal{D} &= \frac{k_{inc}}{w_B}\frac{k^A_{ads}}{k^B_{ads}}\frac{k^B_{des}}{k^A_{des}}\rho^g_{X_AA}\rho^g_{X_BB}.
\end{aligned}$$

Its discriminant $\Delta = \mathcal{B}^2 - 4\mathcal{A}\mathcal{D}$ is always positive:

$$\begin{aligned}
\Delta = \frac{k_{inc}}{w_B}^2&\left(\frac{k^B_{ads}}{k^B_{des}}\rho^g_{X_BB}\cosh(\pi_B\mathcal{L}) - \alpha\frac{k^A_{ads}}{k^A_{des}}\rho^g_{X_AA}\cosh(\pi_A\mathcal{L})\right)^2 + D_A^2\pi_A^2\sinh^2(\pi_A\mathcal{L})\\
&+2\frac{k_{inc}}{w_B}D_A\pi_A\sinh(\pi_A\mathcal{L})\left(\frac{k^B_{ads}}{k^B_{des}}\rho^g_{X_BB}\cosh(\pi_B\mathcal{L}) + \alpha\frac{k^A_{ads}}{k^A_{des}}\rho^g_{X_AA}\cosh(\pi_A\mathcal{L})\right) > 0
\end{aligned}$$

thus insuring the existence of two real roots of (4.31):

$$c_{1,2} = \frac{-\mathcal{B} \pm \sqrt{\Delta}}{2\mathcal{A}}.$$

It can easily be shown that these two real roots are (strictly) negative. Moreover, one can easily show that: $\forall\ x \in [0, \mathcal{L}]$,

$$\rho_A(x = \mathcal{L}) \leq \rho_A(x) \leq \rho_A(x = 0),$$

where

$$\rho_A(x=0) = c_{1,2} + \frac{k^A_{ads}}{k^A_{des}}\rho^g_{X_AA}$$

and

$$c_1 \;<\; c_2.$$

The integration constants c_1 and c_2 are to be viewed here as functions of the three parameters $\mathcal{L}$, $\rho^g_{X_AA}$ and $\rho^g_{X_BB}$. Given all the material parameters that characterize the physical system of interest (i.e., the adsorption, desorption and incorporation reaction-rate constants as well as the terrace diffusivities of the species, etc.), there exists a region in the three-parameter space for which the following two inequalities hold:

$$\begin{aligned} c_1(\mathcal{L}, \rho^g_{X_AA}, \rho^g_{X_BB}) + \frac{k^A_{ads}}{k^A_{des}}\rho^g_{X_AA} &\leq 0, \qquad \text{and} \\ c_2(\mathcal{L}, \rho^g_{X_AA}, \rho^g_{X_BB})\cosh(\pi_A\mathcal{L}) + \frac{k^A_{ads}}{k^A_{des}}\rho^g_{X_AA} &> 0, \end{aligned}$$

that is, there exists an operating regime for which there is only one *positive* density profile of A-adatoms that satisfies the diffusion equation along the terrace as well as the boundary conditions along the lower and upper steps (corresponding to c_2), the other solution of the quadratic (corresponding to c_1) generating negative mass densities along the terrace. In what follows, we shall assume that we are operating within the regime described above.

We can now compute the net deposition fluxes for the two species:

$$\begin{aligned} \langle R_A \rangle &= \frac{k_{inc}}{w_B}\frac{\rho_A(x=\mathcal{L})\rho_B(x=\mathcal{L})}{\mathcal{L}}, \qquad \text{and} \\ \langle R_B \rangle &= \frac{k_{inc}}{w_A}\frac{\rho_A(x=\mathcal{L})\rho_B(x=\mathcal{L})}{\mathcal{L}} \end{aligned}$$

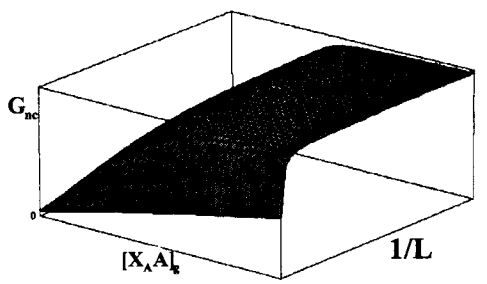

Figure 4.2: The net deposition flux (in the absence of competition for open adsorption sites) $\mathbf{G}_{nc}$ as a function of the inverse of the terrace width $1/\mathcal{L}$ and the concentration of the gas-phase precursor $[X_A A]_g$ for fixed concentration of $[X_B B]_g$.

or, equivalently, we determine the following measure of growth:

$$\begin{aligned}\mathbf{G} =& k_{inc}\frac{\rho_A(x=\mathcal{L})\rho_B(x=\mathcal{L})}{\mathcal{L}} \\ =& \frac{k_{inc}}{\mathcal{L}}\left[c_2(\mathcal{L},\rho^g_{X_AA},\rho^g_{X_BB})\cosh(\pi_A\mathcal{L})+\beta_A\right]\left[\alpha(\mathcal{L})c_2(\mathcal{L},\rho^g_{X_AA},\rho^g_{X_BB})\cosh(\pi_B\mathcal{L})+\beta_B\right],\end{aligned}$$

where

$$\begin{aligned}\beta_A &\stackrel{def}{=} \frac{k^A_{ads}}{k^A_{des}}\rho^g_{X_AA}, \\ \beta_B &\stackrel{def}{=} \frac{k^B_{ads}}{k^B_{des}}\rho^g_{X_BB},\end{aligned}$$

and $\alpha(\mathcal{L})$ is given by (4.30).

The results are shown in Figures 4.2 and 4.3. The former is a plot of the growth rate $\mathbf{G}$ as a function of the slope of the terraced surface (i.e., as a function of the inverse of the terrace width $\mathcal{L}$) and the gas-phase concentration of the precursor X_AA, for a fixed value of the concentration of the other precursor X_BB and a particular choice of material parameters. The latter is a plot of the growth rate $\mathbf{G}$ as a function of the two gas-phase precursor concentrations corrected for the adsorption kinetics $k^A_{ads}[X_AA]_g$ and $k^B_{ads}[x_BB]_g$, for a given fixed value of the terrace width $\mathcal{L}$ and the same choice of material parameters, where $[X_iS_i]_g = \rho^g_{X_iS_i}/w_i$, $\forall\ S_i = A, B$.

Consider Figure 4.2. For a fixed value of $[X_AA]_g$, the growth rate is an increasing function of the slope. That is, as the slope becomes infinite, i.e., as the terrace width becomes infinitely small, the growth rate reaches a maximal value. This is to be

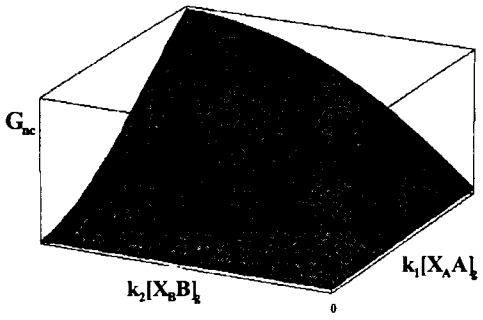

Figure 4.3: The net deposition flux (in the absence of competition for open adsorption sites) $\mathbf{G}_{nc}$ as a function of the concentrations of the gas-phase precursors $[x_A A]_g$ and $[X_B B]_g$ for fixed terrace width $\mathcal{L}$.

expected as, when the terrace width tends to zero, the step density becomes infinite, and since incorporation is confined to the steps (more specifically the upper steps), one would anticipate that the growth rate reaches its maximum. On the other hand, as the terrace width becomes infinitely large, i.e., as the slope tends to zero, the growth rate reaches its minimal value. This is consistent with the fact that, as the density of steps goes to zero, and the growth occurring only at the steps, the growth rate becomes minimal.

From Figure 4.3 we can see that the growth rate is an increasing function of the concentrations of the gas phase precursors. Indeed, there is no blocking effect as the depositing particles are not competing for open adsorption sites along the terraces. Consequently, as the quantities of precursors are increased in the vapor phase, the deposition rates are increased (since they depend exclusively on the precursor concentrations) and the increase in the growth rate of the film follows.

The numerical simulations were performed using specific values of the various material constants w_i, D_i, k^i_{ads}, k^i_{des} and k_{inc}. But the qualitative behavior of the average deposition flux (or growth rate) is independent of this particular choice of parameters. In fact, numerical studies suggest that the following constitutive relation accounts (at least qualitatively) for the main features of the growth rate functional dependence on the surface morphology (via its dependence on the terrace width) and

the molar concentrations of the two gas-phase precursors:

$$\mathbf{G}_{nc}(\mathcal{L}, [X_A A]_g, [X_B B]_g) \;=\; \frac{c_1}{c_2 + \mathcal{L}}([X_A A]_g)^{\alpha_1}([X_B B]_g)^{\alpha_2} \tag{4.32}$$

where α_1 and α_2 are positive numbers. Here, c_1, c_2, α_1 and α_2 replace w_i, D_i, k^i_{ads}, k^i_{des} and k_{inc} as the relevant macroscopic material parameters.

4.5 The Two-species Problem With Competition

Along an individual terrace ($x \in [0, \mathcal{L}]$), the equations governing the mass density distributions of adatoms of species A and B are given by (respectively):

$$D_A \frac{d^2\rho_A}{dx^2}(x) + w_A \left\{ k^A_{ads}[X_A A]_g \left(\Gamma - \frac{\rho_A(x)}{w_A} - \frac{\rho_B(x)}{w_B} \right) - \frac{k^A_{des}}{w_A}\rho_A(x) \right\} = 0, \text{ and} \tag{4.33}$$

$$D_B \frac{d^2\rho_B}{dx^2}(x) + w_B \left\{ k^B_{ads}[X_B B]_g \left(\Gamma - \frac{\rho_A(x)}{w_A} - \frac{\rho_B(x)}{w_B} \right) - \frac{k^B_{des}}{w_B}\rho_B(x) \right\} = 0. \tag{4.34}$$

Notice that the above two equations are coupled because of the dependence of the adsorption reaction rates for both species A and B (the second term on the LHS of (4.33) and (4.34) respectively) on the A-adatom density ρ_A as well as the B-adatom density ρ_B along the terrace.

In addition, we impose the infinite-Schwoebel-barrier boundary condition at the lower step:

$$\frac{d\rho_A}{dx}(x = 0) \;=\; \frac{d\rho_B}{dx}(x = 0) \;=\; 0. \tag{4.35}$$

Finally, at the upper step, the boundary conditions reduce to the following:

$$w_B D_A \frac{d\rho_A}{dx}(x = \mathcal{L}) \;=\; w_A D_B \frac{d\rho_B}{dx}(x = \mathcal{L}) \;=\; -k_{inc}\rho_A(x = \mathcal{L})\rho_B(x = \mathcal{L}). \tag{4.36}$$

We begin by rewriting (4.33) as follows:

$$\frac{d^2\rho_A}{dx^2}(x) - \alpha_A^2\rho_A(x) = -\beta_A + \gamma_A\rho_B(x), \tag{4.37}$$

where

$$\begin{aligned} \alpha_A &= \left(\frac{k_{ads}^A[X_AA]_g + k_{des}^A}{D_A}\right)^{1/2}, \\ \beta_A &= \frac{w_A k_{ads}^A[X_AA]_g}{D_A}\Gamma, \qquad \text{and} \\ \gamma_A &= \frac{w_A}{w_B}\frac{k_{ads}^A[X_AA]_g}{D_A}. \end{aligned}$$

Identically, (4.34) can be rewritten as:

$$\frac{d^2\rho_B}{dx^2}(x) - \alpha_B^2\rho_B(x) = -\beta_B + \gamma_B\rho_A(x), \tag{4.38}$$

with

$$\begin{aligned} \alpha_B &= \left(\frac{k_{ads}^B[X_BB]_g + k_{des}^B}{D_B}\right)^{1/2}, \\ \beta_B &= \frac{w_B k_{ads}^B[X_BB]_g}{D_B}\Gamma, \qquad \text{and} \\ \gamma_B &= \frac{w_B}{w_A}\frac{k_{ads}^B[X_BB]_g}{D_B}. \end{aligned}$$

Taking the second derivative of (4.33) with respect to x, we obtain the following relation:

$$\frac{d^2\rho_B}{dx^2}(x) = \frac{1}{\gamma_A}\left(\frac{d^4\rho_A}{dx^4}(x) - \alpha_A^2\frac{d^2\rho_A}{dx^2}(x)\right). \tag{4.39}$$

Now, substituting (4.39) into (4.34) yields the following fourth order linear ordinary differential equation in $\rho_A(x)$:

$$\frac{d^4\rho_A}{dx^4}(x) - \mathcal{A}\frac{d^2\rho_A}{dx^2}(x) + \mathcal{B}\rho_A(x) - \mathcal{C} = 0, \tag{4.40}$$

where

$$\mathcal{A} = \alpha_A^2 + \alpha_B^2 = \frac{k_{ads}^A[X_A A]_g + k_{des}^A}{D_A} + \frac{k_{ads}^B[X_B B]_g + k_{des}^B}{D_B}, \tag{4.41}$$

$$\mathcal{B} = \alpha_A^2\alpha_B^2 - \gamma_A\gamma_B = \frac{k_{ads}^A k_{des}^B[X_A A]_g + k_{ads}^B k_{des}^A[X_B B]_g + k_{des}^A k_{des}^B}{D_A D_B}, \text{ and} \tag{4.42}$$

$$\mathcal{C} = \alpha_B^2\beta_A - \gamma_A\beta_B = \frac{w_A k_{ads}^A k_{des}^B}{D_A D_B}\Gamma. \tag{4.43}$$

Consider the homogeneous equation associated with (4.40). The corresponding characteristic equation is the following fourth order algebraic equation:

$$r^4 - \mathcal{A}r^2 + \mathcal{B} = 0. \tag{4.44}$$

Let $s = r^2$. We can rewrite (4.44) as a quadratic in s:

$$s^2 - \mathcal{A}s + \mathcal{B} = 0. \tag{4.45}$$

It can easily be shown that the discriminant of (4.45) is (strictly) positive and that the two real roots thus generated are also (strictly) positive. Consequently, the general solution of (4.40) is of the following form: $\forall\ x \in [0, \mathcal{L}]$,

$$\rho_A(x) = c_1\exp(r_1 x) + c_2\exp(-r_1 x) + c_3\exp(r_2 x) + c_4\exp(-r_2 x) + \frac{\mathcal{C}}{\mathcal{B}}, \tag{4.46}$$

where

$$r_{1,2} \stackrel{def}{=} \left(\frac{\mathcal{A} \pm (\mathcal{A} - 4\mathcal{B})^{1/2}}{2}\right)^{1/2},$$

with $\mathcal{A}$, $\mathcal{B}$ and $\mathcal{C}$ given by (4.41)-(4.43), and $\{c_i\}_{i=1}^4$ are constants yet to be determined.

From (4.37) and (4.46), it follows that the mass density profile of B-adatoms along

the terrace is given by:

$$\rho_B(x) = \frac{1}{\gamma_A}(r_1^2 - \alpha_A^2)\left[c_1 \exp(r_1 x) + c_2 \exp(-r_1 x)\right] + \frac{1}{\gamma_A}\left\{(r_2^2 - \alpha_B^2)\left[c_3 \exp(r_2 x) + c_4 \exp(-r_2 x)\right] + \left(\beta_A - \alpha_A^2 \frac{\mathcal{C}}{\mathcal{B}}\right)\right\}. \quad (4.47)$$

Taking the derivative of (4.46) with respect to x and substituting into (4.35), we obtain the following equation:

$$r_1(c_1 - c_2) + r_2(c_3 - c_4) = 0. \quad (4.48)$$

Similarily, taking the derivative of (4.47) w.r.t. x and substituting in (4.36) yields the following equation:

$$r_1(r_1^2 - \alpha_A^2)(c_1 - c_2) + r_2(r_2^2 - \alpha_A^2)(c_3 - c_4) = 0. \quad (4.49)$$

Next, solving the set of two algebraic linear equations (4.48) and (4.49) for the two unknowns $c_1 - c_2$ and $c_3 - c_4$, and noting that the determinant of the associated matrix never vanishes, we obtain the following two relations:

$$c_1 = c_2, \quad \text{and} \quad c_3 = c_4. \quad (4.50)$$

It follows that the terrace densities of adatoms can be rewritten as:

$$\rho_A(x) = d_1 \cosh(r_1 x) + d_2 \cosh(r_2 x) + \frac{\mathcal{C}}{\mathcal{B}}, \quad \text{and} \quad (4.51)$$

$$\rho_B(x) = \frac{1}{\gamma_A}\left\{d_1(r_1^2 - \alpha_A^2)\cosh(r_1 x) + d_2(r_2^2 - \alpha_A^2)\cosh(r_2 x) + \left(\beta_A - \alpha_A^2 \frac{\mathcal{C}}{\mathcal{B}}\right)\right\}, \quad (4.52)$$

where $d_1 = 2c_1$ and $d_2 = 2c_3$ are yet to be determined.

From (4.36) we have the following proportionality relation between the adatom

mass fluxes at the upper step:

$$\frac{d\rho_B}{dx}(x=\mathcal{L}) \;=\; \frac{w_B}{w_A}\frac{D_A}{D_B}\frac{d\rho_A}{dx}(x=\mathcal{L}). \tag{4.53}$$

Taking the derivatives of (4.51) and (4.52) w.r.t. x and then substituting into (4.53), we obtain the following relation:

$$d_2 = \alpha d_1, \tag{4.54}$$

where

$$\alpha \stackrel{def}{=} -\frac{r_1}{r_2}\frac{D_B(r_1^2-\alpha_A^2)-k_{ads}^A[X_AA]_g}{D_B(r_2^2-\alpha_A^2)-k_{ads}^A[X_AA]_g}\frac{\sinh(r_1\mathcal{L})}{\sinh(r_2\mathcal{L})}.$$

We are thus left with only one constant to determine, i.e., d_1. Once d_1 is known, the mass density profiles of A- and B-adatoms along the terrace can be explicitly expressed, and consequently, the net deposition fluxes will be determined thus yielding the functional dependence of the growth rate of the thin solid film on the terrace width as well as the concentrations of the gas-phase precursors. For simplicity, we replace the notation d_1 by d. Substituting (4.54) into the boundary condition at the upper step

$$\frac{d\rho_A}{dx}(x=\mathcal{L}) \;=\; -\frac{k_{inc}}{w_BD_A}\rho_A(x=\mathcal{L})\rho_B(x=\mathcal{L}), \tag{4.55}$$

and after some tedious but straightforward algebra, we can express the above condition as a quadratic equation in d:

$$\mathcal{D}d^2+\mathcal{E}d+\mathcal{F}=0, \tag{4.56}$$

where

$$\begin{aligned}
\mathcal{D} &= w_A k^A_{ads}[X_A A]_g \mathcal{M}\mathcal{N}, \\
\mathcal{E} &= w_A k^A_{ads}[X_A A]_g \left\{ \left(\beta_A - \alpha_A^2 \frac{\mathcal{C}}{\mathcal{B}} \right) \mathcal{M} + \frac{\mathcal{C}}{\mathcal{B}} \mathcal{N} \right\}, \qquad \text{and} \\
\mathcal{F} &= w_A k^A_{ads}[X_A A]_g \left(\beta_A - \alpha_A^2 \frac{\mathcal{C}}{\mathcal{B}} \right) \frac{\mathcal{C}}{\mathcal{B}},
\end{aligned}$$

with

$$\begin{aligned}
\mathcal{M} &= \cosh(r_1 \mathcal{L}) + \alpha \cosh(r_2 \mathcal{L}), \qquad \text{and} \\
\mathcal{N} &= (r_1^2 - \alpha_A^2) \cosh(r_1 \mathcal{L}) + \alpha (r_2^2 - \alpha_A^2) \cosh(r_2 \mathcal{L}).
\end{aligned}$$

The coefficients $\mathcal{D}$, $\mathcal{E}$ and $\mathcal{F}$ of the quadratic above are functions of the terrace width $\mathcal{L}$ as well as the molar consentrations of the gas-phase precursors $[X_A A]_g$ and $[X_B B]_g$. In what follows, we shall assume that there exists a region of the parameter space within which (i) the 3 coefficients listed above, (ii) the discriminant of (4.56), and (iii) α are all strictly positive. From (ii) it follows that, within the region of interest, we have two real and distinct roots of (4.56), denoted below by $\mathbf{d}_1$ and $\mathbf{d}_2$. It is a trivial matter to show that, when (i) and (ii) are simultaneously satisfied, the two roots are both negative. We then end up with two distinct density profiles of A-adatoms along the terrace:

$$\rho_A^{1,2}(x) = \mathbf{d}_{1,2}(\cosh(r_1 x) + \alpha \cosh(r_2 x)) + \frac{\mathcal{C}}{\mathcal{B}}, \tag{4.57}$$

where

$$\begin{aligned}
\mathcal{B} &= \mathcal{B}([X_A A]_g, [X_B B]_g), \\
r_{1,2} &= r_{1,2}([X_A A]_g, [X_B B]_g), \\
\alpha &= \alpha(\mathcal{L}, [X_A A]_g, [X_B B]_g), \qquad \text{and} \\
\mathbf{d}_{1,2} &= \mathbf{d}_{1,2}(\mathcal{L}, [X_A A]_g, [X_B B]_g).
\end{aligned}$$

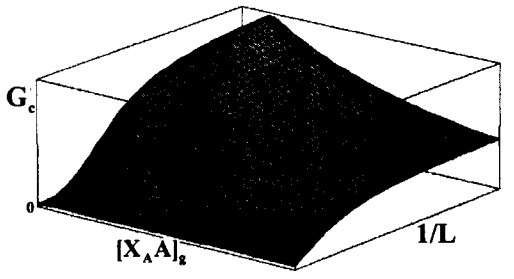

Figure 4.4: The net deposition flux (in the presence of competition for open adsorption sites) $\mathbf{G}_c$ as a function of the inverse of the terrace width $1/\mathcal{L}$ and the concentration of the gas-phase precursor $[X_A A]_g$ for fixed concentration of $[X_B B]_g$.

It can easily be shown that: $\forall\ x \in [0, \mathcal{L}]$,

$$\rho_A(x = \mathcal{L}) \leq \rho_A(x) \leq \rho_A(x = 0).$$

In addition, we will assume that there exists a subregion of the region defined above within which the following two inequalities hold:

$$\begin{aligned} \mathbf{d}_1(1+\alpha) + \frac{\mathcal{C}}{\mathcal{B}} &\leq 0, \\ \mathbf{d}_2(\cosh(r_1\mathcal{L}) + \alpha\cosh(r_2\mathcal{L})) + \frac{\mathcal{C}}{\mathcal{B}} &> 0, \end{aligned}$$

that is, only one of the two roots of (4.56) generates a *positive* density profile of A-adatoms along the terrace.

We are now in a position to compute the growth rate as a function of the terrace width and the gas-phase precursor concentrations:

$$\mathbf{G} = k_{inc}\frac{\rho_A(x = \mathcal{L})\rho_B(x = \mathcal{L})}{\mathcal{L}}.$$

The results are shown in Figure 4.4 and 4.5 for a particular choice of material parameters. As in the case of adsorption without competition, we can conclude from Figure 4.4 that for fixed precursor concentrations, the average flux increases with decreasing step width (increasing step density). This behavior is to be expected as, for both mechanisms, the formation of the compound is restricted to the steps (more precisely the upper ones). The more interesting behavior is illustrated in Figure 4.5 which shows the average deposition flux as a function of the two precursor

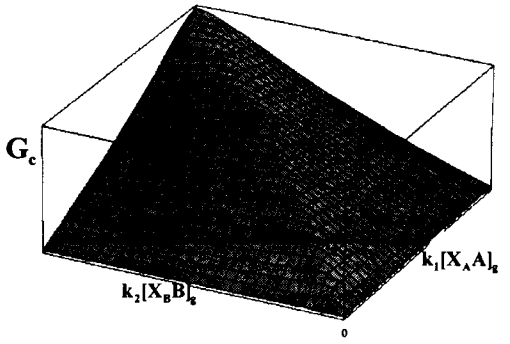

Figure 4.5: The net deposition flux (in the presence of competition for open adsorption sites) $\mathbf{G}_c$ as a function of the concentrations of the gas-phase precursors $[x_A A]_g$ and $[X_B B]_g$ for fixed terrace width $\mathcal{L}$.

concentrations. Notice that the flux has a peak along the line $k_1[X_A A]_g = k_2[X_B B]_g$ which corresponds to the stochiometric ratio corrected for the kinetics. Any excess of either precursor is adsorbed to the terrace thus blocking the open sites for adsorption and diffusion of the other species. This decreases the concentration of the other species at the step thereby inhibiting the formation of the compound and reducing the total deposition flux. This shows the need for controlling the gas phase composition to a narrow range if experimental results suggest that the growth mechanism is one for which the depositing species compete for open adsorption sites. An excess of one precursor can in fact slow the overall growth process. Worse, the excess of the abundant species on the terrace can also lead to the formation of precipitates of different stoichiometry (a scenario beyond the scope of the present chapter).

Though Figures 4.4 and 4.5 were obtained using specific values of material constants k^i_{ads}, D_i, w_i and k_{inc}, the qualitative behavior of the average flux is independent of this particular choice. In fact, extensive numerical studies suggest the following constitutive relation which we believe accounts for the main features of the dependence of the net deposition flux on the surface morphology and the gas-phase concentrations:

$$\mathbf{G}_c(\mathcal{L}, [X_A A]_g, [X_B B]_g) = \frac{c_1}{c_2 + \mathcal{L}} \exp(-c_3 \, |[X_A A]_g - c_4 [X_B B]_g|)(1 - \exp(-[X_A A]_g))(1 - \exp(-[X_B B]_g)),$$

where c_1, c_2, c_3, c_4 replace k^i_{ads}, D_i, w_i and k_{inc} as macroscopic material parameters (to be determined empirically).

Chapter 5 Conclusion

The objective of this work was to adress several issues concerning the modeling of the chemical vapor deposition of multispecies thin solid films. The chosen approach was to consider a general setting characterized by the presence of N chemical species, where $N \geq 2$. The goals were (i) to develop a unified framework within which to couple the gas flow to the growing solid film via an understanding of the fundamental physics governing the morphologial evolution of the gas-film interface, (ii) to investigate the behavior of the multicomponent gas flow for a particular reactor geometry and growth regime, and (iii) to have a better understanding of the complex interaction between the surface microstructure and the heterogeneous chemical kinetics.

In chapter 2, a macroscopic thermomechanical model describing the growth of a thin solid film by chemical vapor deposition was developed. The physical system considered consists of three separate phases (the gas flow, the bulk of the thin solid film and the surface phase separating them), each containing multiple chemical species. In each phase, the transport of species occurs by both convection and diffusion. In addition, homogeneous (gas-phase) and heterogeneous (surface) chemical kinetics were included. The gas flow is assumed to behave like a Newtonian multicomponent fluid, the bulk of the film like an elastic compound or substitutional alloy, and the surface like an anisotropic elastic two-dimensional smoothly evolving manifold. The equations governing the behavior of each phase were derived and thermodynamically consistent constitutive assumptions were proposed (sections 2.4 and 2.5). Of particular interest was the coupling of the gas flow to the bulk of the film via the equations describing the morphological evolution of the surface (subsection 2.5.4). Moreover, the driving force at the surface was identified (cf. equation (2.100)), and a kinetic relation linking it to the growth velocity was proposed (cf. equation (2.155)). A specialization to the case of a multispecies ideal gas separated from a linearly elastic film by an anisotropic interface was discussed (section 2.6), and a further specialization to the case of local

equilibrium along an isotropic surface was examined (section 2.7).

In chapter 3, we have focused on the multispecies gas flow in the setting of a vertical axisymmetric stagnation-point flow CVD reactor characterized by a small aspect ratio and operating under conditions ensuring a small Mach number. The Soret effects (i.e., the dependence of the species diffusion on the temperature gradient) as well as the gas-phase and surface chemical kinetics were accounted for. A two-parameter asymptotic analysis was performed, and the leading-order governing equations (cf. equations (3.81)–(3.88) and (3.118)) and corresponding boundary conditions at the showerhead and the gas-film interface (cf. equations (3.89)–(3.95), (3.120) and (3.124)) were derived in the limit of vanishingly small aspect ratio and Mach number. The total mass density, the velocity, the temperature, and the species density profiles were determined analytically under the additional assumptions of steady-state and diffusion-controlled growth regime. It was found that this solution is of the similarity type, thus ensuring the uniformity of the thickness and chemical composition of the thin solid film.

In chapter 4, a mesoscopic model was proposed that accounts for the microstructure of the gas-film interface. This model describes the terrace-and-ledge growth of a compound thin film, during which gas-phase particles adsorb at the terraces along which they then diffuse, and the formation of the compound occurs along the steps. A simple one-dimensional step-flow model was developed whose goal was to determine the average growth rate of the film as a function of the surface morphology (via its dependence on the terrace width) as well as the chemical composition of the gas phase (via its dependence on the molar concentrations of the gas-phase precursors). Finally, the complex interaction between the microstructure of the surface and the heterogeneous chemical kinetics was illustrated by examining the growth of a binary compound.

Future investigations can proceed in the following two directions. First, the asymptotic analysis in chapter 3 holds in the limit of infinitely small aspect ratio, i.e., when the radius of the substrate is infinite. This is an idealization of the actual finite-geometry reactor, but it can serve as a tool to check the validity of com-

plex numerical simulations using Chemkin or other available computational packages . One could consider the governing equations and associated boundary conditions that result from taking into account higher order terms in the two-parameter expansions of the flow fields. These equations would need to be solved numerically, and their solutions would exhibit a radial dependence, thus providing some insight into the edge effects associated with the finite-radius susceptor as well as allowing us to prescribe radially-dependent boundary conditions. Another way of approaching the finite-geometry problem is by expanding the flow fields in terms of Tchebysheff polynomials. The advantadge of using Tchebysheff polynomials resides mainly in the fact that the expansions can often be truncated at low 'degrees' (i.e., only the first few polynomials are needed) while maintaining a high level of 'accuracy' (i.e., polynomial approximations with the smallest maximal deviations from the exact flow fields), which would allow us to capture the main features of the flow behavior due to radial nonuniformities. Second, the step-flow model proposed in chapter 4 was based on the steady-state approximation. Consequently, an initially equidistant train of steps would remain equidistant at all times during the growth process. Moreover, this model makes the assumption of an infinite Schwoebel barrier at the lower steps. These approximations preclude long-range interactions between steps whose homogenization would result in long-range surface diffusion. Generalizing this model to the unsteady train of steps would enable us to study the interactions between steps, and consequently to account for the long-range surface diffusion of interfacial species. In addition, the formation of the compound was restricted to the upper steps and the nucleation of secondary phases was not included in the model. These issues could be addressed via the inclusion of nucleation terms in the equations governing the density profiles of adatoms along the terraces.

Appendix A On the Step-Flow Simulations

The simulations shown in Figures 4.2 and 4.3 were performed using the following values for the physical parameters that enter the non-competitive two-species step-flow model: the diffusion coefficient associated with the A- and B-adatoms have the values $D^A = 1$ and $D^B = 1.5$ respectively; the reaction-rate constants associated with the adsorption of A- and B- adatoms along the terraces have the values $k^A_{ads} = k^B_{ads} = 10$, while the reaction-rate constants associated with the desorption of the adatoms in question have the values $k^A_{des} = k^B_{des} = 1$. The reaction-rate constant associated with the formation of the AB-compound at the upper steps is assigned the value 1. Finally, the molecular weights of the A and B species are taken to be $w_A = 2$ and $w_B = 3$.

Figures A1 and A2 represent plots of the constitutive function (4.32) for the following choice of the constants c_1, c_2, α_1 and α_2: $c_1 = 20$, $c_2 = .6$, $\alpha_1 = 1.5$ and $\alpha_2 = .55$. Figure A1 is plotted over the same domain as Figure 4.2 and for the same fixed value of $[X_bB]_g$. Identically, Figure A2 was computed over the same range of gas-phase concentrations and for the same fixed value of $\mathcal{L}$.

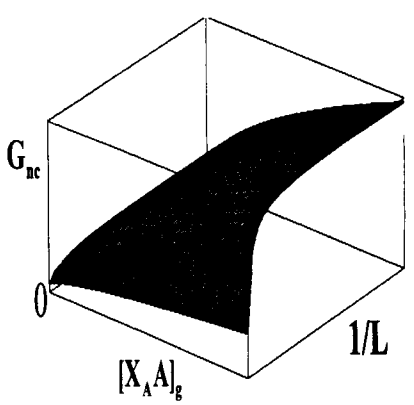

Figure A1: Plot of the average growth rate as a function of the inverse of terrace width and the gas-phase molar concentration of the precursor $[X_AA]_g$ for a fixed value of $[X_BB]_g$ as proposed in the constitutive relation (4.32) and over the same domain as Figure 4.2.

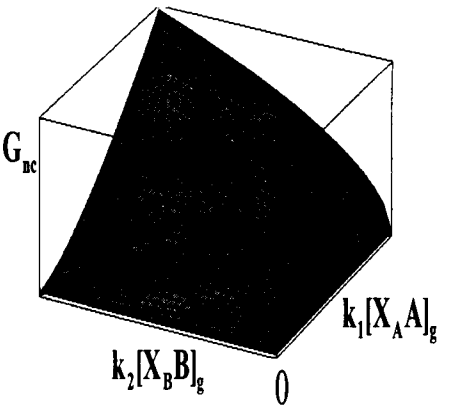

Figure A2: Plot of the average growth rate as a function of the molar concentrations of the gas-phase precursors $[X_A A]_g$ and $[X_B B]_g$ for a fixed value of $\mathcal{L}$ as proposed in the constitutive relation (4.32) and over the same domain as Figure 4.3.

Identically, in the simulations shown in Figures 4.4 and 4.5, we have used the following values for the physical parameters that enter the competitive two-species step-flow model: the diffusion coefficient associated with the A- and B-adatoms have the values $D^A = D^B = 1$ and the reaction-rate constants associated with the adsorption of A- and B- adatoms along the terraces have the values $k^A_{ads} = k^B_{ads} = 10$, while the reaction-rate constants associated with the desorption of the adatoms in question have the values $k^A_{des} = k^B_{des} = 1$. The reaction-rate constant associated with the formation of the AB-compound at the upper steps is assigned the value 1. Finally, the molecular weights of the A and B species are taken to be $w_A = 2$ and $w_B = 1$.

Finally, Figures A3 and A4 (shown on the next page) represent plots of the constitutive function proposed for $\mathbf{G}_c$ on page 143 for the following choice of the constants: $c_1 = 1.5$, $c_2 = .3$, $c_3 = 1.4$ and $c_4 = 1$. Figure A3 is plotted over the same domain as Figure 4.4 and for the same fixed value of $[X_b B]_g$ and Figure A4 was computed over the same range of gas-phase concentrations and for the same fixed value of $\mathcal{L}$.

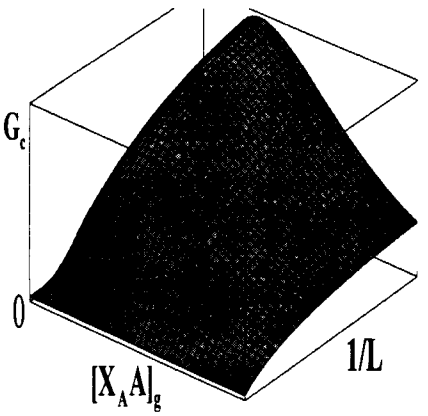

Figure A3: Plot of the average growth rate as a function of the inverse of terrace width and the gas-phase molar concentration of the precursor $[X_A A]_g$ for a fixed value of $[X_B B]_g$ as proposed in the constitutive relation on page 143 and over the same domain as Figure 4.4.

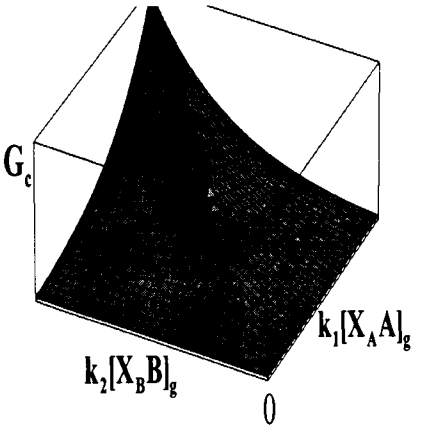

Figure A4: Plot of the average growth rate as a function of the molar concentrations of the gas-phase precursors $[X_A A]_g$ and $[X_B B]_g$ for a fixed value of $\mathcal{L}$ as proposed in the constitutive relation on page 143 and over the same domain as Figure 4.5.

Bibliography

[AK] R. Abeyaratne and J.K. Knowles, On the driving traction acting on a surface of strain discontinuity in a continuum, *J. Mech. Phys. Solids*, **38**, 345-360 (1990).

[BZ] G.S. Bales and A. Zangwill, Morphological instability of a terrace edge during step-flow growth, *Phys. Rev. B*, **41**, 5500-5508 (1990).

[BSB1] C.C. Battaile, D.J. Srolovitz and J.E. Butler, Morphologies of diamond films from atomic-scale simulations of chemical vapor deposition, *Diam. Relat. Mater.*, **9**, 1198-1206 (1997).

[BSB2] C.C. Battaile, D.J. Srolovitz and J.E. Butler, A kinetic Monte Carlo method for the atomic-scale simulation of chemical vapor deposition: Application to diamond, *J. Appl. Phys.*, **82**, 6293-6300 (1997).

[BSB3] C.C. Battaile, D.J. Srolovitz and J.E. Butler, Atomic-scale simulations of chemical vapor deposition on flat and vicinal diamond substrates, *J. Crys. Growth*, **194**, 353-368 (1998).

[BD] A. Bedford and D.S. Drumheller, Theories of immiscible and structured mixtures, *Int. J. Engng Sci.*, **8**, 863-960 (1983).

[BB] A. Bourdillon and N.X. Tan Bourdillon, High-temperature superconductors: processing and science, Academic Press, New York (1994).

[BCF] W.K. Burton, N. Cabrera and F.C. Frank, The growth of crystals and the equilibrium structure of their surfaces, *Philos. trans. R. Soc. London A*, **243**, 299-358 (1951).

[C] H.B. Callen, Thermodynamics and an introduction to thermostatistics (2^{nd} edition), John Wiley & Sons, 56-58 (1985).

[CN] B.D. Coleman and W. Noll, The thermodynamics of elastic materials with heat conduction and viscosity, *Arch. Rat. Mech. Anal.*, **13**, 167-178 (1963).

[CKM1] M.E. Coltrin, R.J. Kee and J.A. Miller, A mathematical model of the coupled fluid mechanics and chemical kinetics in a chemical vapor deposition reactor, *J. Electrochem. Soc.*, **131**, 425-434 (February 1984).

[CKM2] M.E. Coltrin, R.J. Kee and J.A. Miller, A mathematical model of Silicon chemical vapor deposition. Further refinements and the effects of thermal diffusion, *J. Electrochem. Soc.*, **113**, 1206 (June 1986).

[CK] M.E. Coltrin and R.J. Kee, A mathematical model of the gas-phase and surface chemistry in GaAs MOCVD, *Mat. Res. Soc. Symp. Proc.*, **145**, 119-124 (1989).

[CKR] M.E. Coltrin, R.J. Kee and F.M. Rupley, Surface Chemkin (version 3.7): a Fortran package for analyzing heterogeneous chemical kinetics at solid-surface –gas-phase interface, *Sandia Report*, SAND90-8003•UC-401 (August 1990).

[DG] F. Davi and M.E. Gurtin, On the motion of a phase interface by surface diffusion, *J. Appl. Math. Phys.*, **41**, 782 (November 1990).

[VE] I. Elkinani and J. Villain, Growth roughness and instabilities due to the Schwoebel effect- a one-dimensional model, *J. De Physique I*, **4**, 949-973 (1994).

[EG] G. Evans and R. Greif, A numerical model of the flow and heat transfer in a rotating disk chemical vapor deposition reactor, *Transactions of the ASME*, **109**, 928-935 (1987).

[G] J.W. Gibbs, The collected works of J. Willard Gibbs, Longmans, Green and Co., 55-354 (1928).

[GG] D.G. Goodwin and G.G. Gavillet, Numerical modeling of the filament-assisted diamond growth environment, *J. Appl. Phys.*, **68**, 6393-6400 (December 1990).

[GB] D.G. Goodwin and J.E. Butler, Theory of diamond chemical vapor deposition, *in* Handook of industrial diamonds and diamond films, M. A. Prelas, G. Popovici, and L. K. Bigelow (editors), Marcel Dekker (1997).

[G1] D. Goodwin, private communication.

[G2] M.E. Gurtin, An introduction to Continuum Mechanics, Academic Press, New York, 101-105 (1981).

[G3] M.E. Gurtin, The nature of configurational forces, *Arch. Rat. Mech. Anal.*, **131**, 67-100 (1995).

[GM] M.E. Gurtin and A.I. Murdoch, A continuum theory of elastic material surfaces, *Arch. Rat. Mech. Anal.*, **57**, 291-323 (1975).

[GP] M.E.Gurtin and P. Podio-Guidugli, On configurational inertial forces at a phase interface, *J. Elasticity*, **44**, 255-269 (September 1996).

[GV1] M.E.Gurtin and P.W. Voorhees, The thermodynamics of evolving interfaces far from equilibrium, *Acta mater.*, **44**, 235-247 (1996).

[GV2] M.E. Gurtin and P.W. Voorhees, The continuum mechanics of coherent two-phase elastic bodies with mass transport, *Proc. R. Soc. Lond.* A, **440**, 323-343 (1993).

[GV] J.E. Guyer and P.W. Voorhees, Morphological stability of alloy thin films, *Phys. Rev.* B, **54**, 11710-11724 (1996).

[H1] C. Herring, Surface tension as a motivation for sintering, In *The physics of powder metallurgy* (W.E. Kingston, ed.), McGraw-Hill, New York, 143-179 (1951).

[TH] T.L. Hill, An introduction to statistical thermodynamics, Dover, New York, 177-198 (1986).

[HGB] W.G. Houf, J.F. Grcar and W.G. Breiland, A model for low pressure chemical vapor deposition in a hot-wall tubular reactor, *Mater. Sci. Engng. B*, **17**, 163-171 (1993).

[HGJ] C. Houtman, D.B. Graves and K.F. Jensen, CVD in stagnation point flow, *J. Electrochem. Soc.*, **133**, 961-970 (May 1986).

[H2] W. Hurewicz, Lectures on ordinary differential equations, Dover, New York, 8 (1990).

[K] Th. v. Kármán, Uber laminare und turbulent reibung, *Z. Angew. Math. Mech.*, **1**, 233-252 (1921).

[K] C.R. Kleijn, Chemical vapor deposition processes, *in* Computational Modeling in Semiconductor Processing, The Artech House Materials Science Library, M. Meyyappan (Editor), 97-145 (1995).

[LS] P.H. Leo and R.F. Sekerka, The effect of surface stress on crystal-melt and crystal-crystal equilibrium, *Acta Metall.*, **37**, 3119-3138 (1989).

[LR] H.W. Liepmann and A. Roshko, Elements of gasdynamics, John Wiley & Sons, New York, 50-51 (1957).

[MKD] E. Meeks, R.J. Kee and D.S. Dandy, Computational simulation of diamond chemical vapor deposition in premixed $C_2H_2/O_2/H_2$ and CH_4/O_2-strained flames, *Combust. Flame*, **92**, 144-160 (1993).

[JM] T.J. Mountziaris and K.F. Jensen, Gas-phase and surface reaction mechanisms in MOCVD of GaAs with Trimethyl-Gallium and Arsine, *J. Electrochem. Soc.*, **138**, 2426-2439 (August 1991).

[M] W.W. Mullins, Theory of thermal grooving, *J. Appl. Phys.*, **28**, 333-339 (1957).

[MS] W.W. Mullins and R.F. Sekerka, Morphological stability of a particle growing by diffusion or heat flow, *J. Appl. Phys.*, **34**, 323-329 (February 1963).

[OSLJ] R. Omstead, P.M. van Sickle, P.W. Lee and K.F. Jensen, Gas phase and surface reactions in the MOCVD of $GaAs$ from triethylgallium trimethylgallium, and tertiarybutylarsine, *J. Cryst. Growth* **93**, 20-28 (1998).

[PN] R. Pollard and J. Newman, Silicon deposition on a rotating disk, *J. Electrochem. Soc.*, **127**, 744-752 (1980).

[RH] I.D. Raistrick and M. Hawley, Scanning tunneling and atomic force microscope studies of thin sputtered films of $YBa_2Cu_3O_{7-\delta}$, in *Interfaces in high-T_c superconducing systems*, S.L. Shindé and D.A. Rudman (editors), Springer-Verlag 28-70 (1993).

[RSV] C. Ratsch, P. Smilauer, D.D. Vvedensky, et al., Mechanism for coherent island formation during heteroepitaxy, *J. Phys. I*, **6**, 575-581 (1996).

[S] Y. Saito, Statistical physics of crystal growth, World Scientific, 7-8 (1996).

[SB] N.K. Simha and K. Bhattacharya, Kinetics of phase boundaries with edges and junctions in a three-dimensional multi-phase body, to appear in *J. Mech. Phys. Solids.*

[SVD] B.J. Spencer, P.W. Voorhees and S.H. Davis, Morphological instability in epitaxially strained dislocation-free solid films: linear stability theory, *J. Appl. Phys.*, **73**, 4955-4970 (1993).

[V] J. Villain, Continuum models of crystal growth from atomic beams with and without desorption, *J. Phys. I*, **1**, 19-42 (1991).

[VP] J. Villain and A. Pimpinelli, Physics of crystal growth, Cambridge University Press (1998).

[V] D.D. Vvedensky, Atomistic modeling of epitaxial growth: Comparisons between lattice models and experiment, *Comp.Mater. Sci.*, **6**, 182-187 (1996).

[VHS] D.D. Vvedensky, N. Haider, T. Shitara, et al., Evolution of surface-morphology during epitaxial-growth, *Philos. T. Roy. Soc. A*, **344**, 493-505 (1993).

[W] E. Waffenschmidt, K.H. Waffenschmidt, F. Arndt, E. Boeke, J. Musolf, X. He, M. Heuken, and K. Heime, Local stochiometry measurement of Y-Ba-Cu-O thin

layers grown by metal organic chemical vapor deposition, *J. Appl. Phys.*, **75**, 54092-4096 (1994).

[WEM] W.S. Winters, G.H. Evans and C.D. Moen, CURRENT- A computer code for modeling two-dimensional, chemically reacting, low Mach number flows, *Sandia Report* SAND97-8202•UC-1409 (October 1996).

[YHC] G.W. Young, S.I. Hariharan and R. Carnahan, Flow effects in a vertical CVD reactor, *SIAM J. Appl. Math.*, **52**, 1509-1532 (December 1992).

[Z] A. Zangwill, Theory of growth-induced surface roughness, to appear in *Microstructural evolution of thin films*, H.A. Atwater and C.V. Thompson (editors), Academic Press, New York.